Chapter 3. Attribution of the Causes of Climate Variations and Trends over North America during the Modern Reanalysis Period

Convening Lead Author: Martin Hoerling, NOAA

Lead Authors: Gabriele Hegerl, Duke University; David Karoly, University of Melbourne; Arun Kumar, NOAA; David Rind, NASA

Contributing Author: Randall Dole, NOAA

KEY FINDINGS

- Significant advances have occurred over the past decade in capabilities to attribute causes for observed climate variations and change.
- Methods now exist for establishing attribution for the causes of North American climate variations and trends due to internal climate variations and/or changes in external climate forcing.

Annual, area-average change since 1951 across North America show:

- Seven of the warmest ten years for annual surface temperatures since 1951 have occurred in the last decade (1997 to 2006).

- The 56-year linear trend (1951 to 2006) of annual surface temperature is +0.90°C +/-0.1°C.
- Virtually all of the warming since 1951 has occurred after 1970.
- More than half of the warming is *likely* the result of anthropogenic forcing.
- Changes in ocean temperatures *likely* explain a substantial fraction of the anthropogenic warming of North America.
- There is no discernible trend in precipitation since 1951, in contrast to trends observed in extreme precipitation events (CCSP, in press).

Spatial variations in annual-average change since 1951 across North America show:

- Observed surface temperature change has been largest over northern and western North America, with up to +2°C/56 years warming over Alaska, the Yukon Territories, Alberta, and Saskatchewan.
- Observed surface temperature change has been least over the southern United States and eastern Canada, where no significant trends have occurred.
- There is *very high* confidence that changes in free atmospheric circulation have occurred based upon reanalysis data, and that these circulation changes are the *likely* physical basis for much of the spatial variations in surface temperature change over North America, especially during winter.
- The spatial variations in surface temperature change over North America are *unlikely* the result of anthropogenic forcing alone.

- The spatial variations in surface temperature change over North America are very *likely* influenced by variations in global sea surface temperatures through the effects of the latter on atmospheric circulation, especially during winter.

Spatial variations of seasonal average change since 1951 across the United States show:

- Six of the warmest ten summers and winters for conterminous United States averaged surface temperatures since 1951 have occurred in the last decade (1997 to 2006).
- During summer, surface temperatures have warmed most over western states, with insignificant change between the Rocky and Appalachian Mountains. During winter, surface temperatures have warmed most over northern and western states, with insignificant change over the central Gulf of Mexico, and Maine.
- The spatial variations in summertime surface temperature change are *unlikely* the result of anthropogenic forcing alone.
- The spatial variations and seasonal differences in precipitation change are *unlikely* the result of anthropogenic forcing alone.
- Some of the spatial variations and seasonal differences in precipitation change and variations are *likely* the result of regional variations in sea surface temperatures.

With respect to abrupt climate change over North America in the reanalysis period:

- Current reanalysis data extends back until only the middle of the last century, posing limitations for detecting rapid climate shifts and distinguishing them from quasi-cyclical variations.

For droughts:

- It is *unlikely* that a systematic change in either the frequency or area coverage of severe drought occurred over the conterminous United States during the past half-century.
- It is *very likely* that short-term (monthly-to-seasonal) severe droughts that have impacted North America during the past half-century are mostly due to atmospheric variability, in some cases amplified by local soil moisture conditions.
- It is *likely* that sea surface temperature anomalies have been important in forcing long-term (multi-year) severe droughts that have impacted North America during the past half-century.
- It is *likely* that anthropogenic warming has increased the severity of both short-term and long-term droughts over North America in recent decades.

INTRODUCTION

Increasingly, climate scientists are being asked to go beyond descriptions of *what* the current climate conditions are and how they compare with the past, to also explain *why* climate is evolving as observed; that is, to provide attribution of the causes for observed climate variations and change.

Today, a fundamental concern for policy-makers is to understand the extent to which anthropogenic factors and natural climate variations are responsible for the observed evolution of climate. A central focus for such efforts, as articulated in the IPCC assessments, has been to establish the cause, or causes, for global-mean temperature increases over roughly the past century. However, requests for climate attribution far transcend this single variable, with notable interest in explaining regional variations and the causes for high-impact climate events, such as the recent multi-year drought in the western United States and the record setting 2006 United States warmth. For many decision makers who must assess potential impacts and management options, a particularly important question is: What are and how well do we understand the causes for regional and seasonal differences in climate variations and trends? For example, is the source for the recent drought in the western United States due mainly to factors internal to the climate system, in which case a return toward previous climate conditions might be anticipated, or is it rather a manifestation of a longer-term trend toward increasing aridity in the region that is driven primarily by anthropogenic forcing? Why do some droughts last longer than others? Such examples illustrate that to support informed decision making, the capability to attribute causes for past and current climate conditions can be of fundamental importance.

The recently completed IPCC Fourth Assessment Report (AR4) from Working Group I contains a full chapter devoted to the topic "Understanding and Attributing Climate Change" (IPCC, 2007a). In the present chapter, we have attempted to minimize overlap with the IPCC report by focusing on a subset of questions of particular interest to the United States public, decision makers, and policymakers that may not have been covered in detail (or in some cases, at all) in the IPCC report. The specific emphasis here is on our present ability – or inability – to attribute the causes for observed climate variations and change over North America. For a more detailed discussion of attribution, especially for other regions and at the global scale, the interested reader is referred to chapter 9 of the AR4 Working Group I report.

Figure 3.1 illustrates methods and tools used in climate attribution. The North American map (right side) shows an observed surface condition whose causes are sought. A roadmap for attribution involves the systematic probing of cause-effect relationships. Plausible forcings are identified along the top of Figure 3.1 (brown oblongs), and arrows illustrate connections among these and also pathways for explaining the observed condition.

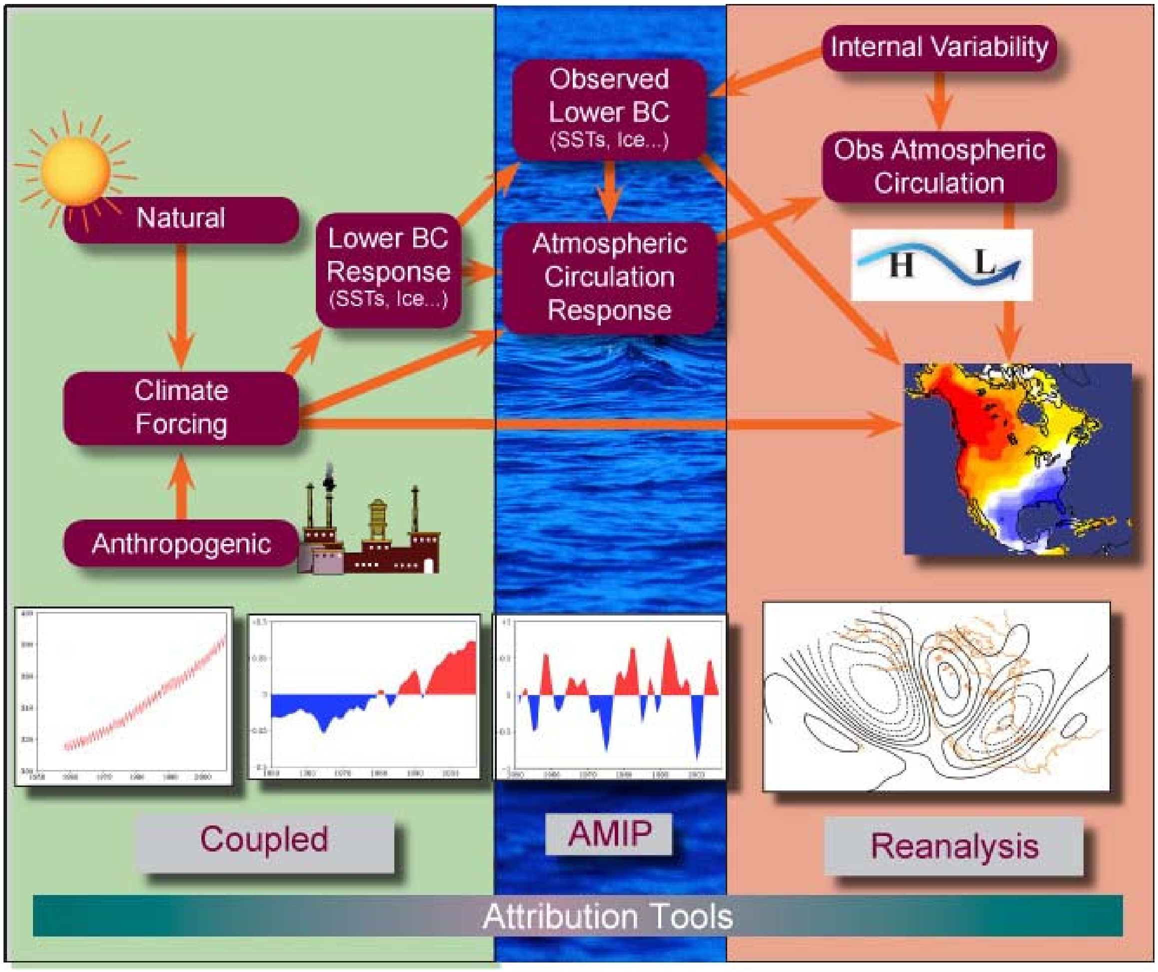

Figure 3.1 Schematic illustration of the data sets and modeling strategies for performing attribution. The right-side map displays a North American climate condition whose origin is in question. Various candidate causal mechanisms are illustrated in the right-to-left sequences of figures, together with the attribution tool. Listed above each in brown oblongs is a plausible cause that could be assigned to the demonstrated mechanism depending upon the diagnosis of forcing-response relationships derived from attribution methods. The efficacy of the first mechanism is tested, often empirically, by determining consistency with patterns of atmospheric variability, such as the teleconnection processes identifiable from reanalysis data. This step places the current condition within a global and historical context. The efficacy of the second mechanism tests the role of boundary forcings, most often with atmospheric models (AMIP). The efficacy of the third mechanism tests the role of external forcings, most often with coupled ocean-atmosphere models. The processes responsible for the climate condition in question may, or may not, involve teleconnections, but may result from local changes in direct radiative forcing or other near-surface forcing such as from land surface anomalies. The lower panels illustrate representative process: from left-to-right; time-evolving atmospheric carbon dioxide at Mauna Loa, the multi-decadal warming trend in tropical west Pacific-Indian Ocean warm pool SSTs, the yearly SST variability over the tropical east Pacific due to ENSO, the atmospheric pattern over the North Pacific/ North America referred to as the PNA teleconnection.

The attribution process begins by examining conditions of atmospheric circulation that coincide with the North American surface climate anomaly. It is possible, for instance, that the surface condition evolved in concert with a change in the tropospheric jet stream, such as accompanies the Pacific-North American pattern (Chapter 2). Reanalysis data is the essential tool for this purpose because it provides a global description of the state of the tropospheric climate that is physically consistent in space and time. Reanalysis as an attribution tool, however, only offers a connection between the surface and tropospheric climate without necessarily *explaining* its causes.

Additional tools are often needed to explain the circulation pattern itself. Is it, for instance, due to chaotic internal atmospheric variations, or is it related to forcing external to the atmosphere (*e.g.*, sea surface temperature forcing, or radiative forcing)? The middle column in Figure 3.1 illustrates the common approach used to assess the forcing-response associated with Earth's lower boundary conditions, in particular sea surface temperatures. The principal tool is atmospheric general circulation models forced with the specified history of surface boundary conditions (Gates, 1992). Reanalysis would continue to be important in this stage of attribution in order to evaluate the suitability of the models as an attribution tool, including the realism of simulated circulation variability (Box 3.1).

In the event that diagnosis of the AMIP simulation fails to confirm a role for Earth's lower boundary conditions, then two plausible explanations for the circulation (and its associated North American surface condition) remain. One is that it was unforced, being instead due to chaotic atmospheric variability. Reanalysis data would be useful to determine whether the circulation state was within the scope of known variations during the reanalysis record. Alternatively, external natural (*e.g.*, volcanic and solar) or external anthropogenic perturbations may directly have caused the responsible circulation pattern. Coupled ocean-atmosphere climate models would be used to explore the forcing-response relationships involving such external forcings. Illustrated by the left column, coupled models have been widely employed in the reports of the IPCC. Here again, reanalysis is important for assessing the suitability of this attribution tool, including the realism of simulated ocean-atmosphere variations such as El Niño and accompanying atmospheric teleconnections that influence North American surface climate (Box 3.1).

In the event that diagnosis of the AMIP simulations confirms a role for Earth's lower boundary conditions, it becomes important to explain the cause for the boundary condition itself. Comparison of the observed sea surface temperatures with coupled model simulations would be the principal approach. If anthropogenically forced coupled models fail to yield the observed boundary conditions, then they may be attributed to chaotic intrinsic coupled ocean-atmosphere variations. If instead coupled models replicate the observed boundary conditions, this establishes a consistency with external forcing as an ultimate cause. (It is also necessary to confirm that the coupled models also generate the atmospheric circulation patterns; that is, to demonstrate that the models got the result for the correct physical reason).

The schematic illustrates basic approaches applied in the following sections of Chapter 3. It is evident that a physically-based scientific interpretation for the causes of a climate condition requires accurately measured and analyzed features of the time and space characteristics of atmospheric circulation and surface conditions. In addition, it relies heavily upon the use of climate models to test candidate cause-effect relations. Reanalysis is essential for both components of such attribution science.

While this Chapter considers the approximate period covered by modern reanalyses (roughly 1950 to the present), data sets other than reanalyses such as gridded surface station analyses of temperature and precipitation are also used. In fact, the surface condition illustrated in Figure 3.1 are generally derived from such data sets, and these are extensively employed to describe various key features of the recent North American climate variability in Chapter 3. These, together with modern reanalysis data, provide a necessary historical context against which the uniqueness of current climate conditions both at Earth's surface and in the free atmosphere can be assessed.

3.1 WHAT IS CLIMATE ATTRIBUTION, AND WHAT ARE THE SCIENTIFIC METHODS USED FOR ESTABLISHING ATTRIBUTION?

3.1.1 What is Attribution?

Climate attribution is a scientific process for establishing the principal causes or physical explanation for observed climate conditions and phenomena. Within its reports, the IPCC states that "attribution of causes of *climate change* is the process of establishing the most likely causes for the detected change with some level of confidence." As noted in the

Introduction, the definition is expanded herein to include attribution of the causes of observed *climate variations* that may not be unusual in a statistical sense but for which great public interest exists because they produce profound societal impacts.

It is useful at the outset to outline some general classes of mechanisms that may produce climate variations or change. One important class is *external forcing*, which contains both *natural* and *anthropogenic* sources. Examples of natural external forcing include solar variability and volcanic eruptions. Examples of anthropogenic forcing are changing concentrations of greenhouse gases and aerosols, and land cover changes produced by human activities. A second class involves *internal mechanisms* within the climate system that can produce climate variations manifesting themselves over seasons, decades, and longer. Internal mechanisms include processes that are due primarily to interactions within the atmosphere as well as those that involve coupling of the atmosphere with various components of the climate system. Climate variability due to purely internal mechanisms is often called *internal variability*.

For attribution to be established, the relationship between the observed climate state and the proposed causal mechanism needs to be demonstrated, and alternative explanations need to be determined as unlikely. In the case of attributing the cause of a climate condition to internal variations, for example, due to El Niño-related tropical east Pacific sea surface conditions, the influence of alternative modes of internal climate variability must also be assessed. Before attributing a climate condition to anthropogenic forcing, it is important to determine that the climate condition was unlikely to have resulted from natural external forcing or internal variations alone.

Attribution is most frequently associated with the process of explaining a *detected change*. In particular, attribution of anthropogenic climate change - the focus of the IPCC reports (Houghton *et al.*, 1996; Houghton *et al.*, 2001; IPCC, 2007a) - has the specific objective of explaining a detected climate change that is significantly different from that which could be expected from natural external forcing or internal variations of the climate system. According to the Third Assessment Report (TAR), the attribution requirements for a detected change are: (1) a demonstrated consistency with a combination of anthropogenic and natural external forcings, and (2) an inconsistency with "alternative, physically plausible explanations of recent climate change that exclude important elements of the given combination of forcings" (Houghton *et al.*, 2001).

3.1.2 How is Attribution Performed?

The methods used for attributing the causes for observed climate conditions depend on the specific problem or context. To establish the cause requires identifying candidate forcings, determining the response produced by such forcings, and determining the agreement between the forced response and the observed condition. It is also necessary to demonstrate that the observed climate condition is unlikely to have originated from other forcing mechanisms.

The methods for signal identification, as discussed in more detail below, involve both empirical analysis of past climate relationships and experiments with climate models in which forcing-response relations are evaluated. Similarly, estimates of internal variability can be derived from the instrumental records of historical data including reanalyses and from simulations performed by climate models in the absence of the candidate forcings. Both empirical and modeling approaches have limitations. The former is hampered by the relatively short duration of the climate record, the confounding of influences from various forcing mechanisms, and by possible non-physical inhomogeneities in the climate record that can result from changing monitoring techniques and analysis procedures (see Chapter 2 for examples of non-physical trends in precipitation owing to shifts in reanalysis methods). The climate models are hampered by uncertainties in the representation of physical processes and by coarse spatial resolution (currently on the order of several hundred kilometers) that can lead to model biases. In each case, the identified signal (forcing-response relationship) must be robust to these uncertainties. This includes demonstrating that an empirical analysis is both physically meaningful and is robust to sample size, and that a numerical result is replicated when using different climate models. Best attribution practices employ combinations of empirical and numerical approaches using multiple climate models, to minimize the effects of possible biases resulting from a single line of approach. Following this approach, Table 3.1 and Table 3.2 lists the observational and model data sets used to generate analyses in Chapter 3.

Table 3.1 Acronyms of climate models referenced in this Chapter. All 19 models performed simulations of 20th century climate change ("20CEN") as well as the 720 ppm stabilization scenario (SRESA1B) in support of the IPCC Fourth Assessment Report. The ensemble size "ES" is the number of independent realizations of the 20CEN experiment that were analyzed here.

	MODEL ACRONYM	COUNTRY	INSTITUTION	ES
1	CCCma-CGCM3.1(T47)	Canada	Canadian Centre for Climate Modelling and Analysis	1
2	CCSM3	United States	National Center for Atmospheric Research	6
3	CNRM-CM3	France	Météo-France/Centre National de Recherches Météorologiques	1
4	CSIRO-Mk3.0	Australia	CSIRO[1] Marine and Atmospheric Research	1
5	ECHAM5/MPI-OM	Germany	Max-Planck Institute for Meteorology	3
6	FGOALS-g1.0	China	Institute for Atmospheric Physics	1
7	GFDL-CM2.0	United States	Geophysical Fluid Dynamics Laboratory	1
8	GFDL-CM2.1	United States	Geophysical Fluid Dynamics Laboratory	1
9	GISS-AOM	United States	Goddard Institute for Space Studies	2
10	GISS-EH	United States	Goddard Institute for Space Studies	3
11	GISS-ER	United States	Goddard Institute for Space Studies	2
12	INM-CM3.0	Russia	Institute for Numerical Mathematics	1
13	IPSL-CM4	France	Institute Pierre Simon Laplace	1
14	MIROC3.2(medres)	Japan	Center for Climate System Research / NIES[2] / JAMSTEC[3]	3
15	MIROC3.2(hires)	Japan	Center for Climate System Research / NIES[2] / JAMSTEC[3]	1
16	MRI-CGCM2.3.2	Japan	Meteorological Research Institute	5
17	PCM	United States	National Center for Atmospheric Research	4
18	UKMO-HadCM3	United Kingdom	Hadley Centre for Climate Prediction and Research	1
19	UKMO-HadGEM1	United Kingdom	Hadley Centre for Climate Prediction and Research	1

[1]CSIRO is the Commonwealth Scientific and Industrial Research Organization.
[2]NIES is the National Institute for Environmental Studies.
[3]JAMSTEC is the Frontier Research Center for Global Change in Japan.

Table 3.2 Data sets utilized in the report. The versions of these data used in this report include data through December 2006. The web sites listed below provide URLs to the latest versions of these data sets, which may incorporate changes made after December 2006.

CRU HadCRUT3v Climatic Research Unit of the University of East Anglia and the Hadley Centre of the UK Met Office
http://www.cru.uea.uk/cru/data/temperature/

NOAA Land/Sea Merged Temperature NOAA's National Climatic Data Center (NCDC)
http://www.ncdc.noaa.gov/oa/climate/research/anomalies/

NASA Land+Ocean Temperature NASA's Goddard Institute for Space Studies (GISS)
http://data.giss.noaa.gov/gistemp/

NCDC Gridded Land Temperature NOAA's National Climatic Data Center (NCDC)
Gridded Land Precipitation
http://www.ncdc.noaa.gov/oa/climate/research/ghcn/

NCDCdiv Contiguous U.S. Climate Division Data (temperature and precipitation)
http://www.ncdc.noaa.gov/oa/climate/onlineprod/

PRISM Spatial Climate Gridded Data Sets (temperature and precipitation) Oregon State University's Oregon Climate Service (OCS)
http://prism.oregonstate.edu

CHEN Global Land Precipitation NOAA's Climate Prediction Center (CPC)
http://www.cpc.noaa.gov/products/precip/

GPCC Global Gridded Precipitation Analysis Global Precipitation Climatology Centre (GPCC)
http://www/dwd/de/en/FundE/Klima/KLIS/int/GPCC/

CMIP3 CMIP3 World Climate Research Programme's (WCRP's) Coupled Model Intercomparison Project phase 3 (CMIP3) multi-model dataset
http://www-pcmdi.llnl.gov/ipcc/

Reanalysis NCEP50 National Centers for Environmental Prediction (NCEP), NOAA, and the National Center for Atmospheric Research (NCAR)
http://dss.ucar.edu/pub/reanalysis/data_usr.html/

ECHAM4.5 ECHAM4.5
http://iridl.ldeo.columbia.edu/SOURCES/.IRI/.FD/.ECHAM4p5/.History/.MONTHLY

NASA/NSIPP Runs

The specific attribution method can also differ according to the forcing-response relation being probed. As discussed below, three methods have been widely employed. These consider different hierarchical links in causal relationships as illustrated in the schematic Figure 3.1 as discussed in Section 3.1.2.1: (i) climate conditions rising from mechanisms internal to the atmosphere, (ii) climate conditions forced from changes in atmospheric lower boundary conditions (for example, changes in ocean or land surface conditions), and (iii) climate conditions forced externally, whether natural or anthropogenic. Note that in some cases, more than one of these links, or pathways, can be involved. For example, changes in greenhouse gas forcing may induce changes in the ocean component of the climate system. These ocean conditions can then force a response in the atmosphere that leads to regional temperature or precipitation changes.

3.1.2.1 Signal determination

i) Attribution to internal atmospheric variations

Pioneering empirical research, based only on surface information, discovered statistical linkages between anomalous climate conditions that were separated by continents and oceans (Walker and Bliss, 1932), structures that are referred to today as teleconnection patterns. The North Atlantic Oscillation (NAO); a see-saw in anomalous pressure between the subtropical North Atlantic and the Arctic, and the Pacific-North American (PNA) pattern; a wave pattern of anomalous climate conditions arching across the North Pacific and North American regions, are of particular relevance to understanding North American climate variations. Chapter 2 has illustrated the use of reanalysis data to diagnose the tropospheric wintertime atmospheric circulations associated with a specific phase of the PNA and NAO patterns, respectively. They each have widespread impacts on North American climate conditions as revealed by station-based analyses of surface temperature and precipitation anomalies, and the reanalysis data of free atmospheric conditions provides the foundation for a physical explanation of the origins of those fingerprints. The reanalysis data are also used to validate the realism of atmospheric circulation in climate models, as illustrated in Box. 3.1**.**

BOX 3.1 Assessing Model Suitability

A principal tool for attributing the causes of climate variations and change involves climate models. For instance, atmospheric models using specified sea surface temperatures are widely used to assess the impact of El Niño on seasonal climate variations. Coupled ocean-atmosphere models using specified atmospheric chemical constituents are widely used to assess the impact of greenhouse gases on detected changes in climate conditions. One prerequisite for the use of models as tools is their capacity to simulate the known leading patterns of atmospheric (and for the coupled models, oceanic) modes of variations. Realism of the models enhances confidence in their use for probing forcing-response relationships, and it is for this reason that an entire chapter of the IPCC Fourth Assessment Report is devoted to evaluation of the models for simulating known features of large-scale climate variability. That report emphasizes the considerable scrutiny and evaluations under which these models are being placed, making it "less likely that significant model errors are being overlooked". *Reanalysis data of global climate variability of the past half-century provide valuable benchmarks against which key features of model simulations can be meaningfully assessed*.

The figure below illustrates a simple use of reanalysis for validation of models that are employed for attribution elsewhere in this report. Chapter 8 of the Working Group I report of IPCC AR4 and the references therein provide numerous additional examples of validation studies of the IPCC coupled models that are used in this SAP. Shown are the leading winter patterns of atmospheric variability, discussed previously in Chapter 2 (Figures 2.8 and 2.9), that have strong influence on North American climate. These are the Pacific-North American pattern (left), the North Atlantic Oscillation pattern (middle), and the El Niño/Southern Oscillation pattern (right). The spatial expressions of these patterns is depicted using correlations between observed (simulated) indices of the PNA, NAO, and ENSO with wintertime 500 hPa geopotential heights derived from reanalysis (simulation) data for 1951 to 2006. Both atmospheric (middle) and coupled ocean-atmospheric (bottom) models realistically simulate the phase and spatial scales of the observed (top) patterns over the Pacific-North American domain. The correlations within the PNA and NAO centers of action are close to those observed indicating the fidelity of the models in generating these atmospheric teleconnections. The ENSO correlations are appreciably weaker in the models than in reanalysis. This is in part due to averaging over multiple models and multiple realizations of the same model. It \perhaps also indicates that the tropical-extratropical interactions in these models is weaker than observed, and for the CMIP runs it may also indicate weaker ENSO sea surface temperature variability. These circulation patterns are less pronounced during summer, at which time climate variations become more dependant upon local processes (*e.g.*, convection and land-surface interaction) which poses a greater challenge to climate models.

More advanced applications of reanalysis data to evaluate models include budget diagnoses that test the realism of physical processes associated with climate variations, frequency analysis of the time scales of variations, and multi-variate analysis to assess the realism of coupling between surface and atmospheric fields. It should be noted that despite the exhaustive evaluations that can be conducted, model assessments are not always conclusive about their suitability as an attribution tool. First, the tolerance to biases in models needed to produce reliable assessment of cause-effect relationships is not well understood. It is partly for this reason that large multi-model ensemble methods are employed for attribution studies in order to reduce the random component of biases that exist across individual models. Second, even when known features of the climate system are judged to be realistically simulated in models, there is no assurance that the modeled response to increased greenhouse gas emissions will likewise be realistic under future scenarios. Therefore attribution studies (IPCC, chapter 9) compare observed with climate model simulated change because such sensitivity is difficult to evaluate from historical observations.

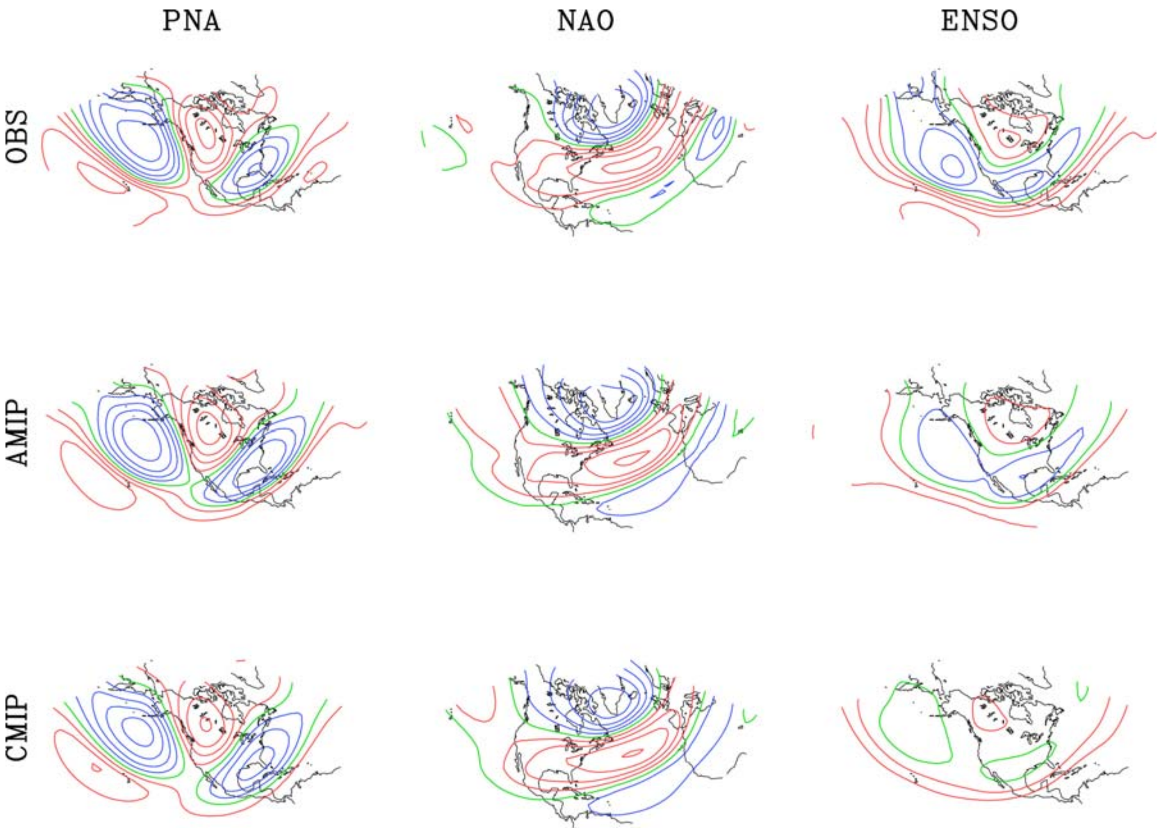

Box Figure B.3-1 Temporal correlation between winter season (December, January, February) 500 hPa geopotential heights and indices of the leading patterns of Northern Hemisphere climate variability: Pacific-North American (PNA, left), North Atlantic Oscillation (middle), and El Niño/Southern Oscillation (ENSO, right) circulation patterns. The ENSO index is based on equatorial Pacific SSTs averaged 170°W-120°W, 5°N-5°S, and the PNA and NAO indices based on averaging heights within centers of maximum observed height variability following Wallace and Gutzler (1981). Assessment period is 1951 to 2006: observations based on reanalysis data (top), simulations based on atmospheric climate models forced by observed specified sea surface temperature variability (middle), and coupled ocean-atmosphere models forced by observed greenhouse gas, aerosol, solar and volcanic variability (bottom). AMIP comprised of 2 models and 33 total simulations. CMIP comprised of 19 models and 19 total simulations. Positive (negative) correlations in red (blue) contours.

***********END BOX 3.1 *****************

Observations of atmospheric circulation patterns in the free atmosphere fueled theories of the dynamics of these teleconnections, clarifying the origins for their regional surface impacts (Rossby, 1939). The relevant atmospheric circulations represent fluctuations in the semi-permanent positions of high and low pressure centers, their displacements being induced by a variety of mechanisms including anomalous atmospheric heating (*e.g.*, due to changes in tropical rainfall patterns), changes in wind flow over mountains, the movement and development of weather systems (*e.g.*, along their storm tracks across the oceans), and other processes (Wallace and Guzzler, 1981; Horel and Wallace, 1981; see Glantz *et al.*, 1991 for a review of the various mechanisms linking worldwide climate anomalies). The PNA and NAO patterns are now recognized as representing preferred structures of extratropical climate variations that are readily triggered by internal atmospheric mechanisms and also by surface boundary forcing, especially from ocean sea surface temperatures (Hoskins and Karoly, 1981; Horel and Wallace, 1981; Simmons *et al.*, 1983).

As indicated in Chapter 2, these and other teleconnection patterns are readily identifiable in the monthly and seasonal averages of atmospheric circulation anomalies in the free atmosphere using reanalysis data. Reanalysis data has also been instrumental in understanding the causes of teleconnection patterns and their North American surface climate impact (Feldstein 2000, 2002; Thompson and Wallace, 1998, 2000a,b). The ability to assess the relationships between teleconnections and their surface impacts provides an important foundation for attribution - North America climate variations are often due to particular atmospheric circulation patterns that connect climate anomalies over distance regions of the globe. Such a connection is illustrated schematically in Figure 3.1.

ii) Attribution to surface boundary forcing

In some situations, teleconnections including those described above are a forced response to anomalous conditions at the Earth's surface. Under such circumstances higher order attribution statements that go beyond the statement of how recurrent features of the atmospheric circulation affect North American surface climate are feasible, and provide an explanation for the cause for the circulation itself.

A particular example is the atmospheric response to tropical Pacific sea surface temperature anomalies, which takes the form of a PNA-like pattern having significant impacts on North American climate especially in the winter and spring seasons. It should be noted, however, that other surface forcings, such as related to sea ice and soil moisture conditions, can also cause appreciable climate anomalies, though their influence is more local and does not usually involve teleconnections.

Jacob Bjerknes (1966, 1969) demonstrated that a surface pressure sea-saw between the western and eastern tropical Pacific (now known as the Southern Oscillation) was linked with the occurrence of anomalous equatorial Pacific SST anomalies referred to as El Niño. This so-called El Niño-Southern Oscillation (ENSO) phenomenon was discovered to be an important source for year-to-year North American climate variation, with recent examples being the strong El Niño events of 1982 to 1983 and 1997 to 1998 whose major meteorological consequences over North America included flooding and storm damage over a wide portion of the western and southern United States and unusually warm winter temperatures over the northern United States (Rasmusson and Wallace, 1983). The cold phase of the cycle, referred to by La Niña, also has major impacts on North America, in particular an enhanced drought risk across the southern and western United States (Ropelewski and Halpert, 1986; Cole *et al.*, 2002)

The impacts of El Niño on North American climate have been extensively documented using both historical data and with sensitivity experiments using atmospheric climate models forced with specified SST conditions observed during El Niño (see review by Trenberth *et al.*, 1998). Figure 3.2 illustrates the observed wintertime tropospheric circulation pattern during El Niño events of the last half century based on reanalysis data, and the associated North American surface signatures in temperature and precipitation. Reanalysis data is of sufficient fidelity to distinguish between the characteristic circulation pattern of the PNA (Figure 2.8) and that induced by El Niño - the latter having more widespread high pressure over Canada. Surface temperature features consist more of a north-south juxtaposition of warm-cold over North America during El Niño, as compared to the west-east structure associated with the PNA. The capacity to observe such distinctions is vital when conducting attribution because particular climate signatures indicate different candidate causes.

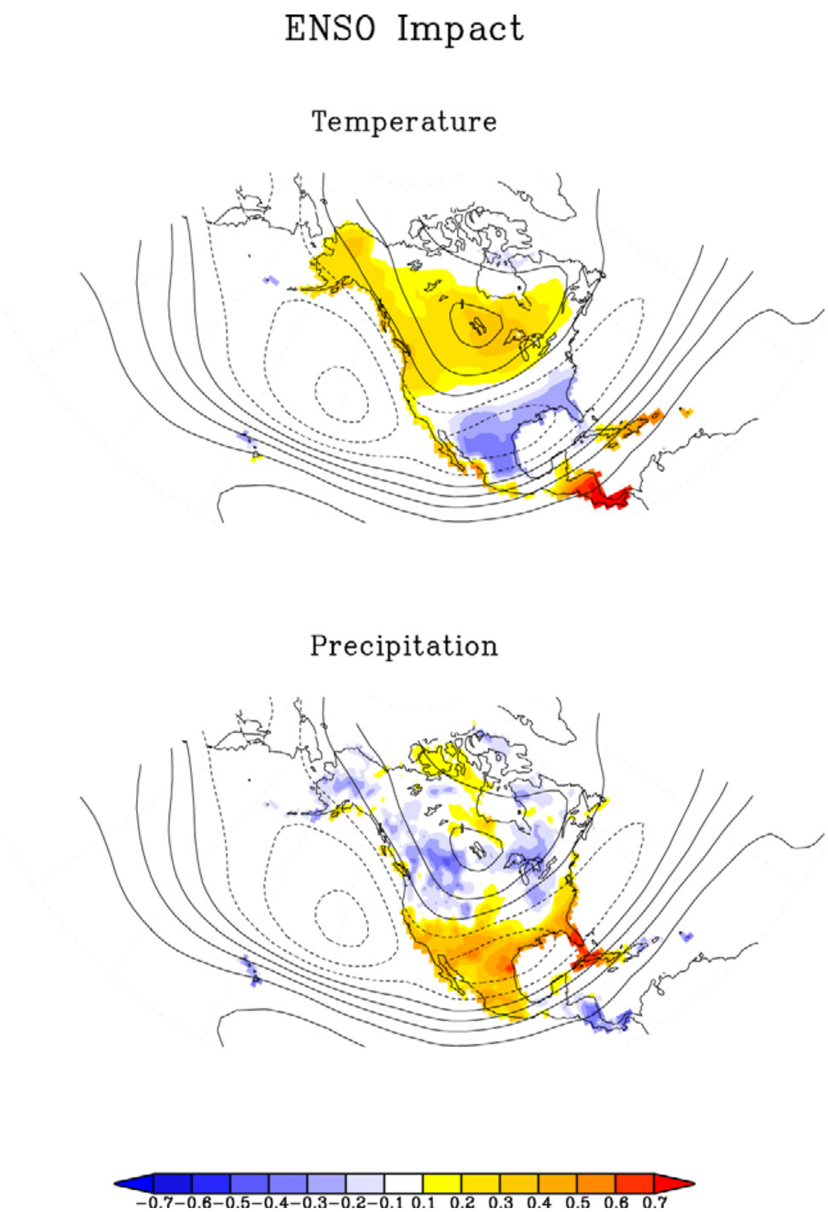

Figure 3.2 The correlation between an SST index of ENSO and 500 mb height field (contours). The shading indicates the correlations between ENSO index and the surface temperature (top panel) and the precipitation (bottom panel). The 500mb height is from the NCEP/NCAR R1 reanalysis. The surface temperature and precipitation are from independent observational data sets. The correlations are based on seasonal mean winter (December-January-February) data for the period 1951 to 2006. The contours with negative correlation are dashed.

The use of climate models subjected to specified SSTs has been essential for elucidating the role of oceans in climate, and such tools are now extensively employed in seasonal climate forecast practices. The atmospheric models are often subjected to realistic globally complete, monthly evolving SSTs (so-called AMIP experiments (Atmospheric Model Intercomparison Project; Gates, 1992)) or to regionally confined idealized SST anomalies in order to explore specific cause-effect relations. These same models have also been used to assess the role of sea ice and soil moisture conditions on climate. The process of forcing a climate model is discussed further in Box 3.2.

BOX 3.2 Forcing a Climate Model

The term "forcing" as used in Chapter 3 refers to a process for subjecting a climate model to a specified influence, often with the intention to probe cause-effect relationships. The imposed conditions could be "fixed" in time, such as a might be used to represent a sudden emission of aerosols by volcanic activity. It may be "time evolving" such as by specifying the history of sea surface temperature variations in an atmospheric model. The purpose of forcing a model is to study the Earth system response, and the degrees of freedom sensitivity of that response to both the model and the forcing employed. The schematic of the climate system helps to better understand the forcings used in various models of Chapter 3.

For atmospheric model simulations used in this SAP, the forcing consists of specified monthly evolving global sea surface temperatures during 1951 to 2006. By so restricting the lower boundary condition of the simulations, the response of unconstrained features of the climate system can be probed. In this SAP, the atmosphere and land surface are free to respond. Included in the former are the atmospheric hydrologic cycle involving clouds, precipitation, water vapor, temperature, and free atmospheric circulation. Included in the latter is soil moisture and snow cover, and changes in these can further feedback upon the atmosphere. Sea ice has been specified to climatological conditions in the simulations of this report, as has the chemical composition of the atmosphere including greenhouse gases, aerosols, and solar output.

For coupled ocean-atmosphere model simulations used in this SAP, the forcing consists of specified variations in atmospheric chemical composition (*e.g,*, carbon dioxide, methane, nitrous oxide), solar radiation, volcanic and anthropogenic aerosols. These are estimated from observations during 1951 to 2000, and then based upon a emissions scenario for 2001 to 2006. The atmosphere, land surface, ocean, and sea ice are free to respond to these specified conditions. The atmospheric response to those external forcings could result from the altered radiative forcing directly, though interactions and feedbacks involving the responses of the lower boundary conditions (*e.g.*, oceans and cryosphere) are often of leading importance. For instance, much of the high-latitude amplification of surface air temperature warming due to greenhouse gas emissions is believed to result from such sea ice and snow cover feedback processes. Neither the coupled ocean-atmospheric models nor the atmospheric models used in this SAP include changes in land surface, vegetation, or ecosystems. Nor does the oceanic response in the coupled models include changes in biogeochemistry.

Multiple realizations of the climate models subjected to the same forcings are required in order to effectively separate the climate model's response from low-frequency climate variability. Ensemble methods are therefore used in Chapter 3. In the case of the atmospheric models, 33 total simulations (derived from two different models) forced as discussed above are studied. In the case of the coupled ocean-atmosphere models, 41 total simulations (derived from 19 different models) forced as discussed above are studied.

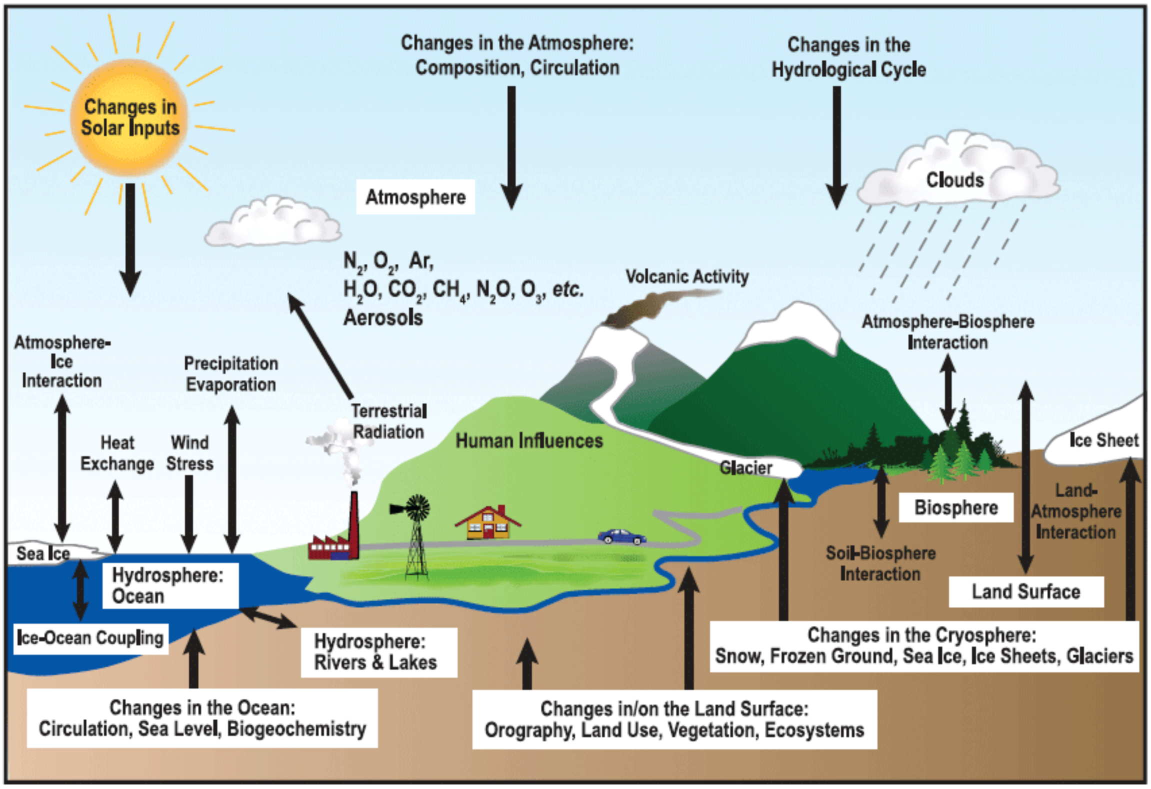

Box Figure 3.2-1 Schematic view of the components of the climate system, their processes and interactions (from "Climate Change 2007: The Physical Science Basis"; IPCC, 2007a).

******** END BOX 3.2 *************

iii) Attribution to external forcing

Explaining the origins for the surface boundary conditions themselves is another stage in attribution. El Niño, for example, is a known internal variation of the coupled ocean-atmosphere. On the other hand, a warming trend of ocean SST, as seen in recent decades over the tropical warm pool of the Indian and west Pacific Oceans, is recognized to result in part from changes in greenhouse gas forcing (Santer *et al.*, 2006; Knutson *et al.*, 2006). Figure 3.1 highlights the very different character of time variations in SSTs over the east and west tropical Pacific that captures different processes occurring in those regions. The climate effects of recent warm-pool warming on North American climate might thus be judged to be of external origins to the ocean-atmosphere system, tied in part to changes in the atmosphere's chemical composition.

The third link in the attribution chain thus involves attribution of observed climate conditions to external forcing. The external forcing could be natural, for instance originating from volcanic aerosol effects or solar fluctuations. Or, the external forcing could be anthropogenic resulting from human activities. As discussed extensively in the IPCC reports, the attribution of climate conditions to external driving can be done directly by specifying the natural and anthropogenic forcings within coupled ocean-atmosphere-land models. An indirect approach can also be employed to attribute a climate conditions to external forcing. An example would be probing the response of an atmospheric model to SST conditions believed to have been externally forced (Hoerling *et al.*, 2004). Note, however, that if an indirect chain is used, it can only be *qualitatively* determined that external forcing contributed to the event - an accurate *quantification* of the magnitude of the impact by external forcing can only be determined in a direct approach.

The tool used for attribution of external forcing, either to test the signal due to anthropogenic greenhouse gas, aerosol changes or land use changes, or natural external forcing due to volcanic and solar forcing, involves coupled ocean-atmosphere-land models forced by observed external forcing variations. As illustrated in Figure 3.1, this methodology has been widely used in the IPCC reports to date. Several studies have used reanalysis data to first detect change in atmospheric circulation, and then test with models whether such change resulted from human influences (Chapter 2 also discusses the use of reanalysis data in establishing the suitability of climate models used for attribution). For instance, a trend in wintertime sea level pressure has been observed and confirmed in reanalysis data that resembles the positive polarity of the NAO, and greenhouse gas and sulphate aerosol changes due to human activities have been implicated as a contributing factor (Gillett *et al.*, 2003; Figure 3.7). Reanalysis data have been used to detect an increase in the height of the tropopause - a boundary separating the troposphere and stratosphere, and modeling results have established human induced changes in stratospheric ozone and greenhouse gases as the primary cause (Santer *et al.*, 2003).

3.1.2.2 Fingerprinting

Many studies use climate models to predict the expected pattern of response to a forcing, referred to as "fingerprints" in the classic climate change literature, or more generally referred to as the "signal" (Mitchell *et al.*, 2001; IDAG, 2005; Hegerl *et al.*, 2007). The spatial and temporal scales used to analyse climate conditions are typically chosen so as to focus on the spatial-temporal scale of the signal itself, filtering out as much structure that is believed to be unrelated to forcing. For example, it is expected that greenhouse gas forcing would cause a large-scale pattern of warming that evolves slowly over time, and thus scientists often smooth data to remove small-scale variations in both time and space. On the other hand, it is expected that El Niño-related SST forcing yields a regionally focused pattern over the Pacific North American sector, having several nodal positions separating regions of opposite signed signal, and thus large-spatial scale smoothing is inappropriate. Furthermore, to ensure that a robust signal has been derived from climate models, individual realizations of an ensemble - in which each member has been identically forced - are averaged. Ensemble methods thus are essential in separating the model's forced signal from its internal variability so as to minimize the confounding of signal and noise.

The consistency between an observed climate condition and the estimated response to a hypothesised key forcing is determined by (1) estimating the amplitude of the expected fingerprint empirically from observations, (2) assessing whether this estimate is statistically consistent with the expected amplitude derived from forced model experiments, and then (3) inquiring whether the fingerprint related to the key forcing is distinguishable from that due to other forcings. The capability to do so also depends on the amplitude of the expected fingerprint relative to the noise resulting from unforced climatic fluctuations.

In order to separate the contribution by different forcings and investigate if other combinations of forcing can also explain an observed event, the simultaneous effect of multiple forcings are also examined, typically using a multiple regression of observations onto several fingerprints representing climate responses to each forcing that, ideally, are clearly distinct from each other (Hasselmann, 1979; 1997; Allen and Tett, 1999; IDAG, 2005; Hegerl *et al.*, 2007). Examples of this are the known unique sign and global patterns of temperature response to increased anthropogenic sulphate aerosols versus increased carbon dioxide. A further example is the known different spatial patterns of atmospheric circulation response over the North American region to SST forcing from the Indian Ocean compared to the tropical east Pacific ocean (Simmons *et al.*, 1983; Barsugli and Sardeshmukh, 2002). If the responses to these key forcings can be distinguished, and if rescaled combinations of the responses to other forcings do not sufficiently explain the observed change, then the evidence for a causal connection is substantially increased. Thus, the attribution of recent large-scale warming to greenhouse gas forcing becomes more reliable if the influences of other natural external forcings, such as solar variability, are explicitly accounted for in the analysis.

The confidence in attribution will thus be subject to the uncertainty in the fingerprints both estimated empirically from observations and numerically from forced model simulations. The effects of forcing uncertainties, which can be considerable for some forcing agents such as solar and aerosol, also remain difficult to evaluate despite recent advances in research.

Satellite and in situ observations during the reanalysis period yield reliable estimates of SST conditions over the world oceans, thus increasing the reliability of attribution based on SST forced atmospheric models. Estimates of other land surface conditions including soil moisture and snow cover are less reliable. Attribution results based on several models or several forcing histories also provide information on the effects of model and forcing uncertainty. Likewise, empirical estimates of fingerprints derived from various observational datasets provide information of uncertainty.

Finally, attribution requires knowledge of the internal climate variability on the time scales considered - the so-called "noise" within the system against which the signal is to be detected and explained. The residual variability that remains in instrumental observations of the Earth System after the estimated effects of external forcing (greenhouse gases and aerosols) have been removed is sometimes used to estimate internal variability of the coupled system. However, these observational estimates are uncertain because the instrumental records are too short to give a well-constrained estimate of internal variability, and because of uncertainties in the forcings and the corresponding estimates of responses. Thus, internal climate variability is usually estimated from long control simulations from climate models. Subsequently, an assessment is usually made of the consistency between the residual variability referred to above and the model-based estimates of internal variability; and analyses that yield implausibly large residuals are not considered credible. Confidence is further increased by comparisons between variability in observations and climate model data, by the ability of models to simulate modes of climate variability, and by comparisons between proxy reconstructions and climate simulations of the last millennium.

The following sections of this Chapter summarize current understanding on the causes of detected changes in North American climate. Sections 2 through 5 will illustrate uses of reanalysis data in combination with surface temperature and precipitation measurements to examine the nature of North American climate variations, and compare with forced model experiments that test attributable cause. In addition, the section also assesses the state of understanding of causes for other variations of significance in North America's recent climate history, focusing especially on major North American droughts. In the mid-1930s Congress requested that the Weather Bureau explain the causes for the 1930s Dust Bowl drought, with a key concern being to understand whether this event was more likely a multi-year occurrence or a harbinger of longer-term change. As 70 years earlier, fundamental challenges in attribution science today are to distinguish quasi-cyclical variations from long-term trends, and natural from anthropogenic origins.

3.2 WHAT IS THE PRESENT UNDERSTANDING OF THE CAUSES FOR THE NORTH AMERICAN CLIMATE TRENDS IN ANNUAL TEMPERATURE AND PRECIPITATION DURING THE REANALYSIS PERIOD?

3.2.1 Summary of IPCC Fourth Assessment Report

Among the major findings of the IPCC Fourth Assessment (IPCC, 2007b) is that "it is *likely* that there has been significant anthropogenic warming over the past 50 years averaged over each continent except Antarctica". This conclusion was based on recent fingerprint-based studies on the attribution of annual surface temperature involving space-time patterns of temperature variations and trends. Model studies using only natural external forcings were shown to be unable to explain the warming over North America in recent decades, and only experiments including the effects of anthropogenic forcings reproduced the recent upward trend. The IPCC report also stated that for precipitation there was low confidence in detecting and attributing a change, especially at the regional scale.

This assessment focuses in greater detail on North American temperature and precipitation variability during the period 1951 to 2006.

BOX 3.3 Choosing the Assessment Period

This SAP report was asked to examine the strengths and limitations of current reanalysis products, and to assess capabilities for attributing the causes for climate variations and trends during the reanalysis period. This assessment's scope is thus bounded by the reanalysis record (1948 to present). An important further consideration is the availability of sufficient, quality controlled surface observations to define key climate variations accurately. For precipitation, a high quality global gridded analysis is available beginning in 1951, thereby further focusing the attribution to 1951 to 2006.

It is reasonable to ask whether such a 56-year assessment period adequately samples the principal features of climate variability. Does it, for example, capture the major climate events that may be of particular concern to decision makers, such as droughts? Is it a sufficiently long period to permit the distinction between fluctuations in climate conditions that are transient, or are cyclical, from trends that are related to a changing climate? How well do scientists understand the climate conditions prior to 1951, and what insight does analysis of those provide toward explaining post-1950 conditions? These are all important questions to bear in mind when reading this Report, and especially if one wishes to generalize conclusions about the nature of and causes for climate conditions during 1951 to 2006 to earlier or future periods.

As a case in point, the U.S. surface temperature record since 1895 is remarkable for its multi-decadal fluctuations (top panel). A simple linear trend fails to describe all features of U.S. climate variations, and furthermore, a trend analysis for any subset of this 112-year period may be problematic since it may capture merely a segment of a transient oscillation. The decade of the 1930s and 40s was a particularly warm period, one only recently eclipsed. The U.S. has thus undergone two major swings between cold epochs (beginning in the 1890s and 1960s) and warm epochs (1930s and 2000s). It is reasonable to wonder whether the current warmth will also revert to colder conditions in coming decades akin to events following the 1930s peak, and attribution science is therefore important for determine whether the same factors are responsible for both warmings or not. Some studies reveal that the earlier warming may have resulted from a combination of anthropogenic forcing and an unusually large natural multi-decadal fluctuation of climate (Delworth and Knutson, 2000). Other work indicates a contribution to the early 20th century warming by natural forcing of climate, such as changes in solar radiation or volcanism (*e.g.*, Tett *et al.*, 2002; Hegerl *et al.*, 2006). The 1930s warming was part of a warming focused mainly in the northern high latitudes, a pattern reminiscent of an increase in poleward ocean heat transport (Rind and Chandler; 1991), which can itself be looked upon as due to "natural variability". In contrast, the recent warming is part of a global increase in temperatures, and the IPCC Fourth Assessment Report chapter 9 states that it is likely that a significant part of warming over the past 50 years over North America may be anthropogenically related, thus contrasting causes of the warming that occurred in this period from that in 1930s. The physical processes related to this recent warming are further examined in Chapter 3.

The year 1934 continues to stand out as one the warmest years in the U.S. 112-year record, while averaged over the entire globe, 1934 is considerably cooler than the recent decade. The U.S. warmth of the 1930s coincided with the Dust Bowl (lower panel), and drought conditions likely played a major role in driving up land surface temperatures. Prior studies suggest that the low precipitation during the Dust Bowl was related in part to sea surface temperature conditions over the tropical oceans (Schubert *et al.*, 2004a,b; Seager *et al.*, 2005). Our understanding of severe U.S. droughts that have occurred during the reanalysis period as described in Chapter 3 builds upon such studies of the Dust Bowl.

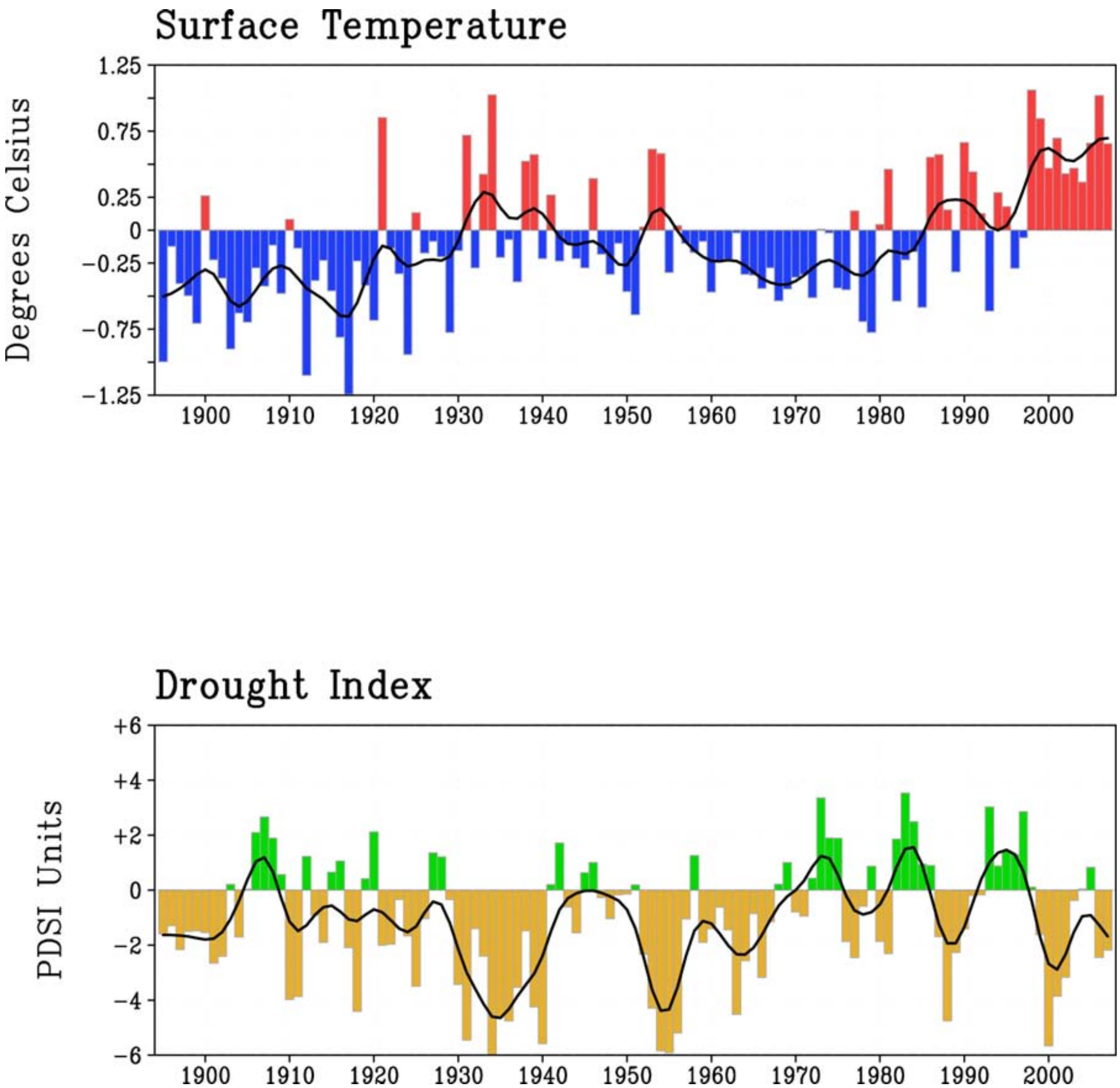

Box Figure 3.3-1 Time series of U.S. area averaged and annually averaged surface air temperature (top) and the Palmer Drought Severity Index (bottom) for the period 1895 to 2006. The smooth curve is a result of applying a 9-point Gaussian filter to the annual values in order to highlight lower frequency variations. Data source is the contiguous U.S. climate division data of NOAA's National Climatic Data Center.

********** END BOX 3.3 ***************

The origins for the North American fluctuations is assessed by examining the impacts on North America from time evolving sea surface conditions (including ENSO and decadal ocean variations), in addition to time evolving anthropogenic effects. The use of reanalysis data to aid in the attribution of surface climate conditions is illustrated.

3.2.2 North American Annual Mean Temperature

3.2.2.1 Description of the observed variability

Seven of the warmest ten years since 1951 have occurred in the last decade (1997 to 2006).

The manner in which North American annual temperatures have risen since 1951, however, has been neither smooth nor consistent; its trajectory has been punctuated by occasional peaks and valleys (Figure 3.3, top). The coldest year since 1951 occurred in 1972, and below average annual temperatures occurred as recently as 1996. Explanations for such substantial variability is no less important than explanations for the warming trend.

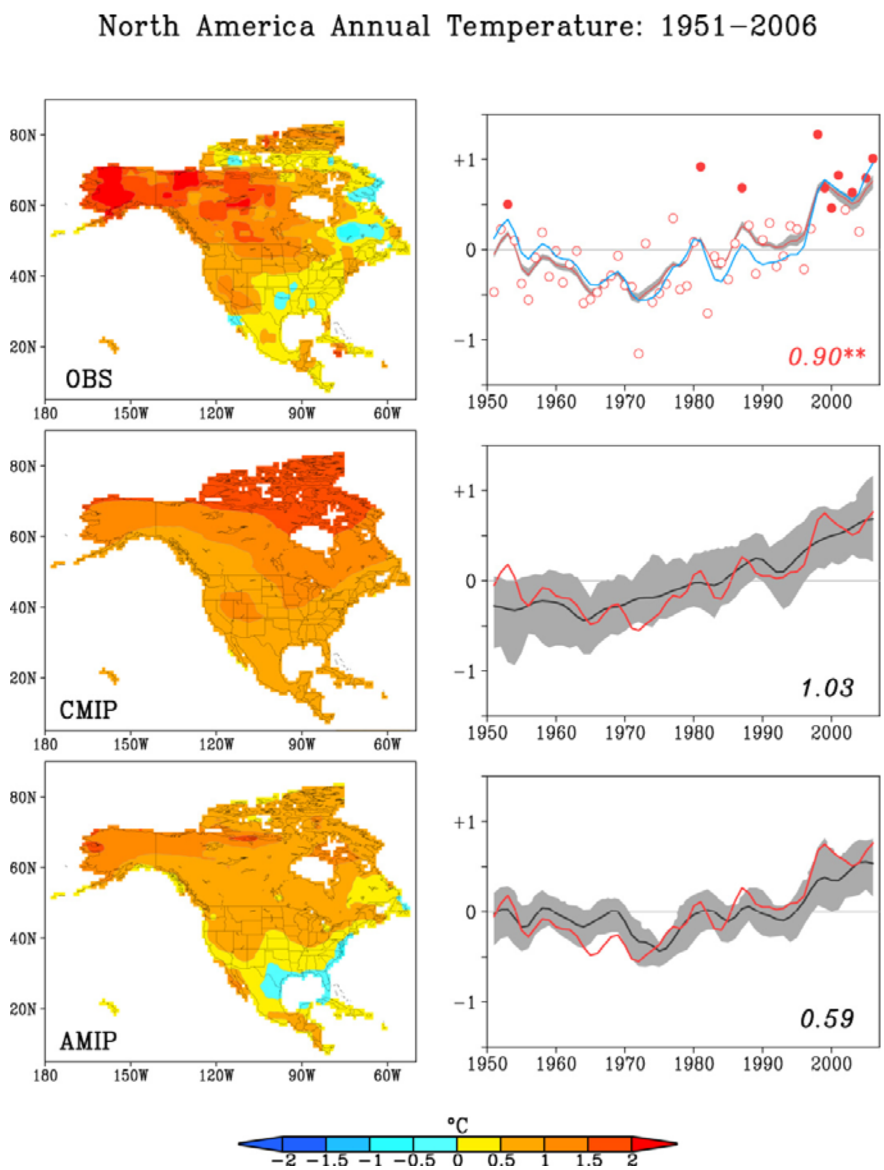

Figure 3.3 The 1951 to 2006 trend in annually averaged North American surface temperature from observations (top), CMIP simulations (middle), AMIP simulations (bottom). Maps (left side) show the linear trend in annual temperatures for 1951 to 2006 (units, °C/56 years). Time series (right side) show the annual values from 1951 to 2006 of surface temperatures averaged over the whole of North America. Curves are smoothed annual values using a 5-point Gaussian filter, based on the average of four gridded surface observational analyses, and the ensemble mean of climate simulations. Unsmoothed annual observed temperatures shown by red circles, with filled circles denoting the ten warmest years since 1951. Plotted values are the total 56-year change (°C), with the double asterisks denoting very high confidence that an observed change was detected. For observations, the gray band denotes the range among four surface temperature analyses. The blue curve is the NCEP/NCAR reanalysis surface temperature time series. For simulations, the gray band contains the 5-95% occurrence of individual model simulations.

Virtually all of the warming averaged over North America since 1951 has occurred after 1970. It is noteworthy that North American temperatures cooled during the period 1951 through the early 1970s. In the 1970s, the public and policy makers were keenly interested to know the reason for this cooling, with concerns about food production and societal disruptions. They turned to the meteorological community for expert assessment. Unfortunately, climate science was at its infancy in the 1970s and attribution was considerably more art than science. The essential tools for performing rigorous attribution such as global climate models were not yet available, nor was much known then about the range of historical climate variations such as has been subsequently revealed by paleoclimate studies. A consistent climate analysis of the historical instrumental record that included descriptions of the free atmosphere was also unavailable.

Barring an explanation of the cause for the cooling, and with no comprehensive climate models available, some scientists responded to the public inquiries on what would happen next by merely extrapolating recent trends thereby portraying enhanced risk for a cooling world (Kukla and Mathews, 1972; Newsweek, 1975). Others suggested, in the mid-1970s that we might be at the brink of a pronounced global warming, arguing that internal variations of the climate were then masking an anthropogenic signal (Broecker, 1975). The 1975 National Academy of Sciences report on (NRC, 1975) understanding climate change emphasized the fragmentary state of knowledge of the mechanisms causing climate variations and change, and posed the question whether we would be able to recognize the first phases of a truly significant climate change when it does occur (NRC, 1975). Perhaps the single most important attribution challenge today regarding the time series of Figure 3.3 is whether the reversal of the cooling trend after 1975 represents such a change, and one for which a causal explanation can be offered.

There is very high confidence in the detection that the observed temperature trend reversed after the early 1970s. The shaded area in Figure 3.3 (top) illustrates the spread among four different analyses of surface measurements (see Table 3.2 for descriptions of these data), and the analysis uncertainty as revealed by their range is small compared to the amplitude of the trend and principal variations. Also shown is the surface temperature time series derived from the reanalysis. Despite the fact that the assimilating model used in producing the NCEP/NCAR reanalysis does not ingest surface temperature observations (Kalnay *et al.*, 1996), the agreement with the in situ observations is strong. This indicates that the surface temperature averaged over the large domain of North America is constrained by and is consistent with climate conditions in the free atmosphere. Both for the emergent warming trend in the 1970s, and for the variations about it, this excellent agreement among time series based on different observational data sets and the reanalysis increases confidence that they are not artifacts of analysis procedure.

The total 1951 to 2006 change in observed North American annual surface temperatures is +0.90°C +/- 0.1°C, with the uncertainty estimated from the range between trends derived from four different observational analyses. Has a *significant* North American warming been detected? Answers to this question require knowledge of the plausible range in 56-year trends that can occur naturally in the absence of any time varying anthropogenic forcing. The brevity of the observational record does not permit such an assessment, but an analysis of such variations in coupled model simulations that exclude variations in anthropogenic forcing provides an indirect estimate. To estimate the confidence that a change in North American temperatures has been detected, a non-parametric test has been applied that estimates the range of 56-year trends attributable to natural variability alone (see Appendix 3.A for methodological details). A diagnosis of 56-year trends from the suite of "naturally forced" CMIP runs is performed, from which a sample of 76 such trends were generated for annual North American averaged surface temperatures. Of these 76 "trends estimates" consistent with natural variability, no single estimate was found to generate a 56-year trend as large as observed.

It is thus *very likely* that a change in North American annual mean surface temperature has been detected. That assessment weighs the realization that the climate models have biases that can affect statistics of their simulated internal climate variability.

3.2.2.1 Attribution of the observed variations

3.2.2.1.1 External Forcing

The Fourth Assessment Report of the IPCC provided strong attribution evidence for a significant anthropogenic warming of North American surface temperatures. Figure 3.4 is drawn from that report, and compares continental-averaged surface temperature changes observed with those simulated using the CMIP coupled models having natural and anthropogenic forcing. It is clear that only experiments using time varying observed

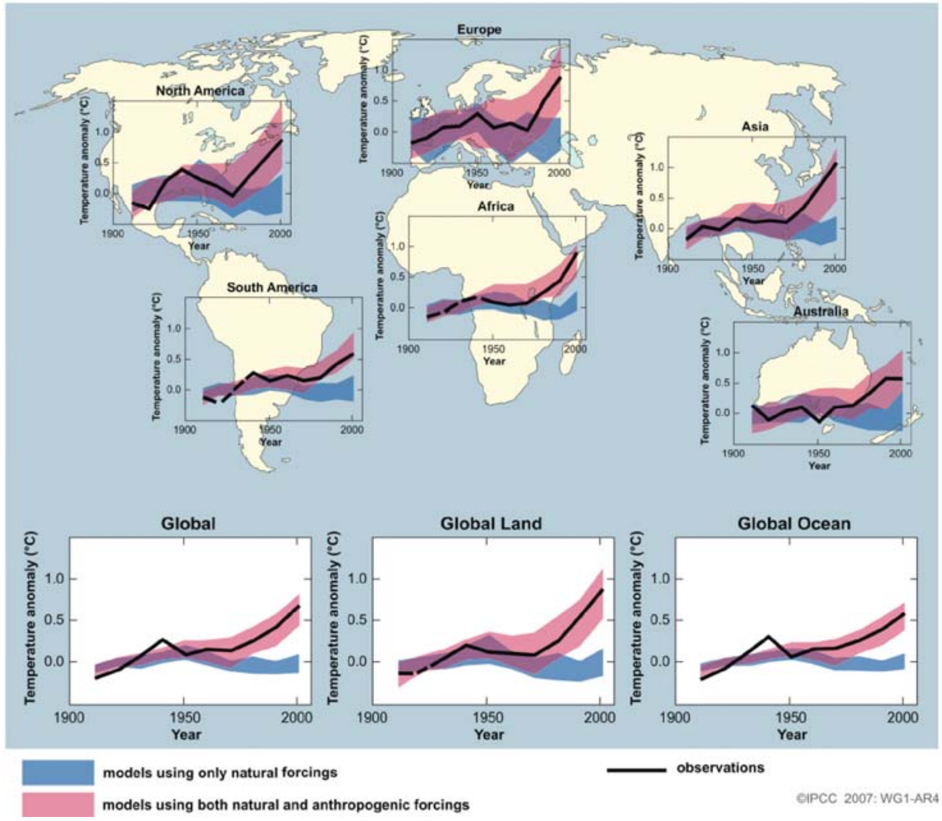

Figure 3.4 Temperature changes relative to the corresponding average for 1901 to 1950 (°C) from decade to decade from 1906 to 2005 over the Earth's continents, as well as the entire globe, global land area and the global ocean (lower graphs). The black line indicates observed temperature change, while the colored bands show the combined range covered by 90% of recent model simulations. Red indicates simulations that include natural and human factors, while blue indicates simulations that include only natural factors. Dashed black lines indicate decades and continental regions for which there are substantially fewer observations. Detailed descriptions of this figure and the methodology used in its production are given in Hegerl (2007).

anthropogenic forcing explain the warming in recent decades. Numerous detection and attribution studies, as reviewed by Hegerl *et al.* (2007), have shown that the observed warming of North American surface temperature since 1950 cannot be explained by natural climate variations alone and is consistent with the response to anthropogenic climate forcing, particularly increases in greenhouse gases (Karoly *et al.*, 2003; Stott, 2003; Zwiers and Zhang, 2003; Knutson *et al.*, 2006; Zhang *et al.*, 2006). The suitability of these coupled climate models for attribution is indicated by the fact that they are able to simulate variability on decadal time scales and longer that is consistent with reanalysis data of the free atmosphere and surface observations over North America (Hegerl *et al.*, 2007, Figure 9.8).

A more detailed examination of the anthropogenic influence on North America is provided in Figure 3.3 (middle) that shows the spatial map of the 1951 to 2006 simulated surface temperature trend, in addition to the time series. There are several key agreements between the CMIP simulations and observations that support the argument for an anthropogenic effect. First, both indicate the bulk of warming to have occurred in the past 30 years. The emergence of North American warming after 1970 is thus *likely* the result of the region's response to anthropogenic forcing. Second, the total 1951 to 2006 change in observed North American annual surface temperatures of +0.90°C compares well to the simulated ensemble averaged warming of +1.03°C. Whereas the observed 56-year trend was shown in the previous subsection to be inconsistent with the population of trends drawn from a state of natural climate variability, the observed warming is found to be consistent with the population of trends drawn from a state that includes observed changes in the anthropogenic forcing during 1951 to 2006.

Further, the observed low frequency variations of annual temperature fall within the 5-95% uncertainty range of the individual model simulations. All CMIP runs that include anthropogenic forcing produce a North American warming during 1951 to 2006. For some simulations, the trend is less than that observed and for some it is greater than that observed. This range results from both the uncertainty in anthropogenic signals (owing to different sensitivities of the 19 models) and the effects of model internal variability (owing to sensitivity of individual runs of the same models to natural coupled-ocean atmosphere fluctuations).

Each of the 41 anthropogenically forced simulations produce a 56-year North American warming (1951 to 2006) that is greater than half of the observed warming. Our assessment of the origin for the observed North American surface temperature trend is that more than half of the warming during 1951 to 2006 is *likely* the result of anthropogenic influences. It is *exceptionally unlikely* that the observed warming has resulted from natural variability alone because there is a clear separation between the ensembles of climate model simulations that include only natural forcings and those that contain both anthropogenic and natural forcings (Hegerl *et al.*, 2007). These confidence statements reflect the uncertainty of the role played by model biases in their sensitivity to external forcing, and also the unknown impact of biases on the range of their unforced natural variability.

BOX 3.4 Use of Expert Assessment

The use of expert assessment is a necessary element in attribution as a means to treat the complexities that generate uncertainties. Expert assessment is used to define levels of confidence, and the terms used in this Report (see Preface) follow those of the IPCC Fourth Assessment Report. The attribution statements used in Chapter 3 of this SAP also employ probabilistic language (for example, "virtually certain") to indicate a likelihood of occurrence.

To appreciate the need for expert assessment, it is useful to highlight the sources of uncertainty that arise in seeking the cause for climate conditions. The scientific process of attribution involves various tools to probe cause-effect relationships such as historical observations, climate system models, and mechanistic theoretical models. Despite ongoing improvements in reanalysis and models, these and other tools have inherent biases rendering explanations of the cause for a climate condition uncertain. Uncertainty can arise in determining a forced signal (*i.e.*, fingerprint identification). For instance, the aerosol-induced climate signal involves direct radiative effects that require on accurate knowledge of the amount and distribution of aerosols in the atmosphere. These are not well observed quantities, leading to so-called "value uncertainties" (IPCC, 2007a) because the forcing itself is poorly known. The aerosol-induced signal also involves an indirect radiative forcing, the latter depending on cloud properties and water droplet distributions. These cloud radiative interactions are poorly represented in current generation climate models (Kiehl, 1999), contributing to so-called "structural uncertainties" IPCC, 2007a). Even if the forcing is known precisely and the model includes the relevant processes and relationships, the induced signal may be difficult to distinguish from other patterns of climate variability thereby confounding the attribution.

The scientific peer-reviewed literature provides a valuable guide to the author team of Chapter 3 for determining attribution confidence. In addition, new analyses in this SAP are also examined in order to provide additional information. These employ methods and techniques that have been extensively tested and used in the scientific literature. In most cases, new analyses involve observational data and model simulations that have merely updated to include recent years through 2006.

********** END BOX 3.4 ************

Regarding the yearly fluctuations in observed North American temperature, it is evident in Figure 3.3 that these are of greater amplitude than those occurring in the ensemble average of externally forced runs. This is consistent with the fact that the former commingles the effects of internal and external influences while the latter estimates only the time evolving impact of external forcings. Nonetheless, several of these observed fluctuations align well with those in the CMIP data. In particular, the model warming trend is at times punctuated by short periods of cooling, and these episodes coincide with major tropical volcanic eruptions (*e.g.*, Aguang in 1963; Mt. Pinatubo in 1991). Such natural externally forced cooling episodes correspond well with periods of observed cooling, as will be discussed further in Section 3.4.

3.2.2.1.1 Sea Surface Temperature Forcing

The oceans play a major role in climate, not only for determining its mean conditions and seasonal cycle, but also for determining its anomalous conditions including interannual to decadal fluctuations. Section 3.1 discussed modes of anomalous SST variations that impact North America, in particular that associated with ENSO. Figure 3.5 illustrates the temporal variations of SSTs over the global oceans and over various ocean basins during

1951 to 2006. Three characteristic features of the observed SST fluctuations are noteworthy. First, SSTs in the east tropical Pacific (top panel) vary strongly from year to year, as warm events alternate with cold events indicative of the ENSO cycle. Extratropical North Pacific and North Atlantic SSTs have strong year-to-year persistence, with decadal periods of cold conditions followed by decadal periods of warm conditions. Finally, the warm pool of the Indian Ocean-west tropical Pacific, the tropically averaged SSTs, and globally averaged SSTs are dominated by a warming trend. These resemble in many ways the time series of North American surface temperatures including a fairly rapid emergence of warmth after the 1970s.

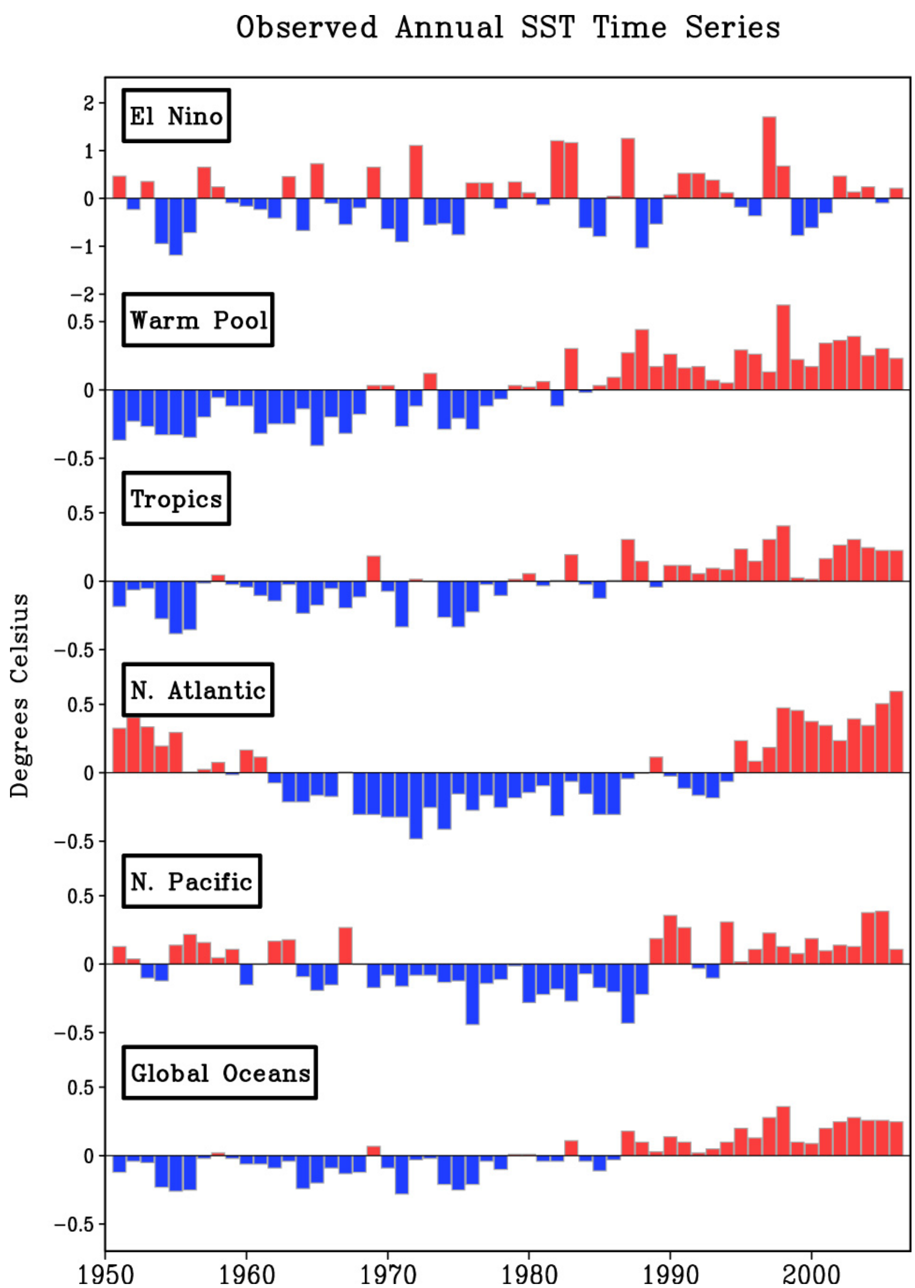

Figure 3.5 Observed annual mean SST time series for 1951 to 2006. The oceanic regions used to compute the indices are 5°N-5°S, 90°W-150°W for El Niño, 10°S-10°N, 60°E-150°E for the warm pool, 30°S-30°N for the tropics, 30°N-60°N for the North Atlantic, 30°N-60°N for the North Pacific, and 40°S-60°N for the global oceans. Data set is the HadiSST monthly gridded fields, and anomalies are calculated relative to a 1951 to 2006 reference.

A common tool for determining the SST effects on climate is atmospheric general circulation models (AGCM) forced with the specified time evolution of the observed

SSTs, in addition to empirical methodologies (see Figure 3.2 for the El Niño impact inferred from reanalysis data, and Box 3.1 for an assessment of model simulated ENSO teleconnections). Such numerical modeling approaches are generally referred to as AMIP simulations (Gates, 1992), and here we adapt that term to refer to model runs spanning the period 1951 to 2006.

Much of the known effect of SSTs has focused on the boreal winter season, a time when El Niño and its North American impacts are at their peak. However, the influence of SSTs on *annual mean* variability over North America is not yet documented in the peer-reviewed literature. Therefore, we present here an expert assessment based on the analysis of two AGCMs (Table 3.1). It is important to note that the AMIP simulations used in this analysis do not include the observed evolution of external forcings, *e.g.*, solar, volcanic aerosols, or anthropogenic greenhouse gases. The specified SSTs may, however, reflect the footprints of such external influences. See Section 3.4 and Figure 3.18 for a discussion of the same SST time series constructed from the CMIP simulations.

North American annual temperature trends, and their temporal evolution, are well replicated in the AMIP simulations (Figure 3.3, bottom). There are several key agreements between the AMIP simulations and observations that support the argument for an SST effect. First, the bulk of the AMIP simulated warming occurs after 1970 as in observations. The time evolution of simulated annual North American surface temperature fluctuations is very realistic, with a temporal correlation of 0.79 between the raw unsmoothed observed and simulated annual values. While slightly greater than the observed versus CMIP agreement of 0.68, much of the positive year-over-year correlation owes to the warming trend. Second, the pattern correlation of 0.87 with the observed trend map highlights the remarkable spatial agreement, and exceeds the 0.79 spatial correlation for the CMIP simulated trend. Several other notable features of the AMIP simulations include the greater warming over western North America and slight cooling over eastern and southern United States regions. The total 1951 to 2006 change in observed North American annual surface temperatures of +0.90°C compares well to the AMIP simulated warming of +0.59°C.

There exists a strong congruence between the AMIP and CMIP simulated North American surface temperature trend patterns and their time evolutions during 1951 to 2006. This comparison of the CMIP and AMIP simulations indicates that a substantial fraction of the area-average anthropogenic warming over North America has *likely* occurred as a consequence of sea surface temperature forcing. The physical processes by which the oceans have led to North American warming is not, however, currently known.

An important attribution challenge is determining which aspects of regional SST variability during 1951 to 2006 have been important in rendering the signals in Figure 3.3. Idealized studies linking regional SST anomalies to atmospheric variability have been conducted (Hoerling *et al.*, 2001; Robertson *et al.*, 2003; Barsugli *et al.*, 2002; Kushnir *et al.*, 2002); however, a comprehensive suite of model simulations to address variability in North American surface temperatures during 1951 to 2006 has yet to be undertaken. Whereas the North American sensitivity to SST forcing from the El Niño region is well understood, less well known is the effect of the progressive tropical-wide SST warming, a condition that has been the major driver of globally averaged SST behavior during the last half century (Figure 3.5). A further question is the effect that recent decadal warming of the North Pacific and North Atlantic Oceans have had on North American climate, either in explaining the spatial inhomogeneity in North American temperature trends, or as a factor in the accelerated pace of North American warming post-1970. Although the desired simulation suite have yet to be conducted, some attribution evidence for regional SST effects can be gleaned empirically from the reanalysis data itself which are capable of describing changes in tropospheric circulation patterns, elements of which are known to have regional SST sources. This will be the subject of further discussion in Section 3.3, where post-1950 observed changes in PNA and NAO circulation patterns are described and their role in North American climate trends is assessed.

3.2.2.1.2 Analysis of Annual Mean Rainfall Variability Over North America

In contrast to temperature, North American precipitation exhibits considerably greater spatial and temporal variability. The annual cycle of precipitation is itself vastly heterogeneous over the continent, with winter maxima along western North America, summertime maxima over Mexico and Central America, and comparatively little amplitude to the seasonal cycle over eastern North America. It is therefore not surprising that the 1951 to 2006 trend in annual precipitation is dominated by regional scale features (Figure 3.6, top). Several of these are discussed further in Section 3.3.

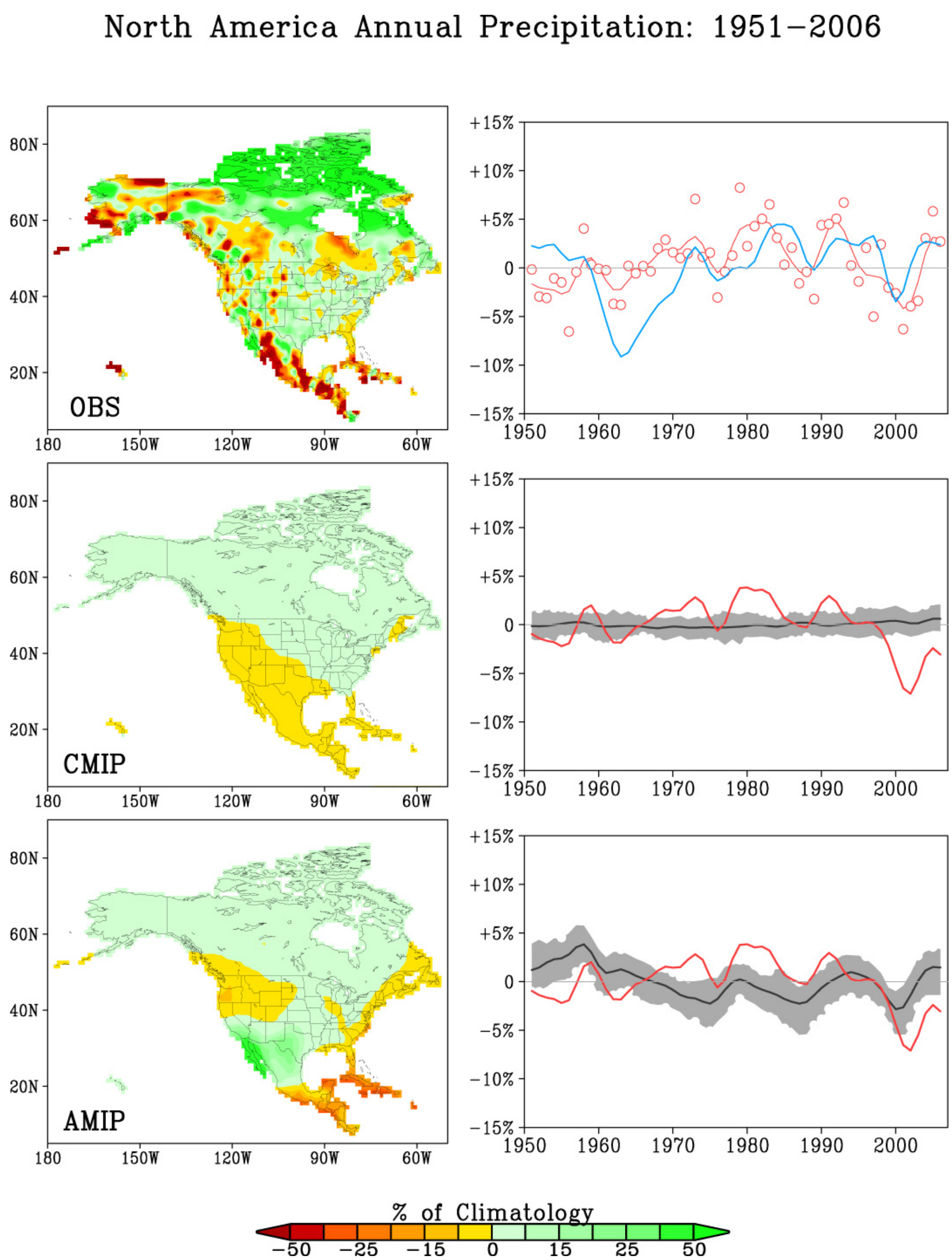

Figure 3.6 The 1951 to 2006 trend in annually averaged North American precipitation from observations (top), CMIP simulations (middle), AMIP simulations (bottom). Maps (left side) show the linear trend in annual precipitations for 1951 to 2006 (units, total 56-year change as % of climatology). Time series (right side) show the annual values from 1951to 2006. Curves are smoothed annual values using a 5-point Gaussian filter, based on the GPCC observational analysis, and the ensemble mean of climate simulations. Unsmoothed annual observed precipitation shown by red circles. The blue curve is the NCEP/NCAR reanalysis precipitation time series. For simulations, the gray band contains the 5-95% occurrence of individual model simulations.

For area-averaged North America as a whole, there is no coherent trend in observed precipitation since 1951. The time series of annual values has varied within 10% of the climatological average, with the most notable feature being the cluster of dry years from the late 1990s to the early 2000s. However, even these annual variations for North American averaged precipitation as a whole are of uncertain physical significance. This is because of the regional focus of precipitation fluctuations, and the considerable cancellation between anomalies of opposite sign when averaging across the continent as is done in Figure 3.6.

Neither externally forced nor SST forced simulations show a significant change in North American-wide precipitation since 1951. In addition, the area averaged annual fluctuations in the simulations are generally within a few percent of climatology (Figure 3.6, middle and bottom panels). The comparison of the observed and CMIP simulated North America precipitation indicates that the anthropogenic signal is small relative to the observed variability on annual and decadal timescales. As a note of caution regarding the suitability of the CMIP models for this particular variable, the time series of low-pass filtered ensemble mean North American precipitation from the individual CMIP simulations also shows almost no decadal variations. Note especially that the recent observed dry anomalies reside well outside the range of all CMIP runs. This suggests that the models may underestimate the observed variability, at least for North American annual and area averages.

A small number of detection and attribution studies of mean precipitation over land have identified a signal due to volcanic aerosol in low frequency variations of precipitation (Gillett *et al.*, 2004; Lambert *et al.*, 2004). Climate models appear to underestimate both the variance of land mean precipitation compared to that observed and the observed changes in response to volcanic eruptions (Gillett *et al.*, 2004; Lambert *et al.*, 2004). Zhang *et al.* (2007) examined the human influence on precipitation trends over land within latitudinal bands during 1950 to 1999, finding evidence for anthropogenic origins for a drying in the subtropics and increased precipitation over sub-polar latitudes, though observed and simulated anthropogenically forced simulations disagreed over much of North America.

The time series of North America precipitation from the AMIP simulations shows better agreement with that observed than the CMIP simulations, including marked negative anomalies over the last decade. This suggests that a part of the observed low frequency variations stems from observed variations of global SST. A connection between ENSO related tropical SST anomalies and rainfall variability over North America has been well documented, particularly for the boreal winter as mentioned earlier, and the recent years of dryness are consistent with the multi-year occurrence of La Niña (Figure 3.5). The influence of tropical-wide SSTs and droughts in the midlatitudes and North America has also been documented in previous studies (Hoerling and Kumar, 2003; Schubert *et al.*, 2004; Lau *et al.*, 2006; Seager *et al.*, 2005; Herweijer *et al.*, 2006). Such causal links do provide an explanation for the success of AMIP integrations in simulating and explaining some aspects of the observed variability in North American area-averaged precipitation, though it is again important to recognize the limited value of such an area average for describing moisture related climate variations.

3.3 WHAT IS THE PRESENT UNDERSTANDING OF THE CAUSES FOR THE SEASONAL AND REGIONAL DIFFERENCES IN UNITED STATES TEMPERATURE AND PRECIPITATION TRENDS DURING THE REANALYSIS PERIOD?

3.3.1 Introduction

As noted in the recent IPCC Fourth Assessment report, identification of anthropogenic causes for variations or trends in temperature and precipitation at regional and seasonal scales is more difficult than for larger area and annual averages. The primary reason is that internal climate variability is greater at these scales - averaging over larger space-time scales reduces the magnitude of the internal climate variations (Hegerl *et al.*, 2007). Early idealized studies (Stott and Tett, 1998) indicated that the spatial variations of surface temperature changes due to changes in external forcing, such as greenhouse gas related, would be detectable only at scales of order 5000 km or more. But these signals will be more easily detectable as the magnitude of the expected forced response increases with time, and the IPCC Fourth Assessment report highlights the acceleration of the warming response in recent decades (IPCC, 2007a).

Consistent with increased external forcing in recent decades, several studies (Karoly and Wu, 2005; Knutson *et al.*, 2006; Wu and Karoly, 2007; Hoerling *et al.*, 2007) have shown that the warming trends over the second half of the 20th century at many individual five degree latitude/longitude cells across the globe can now be detected in observations, and further, these are consistent with the modeled response to anthropogenic climate forcing and cannot be explained by internal variability and response to natural external forcing alone. However, there are a number of regions that do not show significant warming, including the southeast United States although modeling results have yet to consider a range of other possible forcing factors that may be more important at regional scales including changes in carbonaceous and biogenic aerosols (IPCC, 2007a), and changes in land use and land cover, which affect both the radiative forcing and the partitioning between sensible heating and evaporation at the land surface (Pielke *et al.*, 2002; McPherson, 2007).

What is the current capability to explain spatial variations and seasonal differences in North American climate trends over the past half-century? Can various heterogeneities in space and time be accounted for by the climate system's sensitivity to time evolving anthropogenic forcing? To what extent can the influences of non-anthropogenic processes be identified? Recent studies have linked some regional and seasonal variations in temperature and precipitation over the United States to variations in SST (*e.g.*, Livezey *et al.*, 1997; Kumar *et al.*, 2001; Hoerling and Kumar 2002; Schubert *et al.*, 2004; Seager *et al.*, 2005). These published results have either focused on annual mean or winter-only conditions, and herein we will assess both the winter and summer origins change over North America, the conterminous United States, and various sub-regions of the United States.

3.3.2 Temperature Trends

3.3.2.1 North America

The observed annually-averaged temperature trends over North America in Figure 3.3 of the previous section show considerable spatial variation, with largest warming over northern and western North America and minimum warming over the southeastern United States. The ensemble-mean model response to anthropogenic and natural forcing since 1951 (CMIP runs in Figure 3.3) shows a more uniform warming pattern, with larger values in higher latitudes and in the interior of the continent. While the spatial correlation of the CMIP simulated 1951 to 2006 North American surface temperature trend with observations is 0.79, that agreement results almost entirely from the agreement in the *area-mean* temperature trend. Upon removing the area-mean warming, a process that highlights the spatial variations, the resulting pattern correlation between trends in CMIP and observations reduces to only 0.13. Thus, the spatial variations in observed North American surface temperature change since 1951 are *unlikely* due to anthropogenic forcing alone.

An assessment of AMIP simulations indicates that key features of the spatial variations of annually averaged temperature trends are more consistent with a response to SST variations during 1951 to 2006. The ensemble mean model response to observed SST variations (CMIP runs in Figure 3.3) shows a spatial pattern of North American surface temperature trends that agrees well with the observed pattern - the pattern correlation is 0.87. Upon removing the area-mean warming, the resulting correlation is still 0.57. This indicates that the spatial variation of the observed warming over North America is *likely* influenced by observed regional SST variations, consistent with the previously published results of Robinson *et al.* (2002) and Kunkel *et al.*, (2006).

A diagnosis of observed trends in free atmospheric circulation, using the reanalysis data of 500 mb heights, provides a physical basis for the observed regionality in North American surface temperature trends. Figure 3.7 illustrates the 1951 to 2006 November to April surface temperature trends together with the superimposed 500 mb height trends. It is during the cold half of the year that many of the spatial features in the annual trend originate, a time during which teleconnection patterns are also best developed and exert their strongest impacts. The reanalysis data captures two prominent features of circulation change since 1951, one that projects upon the positive phase of the PNA pattern and the other that projects upon the positive phase of the NAO pattern. Recalling from Chapter 2 the surface temperature fingerprints attributable to the PNA and NAO, the diagnosis in Figure 3.7 reveals that the pattern of observed surface temperature trend can be understood as a linear super-positioning of those fingerprints, consistent with prior published results of Hurrell (1995) and Hurrell (1996).

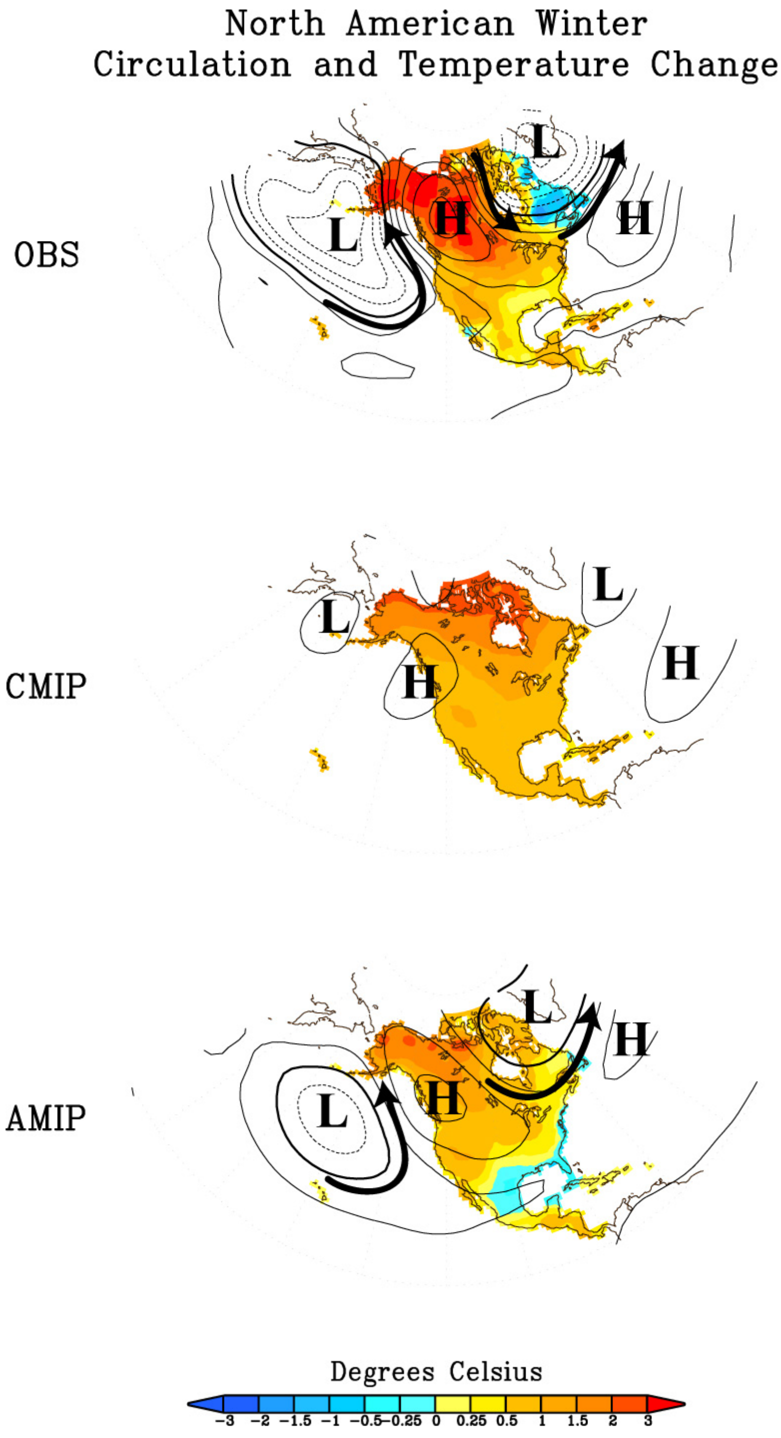

Figure 3.7 The 1951 to 2006 November to April trend of 500 mb heights (contours, units meters/56 years, contour interval 10 m) and North American surface temperature (color shading, units °C/56 years) for observations (top), CMIP ensemble mean(middle), AMIP ensemble mean (bottom). Anomalous High and Low Pressure regions are highlighted. Arrows indicate the anomalous wind direction, which circulates around the High and Low Pressure centers in a clockwise (counterclockwise) direction.

The historical reanalysis data thus proves invaluable for rendering a physically consistent description of the regional structure of North American climate trends. A reason for the inability of the CMIP simulations to replicate key features of the observed spatial variations is revealed by diagnosing their simulated free atmospheric circulation trends, and comparing to the reanalysis data. Shown in the middle panel of Figure 3.7, the CMIP 500 mb height trends have little spatial structure, instead being dominated by a near-uniform increase in heights. Given the strong thermodynamic relation between 500 mb heights and tropospheric column temperature, the relative uniformity of North American surface warming in the CMIP simulations is consistent with the uniformity in its circulation change (there are additional factors that can influence surface temperature patterns, such as local soil moisture, snow cover and sea-ice albedo effects on surface energy balances, that may have little reflection in 500 mb heights).

In contrast, the ability of the AMIP simulations in producing key features of the observed spatial variations in surface temperature stems from the fact that SST variations during 1951 to 2006 force a trend in atmospheric circulation that projects upon the positive phases of both the PNA and NAO patterns (Figure 3.7, bottom panel). Though the amplitude of the ensemble mean AMIP 500 mb height trends is weaker than the observed 500 mb height trends, their spatial agreement is high. It is this wavy aspect to the tropospheric circulation trend since 1951 that permits the reorganization of air mass movements and storm track shifts that is an important factor for explaining key regional details of North American surface climate trends.

3.3.2.2 Conterminous United States

For the United States area-average temperature variations, six of the warmest ten summers (Figure 3.8, top) and 6 of the warmest 10 winters (Figure 3.9, top) during 1951 to 2006 occurred in the last decade (1997 to 2006). This recent clustering of record warm occurrences is consistent with the increasing anthropogenic signal of human induced warming, as evidenced from the CMIP simulations (Figures 3.8 and 3.9, middle panels) that indicate accelerated warming over the United States during the past decade during both summer and winter.

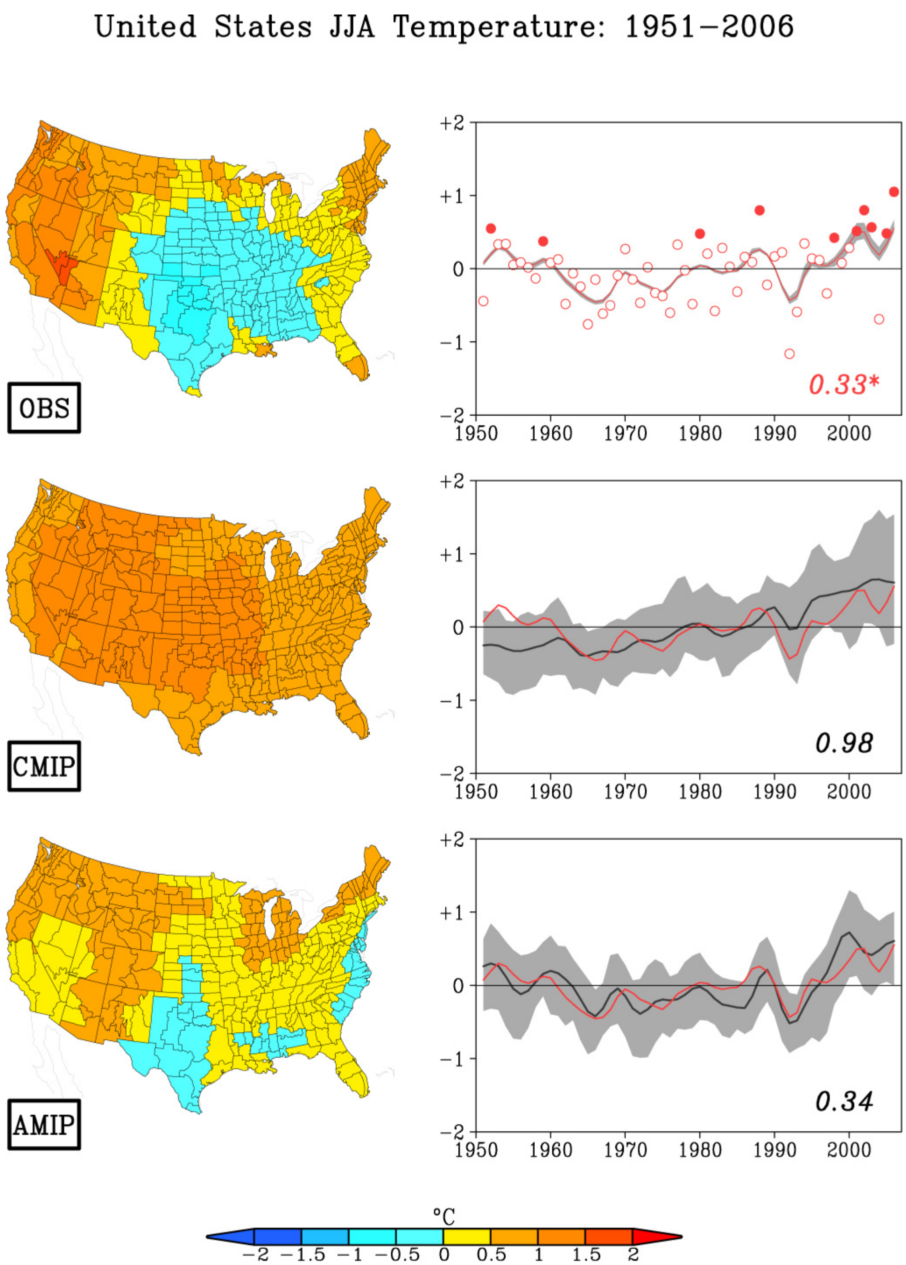

Figure 3.8 Spatial maps of the linear temperature trend (°C/56 years) in summer (June to August) (left side) and time series of the decadal variations of United States area-average temperatures in summer from observations, CMIP model simulations, and AMIP model simulations. Plotted values are the total 56-year change (°C), with the single asterisk denoting high confidence that an observed change was detected Gray band in top panel denotes the range of observed temperatures based on five different analyses, gray band in middle panel denotes the 5-95% range among 41 CMIP model simulations, and gray band in lower panel denotes the 5-95% range among 33 AMIP model simulations. Curves smoothed with 5-point Gaussian filter. Unsmoothed observed annual temperature anomalies shown in open red circles, with warmest 10 years shown in closed red circles.

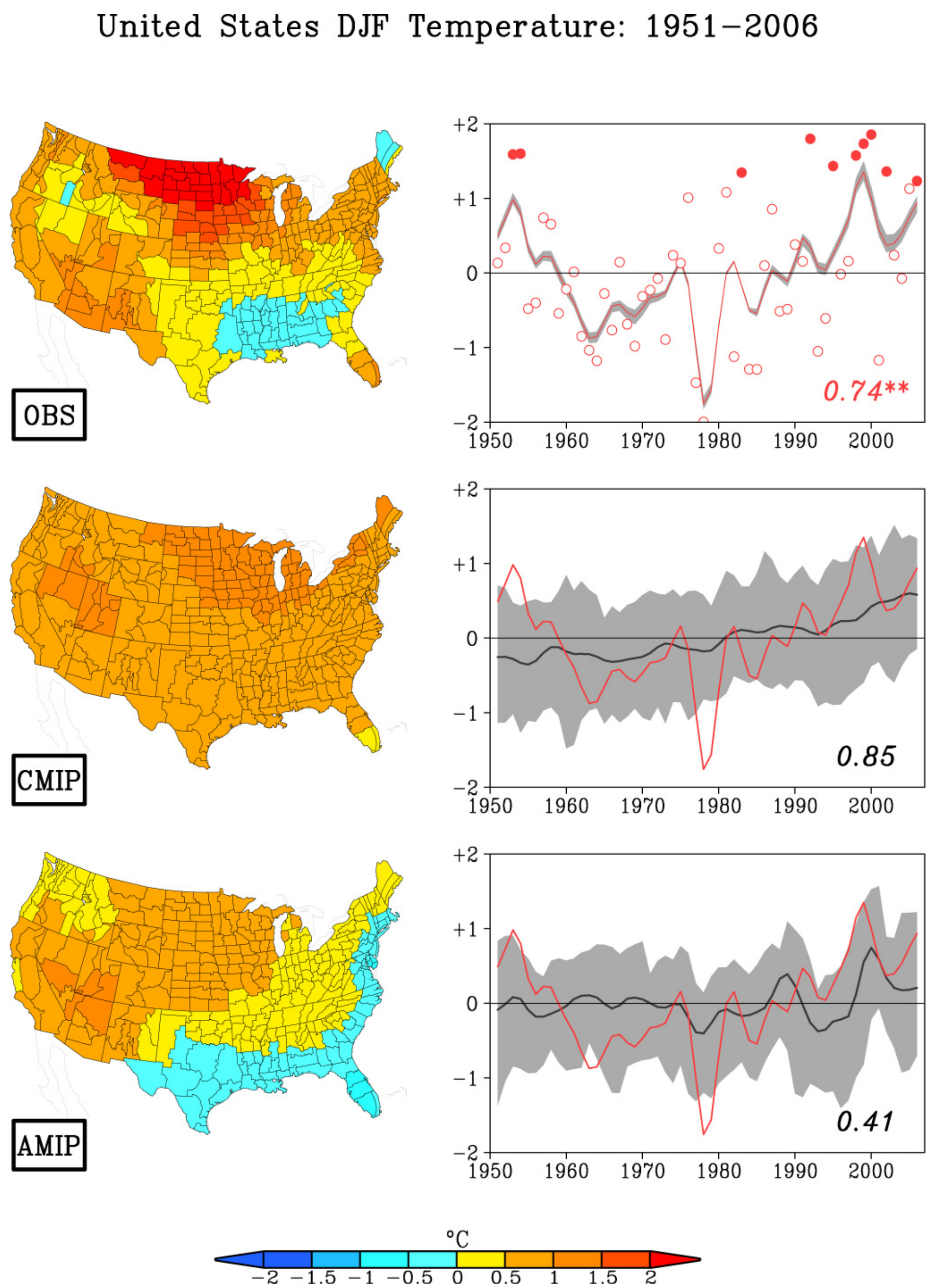

Figure 3.9 Spatial maps of the linear temperature trend (°C/56 years) in winter (December to February) (left side) and time series of the decadal variations of United States area-average temperatures in summer from observations, CMIP model simulations, and AMIP model simulations. Plotted values are the total 56-year change (°C), with the double asterisks denoting very high confidence that an observed change was detected Gray band in top panel denotes the range of observed temperatures based on five different analyses, gray band in middle panel denotes the 5-95% range among 41 CMIP model simulations, and gray band in lower panel denotes the 5-95% range among 33 AMIP model simulations. Curves smoothed with 5-point Gaussian filter. Unsmoothed observed annual temperature anomalies shown in open red circles, with warmest 10 years shown in closed red circles.

During summer, while some regions of the United States have observed strong warming, others experienced no significant change since 1951. The lack of mid-continent warming is a particularly striking feature of the observed trends since 1951, and is juxtaposed with the strong warming in the West. This overall pattern of United States temperature change is *unlikely* due to external anthropogenic forcing alone, an assessment that is supported by several lines of evidence. First, the spatial variations of the CMIP simulated United States temperature trend (Figure 3.8, middle) are uncorrelated with those observed - the pattern correlation is -0.10 when removing the area-mean warming. The ensemble CMIP area-averaged summer warming trend of +0.99°C is also triple the observed area-averaged warming of +0.33°C. In other words, there has been much less summertime warming observed for the United States as a whole than expected based on changes in the external forcing. There is reason to believe - as discussed further below - that internal variations have been masking the anthropogenic warming signal in summer to date, though the possibility that the simulated signal is itself too strong cannot be entirely ruled out.

Second, the spatial variations of the AMIP simulated United States temperature trend (Figure 3.8, bottom) are positively correlated with those observed - the pattern correlation is +0.43 when removing the area-mean warming. The cooling of the southern Plains in the AMIP simulations is in particular agreement with observations, and results in a reduced ensemble AMIP area-averaged United States summer warming trend of only +0.34°C that is close to observations. It thus appears that regional SST variability has played an important role in United States summer temperature trends since 1951. The nature of these important SST variations remains unknown. The extent to which they are due to internal coupled system variations and the contribution from anthropogenic forcing are among the vital questions awaiting future attribution research.

During winter, the pattern of observed surface temperature trends (Figure 3.9, top) consists of strong and significant warming over the West and North, and insignificant change along the Gulf Coast. Both CMIP and AMIP simulations produce key features of the United States temperature trend pattern (spatial correlations of 0.70 and 0.57 respectively upon removing the United States area-mean warming trend), though the cooling along the Gulf Coast appears inconsistent with external forcing, but consistent with SST forcing. The observed United States winter warming trend of +0.75°C has been stronger than that occurring in summer, and compares to an area-averaged warming of +0.85°C in the ensemble of CMIP and +0.41°C in the ensemble of AMIP simulations.

It is worth noting that the United States also experienced warm conditions during the mid-20th century - the early years of available reanalyses (see also Box 3.3 for discussion of the United States warmth in the early 20th century). It is partly for this reason that the 1951 to 2006 observed trends, especially during summer, are not greater. This is an indication for the sensitivity of trends to the beginning and end-years selected for diagnosis, and requires that the trend analysis be accompanied by an assessment of the full temporal evolution during 1951 to 2006.

Regarding confidence levels for the observed United States temperature trends for 1951 to 2006, a non-parametric test has been applied that estimates the probability distribution of 56-year trends attributable to natural variability alone (see Appendix 3.A for methodological details). As in Section 3.2, this involves diagnosis of 56-year trends from the suite of “naturally forced” CMIP runs, from which a sample of 76 such trends were generated for the conterminous United States for winter and summer seasons. The observed area-averaged United States summer trend of +0.33°C is found to exceed the 80% level of trend occurrences in those natural forced runs, indicating a *high* level of confidence that warming has been detected. For winter, the observed trend of +0.75°C is found to exceed the 95% level of trends in the natural forced runs indicating a *very high* level of confidence. These diagnoses support our assessment that a warming of United States area-averaged temperatures during 1951 to 2006 has likely been detected for summer and very likely been detected for winter.

The causes of the reduced warming in the southeast United States, seen during both winter and summer seasons, relative to the remainder of the country have been considered in several studies. Knutson *et al.* (2006) contrasted the area-average temperature variations for the southeast United States with those for the remainder of the United States (as shown in Figure 3.10) for both observations and model simulations with the GFDL CM2 coupled model. While the observed and simulated warming due to anthropogenic forcing agrees well for the remainder of the United States, the observed cooling is outside the range of the small ensemble considered. For a larger ensemble, such as the whole CMIP multi-model ensemble, as considered by Kunkel *et al.* (2006), the cooling in the southeast United States is within the range of model simulated temperature variations but would have to be associated with a very large

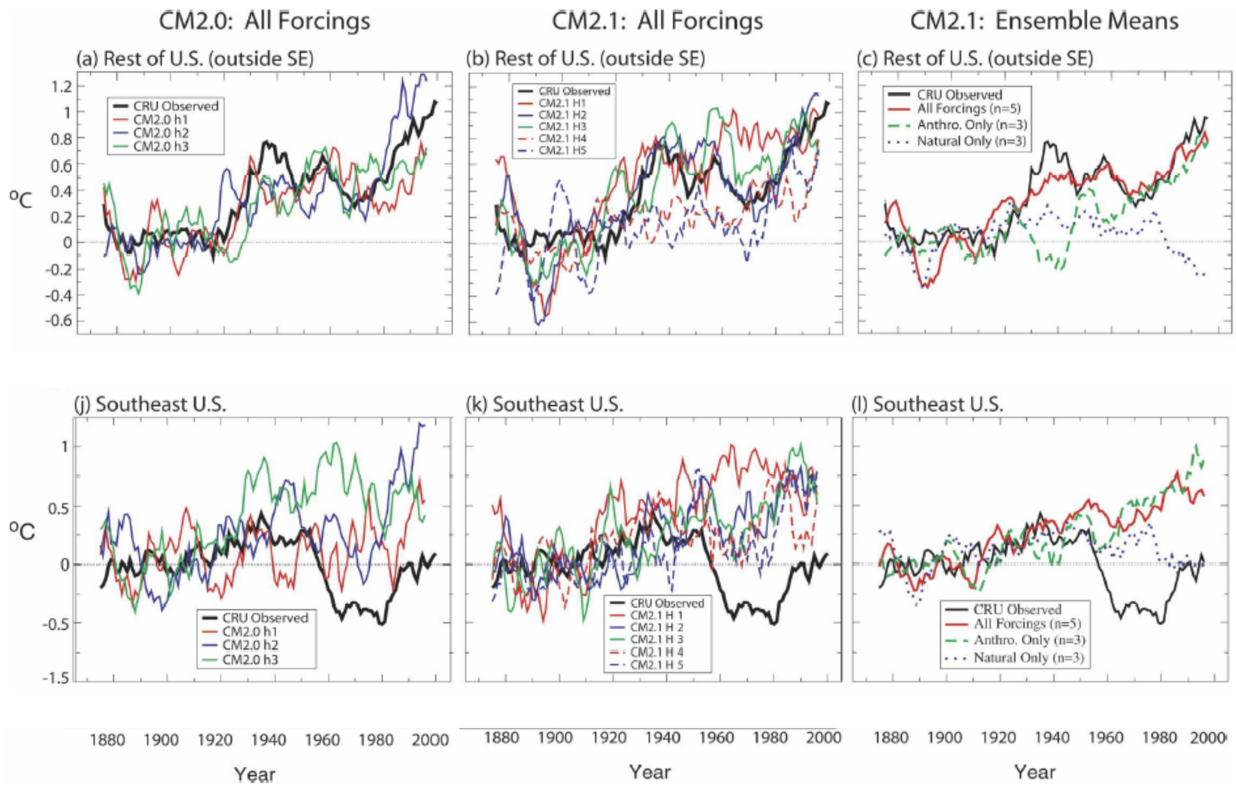

Figure 3.10 Ten-year running-mean area-averaged time series of surface temperature anomalies (°C) relative to 1881 to 1920 for observations and models for various regions: (a)–(c) rest of the contiguous United States, and (j)-(l) southeast United States. The left column and middle columns are based on all-forcing historical runs 1871–2000 and observations 1871 to 2004 for GFDL coupled climate model CM2.0 (n _ 3) and CM2.1 (n _ 5), respectively. The right column is based on observed and model data through 2000, with _2 standard error ranges (shading) obtained by sampling several model runs according to observed missing data. The red, blue, and green curves in the right-hand-column diagrams are ensemble mean results for the CM2.1 all-forcing (n _ 5), natural-only (n _ 3), and anthropogenic-only (n _ 3) forcing historical runs. Model data were masked according to observed data coverage. From Knutson *et al.*, (2006).

case of natural cooling superimposed on anthropogenically-forced larger scale warming. Robinson *et al.* (2002) and Kunkel *et al.* (2006) have shown that this regional cooling in the central and southeast United States is associated with the model response to observed

SST variations, particularly in the tropical Pacific and North Atlantic oceans, and is consistent with the additional assessment of AMIP simulations presented in this Section. For the winter half of year in particular, the southeast cooling is also consistent with the trends in teleconnection patterns that were diagnosed from the reanalysis data.

Other studies have argued that land use and land cover changes are additional candidate factors for explaining the observed spatial variations of warming over the United States since 1951. The marked increase of irrigation in the central valley of California and the northern Great Plains is likely to have lead to a warming of minimum temperatures and a reduced warming of maximum temperatures in summer (Christy *et al.*, 2006; Kueppers *et al.*, 2007; Mahmood *et al.*, 2006). Urbanization, land clearing, deforestation and reforestation are likely to have contributed to some of the spatial patterns of warming over the United States, though a quantification of these factors is lacking (Hale *et al.*, 2006; Kalnay and Cai, 2003; Trenberth, 2004; Vose, 2004; Kalnay *et al.*, 2006).

As a further assessment of the spatial structure of temperature variations, the 1951 to 2006 summer and winter surface temperature time series for nine United States sub-regions are shown in Figure 3.11 and 3.12, respectively. The observed time series is shown by the red bold curve, and the CMIP and AMIP ensemble mean time series are superimposed with blue and green curves, respectively. No attribution of recent climate variations and trends at these scales has been published, aside from the aforementioned

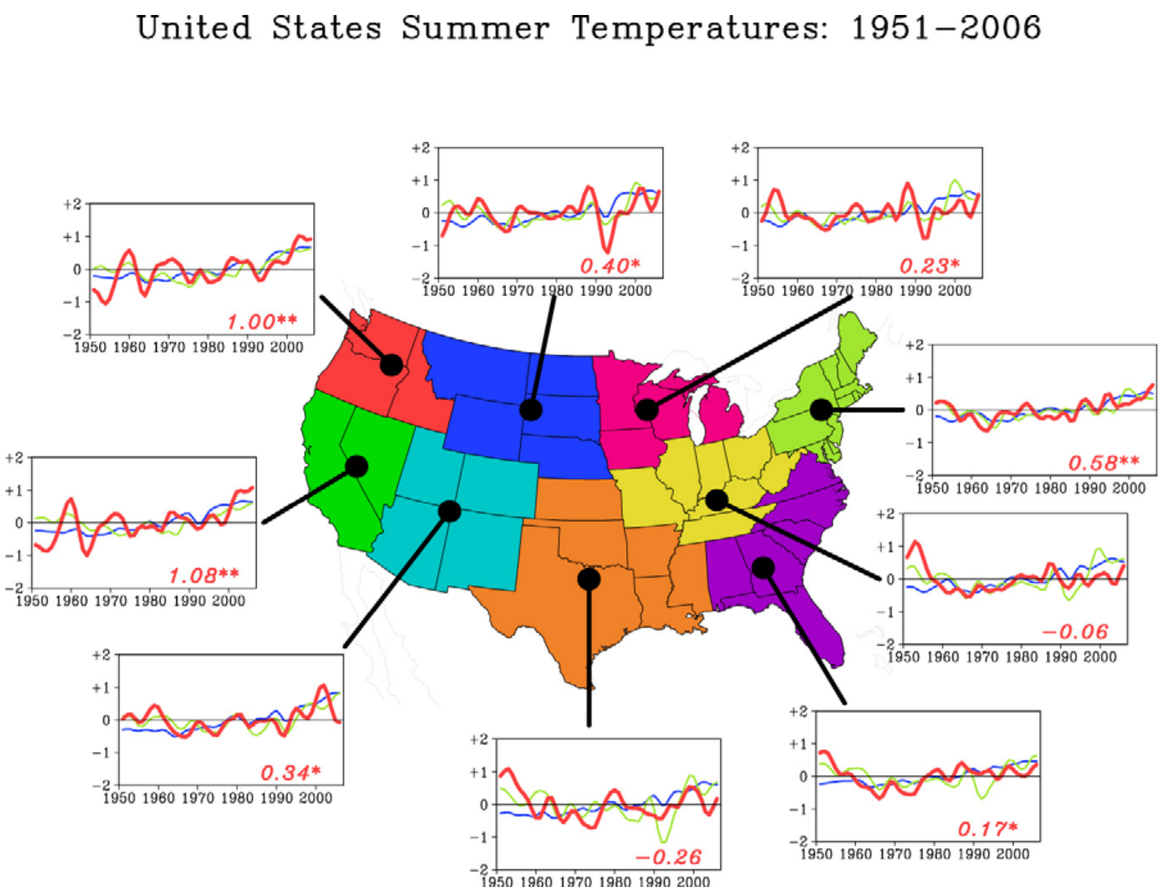

Figure 3.11 The 1951 to 2006 time series of regional United States surface temperatures in summer (June to August). The observations are shown in bold red, ensemble mean CMIP in blue, and ensemble mean AMIP in green. A 5-point Gaussian filter has been applied to the time series to emphasize multi-annual scale time variations. Plotted values in each graph indicate the total 1951 to 2006 temperature change averaged for the sub-region. Double (single) asterisks denote regions where confidence of having detected a change is very high (high).

Knutson *et al.* (2006) and Kunkel *et al.* (2006) studies that examined conditions over the southeast United States. In so far as decision making occurs on these regional scales, and smaller local scales, the need for a systematic explanation of such climate conditions is needed. Here we comment only upon several salient features of the observed and simulated changes, but stress that a complete synthesis has yet to be undertaken. For each region

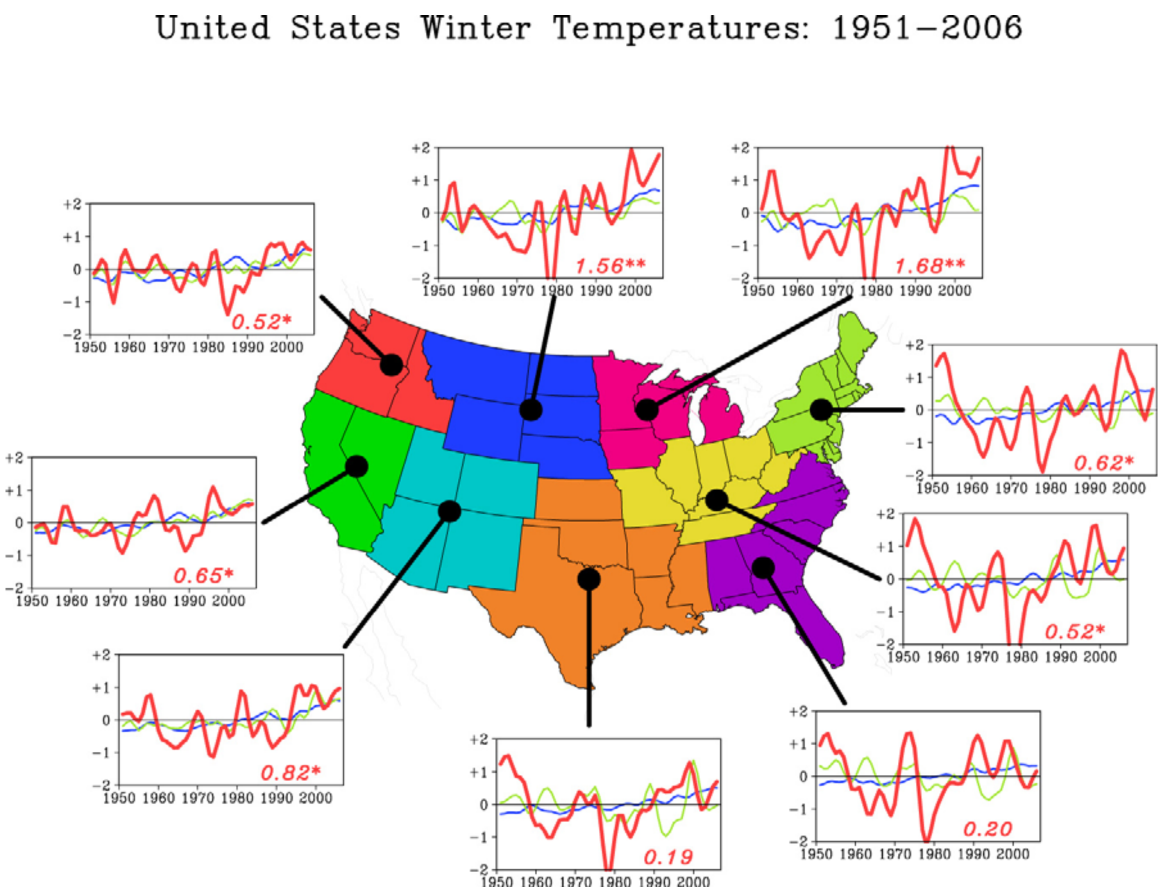

Figure 3.12 The 1951 to 2006 time series of regional United States surface temperatures in winter (December to February). The observations are shown in bold red, ensemble mean CMIP in blue, and ensemble mean AMIP in green. A 5-point Gaussian filter has been applied to the time series to emphasize multi-annual scale time variations. Plotted values in each graph indicate the total 1951 to 2006 temperature change averaged for the sub-region. Double (single) asterisks denote regions where confidence of having detected a change is very high (high).

of the United States, the total 1951 to 2006 observed surface temperature change and its significance is plotted beneath the time series. Single and double asterisks denote high and very high confidence, respectively, that a change has been detected using the methods described above.

During summer (Figure 3.11), there exists *very high* confidence that warming has been observed over Pacific Northwest and Southwest regions. For these, the net warming since

1951 has been about +1°C, exceeding the 95% level of trends in the natural forced runs at these regional scales. *High* confidence of a detected warming also exists for the Northeast, where the observed 56-year change is not as large, but occurs in a region of reduced variability thereby enhancing detectability of a change. These three warming regions also exhibit the best temporal agreement with the warming simulated in the CMIP models. It is also noteworthy that the comparatively weaker observed summertime trends during 1951 to 2006 in the interior West, the southern Great Plains, the Ohio Valley, and the southeast United States results from the very warm conditions at the beginning of the reanalysis record, a period of widespread drought in those regions of the country.

During winter (Figure 3.12), there is *very high* confidence that warming has been detected over the Northern Plains and Great Lakes region. Confidence is *high* that warming during 1951 to 2006 has been detected in the remaining regions, except along the Gulf Coast where no detectable change in temperature has occurred. In the northern regions, most of the net warming of about +1.5°C has happened in the recent two decades. It is noteworthy that the CMIP simulations also produce accelerated winter warming over the northern United States in the past 20 years, suggesting that this regional and seasonal feature may have been influenced by anthropogenic forcing.

The 1950s produced some of the warmest winters during the 1951 to 2006 period for several regions of the United States. The latest decade of surface warmth in the four southern and eastern United States regions still fails to exceed that earlier decadal warmth. The source for the warm winters in those regions in mid-century is not currently known, and it is unclear whether it is related to a widespread warm period across the Northern Hemisphere during the 1930s and 1940s that was attributed primarily to internal variability (Delworth and Knutson, 2000). The fact that neither CMIP nor AMIP ensemble mean responses produce such 1950s warmth supports an interpretation that the United States 1950s warmth was likely unrelated to external or the SST forcing.

3.3.3 Precipitation Trends

3.3.3.1 North America

The observed annual North American precipitation trends during 1951 to 2006 in Figure 3.6 of the previous Section are dominated by regional scale features. Of the identifiable features of change, prominent is the annual drying of Mexico and the greater Caribbean region, and the increase over northern Canada. However, owing to the strong and disparate seasonal cycles of precipitation across the continent, a diagnosis of the annual mean trends is of limited value. We thus focus further discussion on the seasonal and regional analyses below.

Shown in Figure 3.13 (top) is the cold-season (November to April) North American observed precipitation change, with superimposed contours of the tropospheric circulation change (identical to Figure 3.7). The reanalysis data of circulation change provides physical insights on the origins of the observed regional precipitation change. The band of drying that extends from British Columbia across much of southern Canada and part of the northern United States corresponds to upper level high pressure from which one can infer reduced storminess. In contrast, increased precipitation across the southern United States

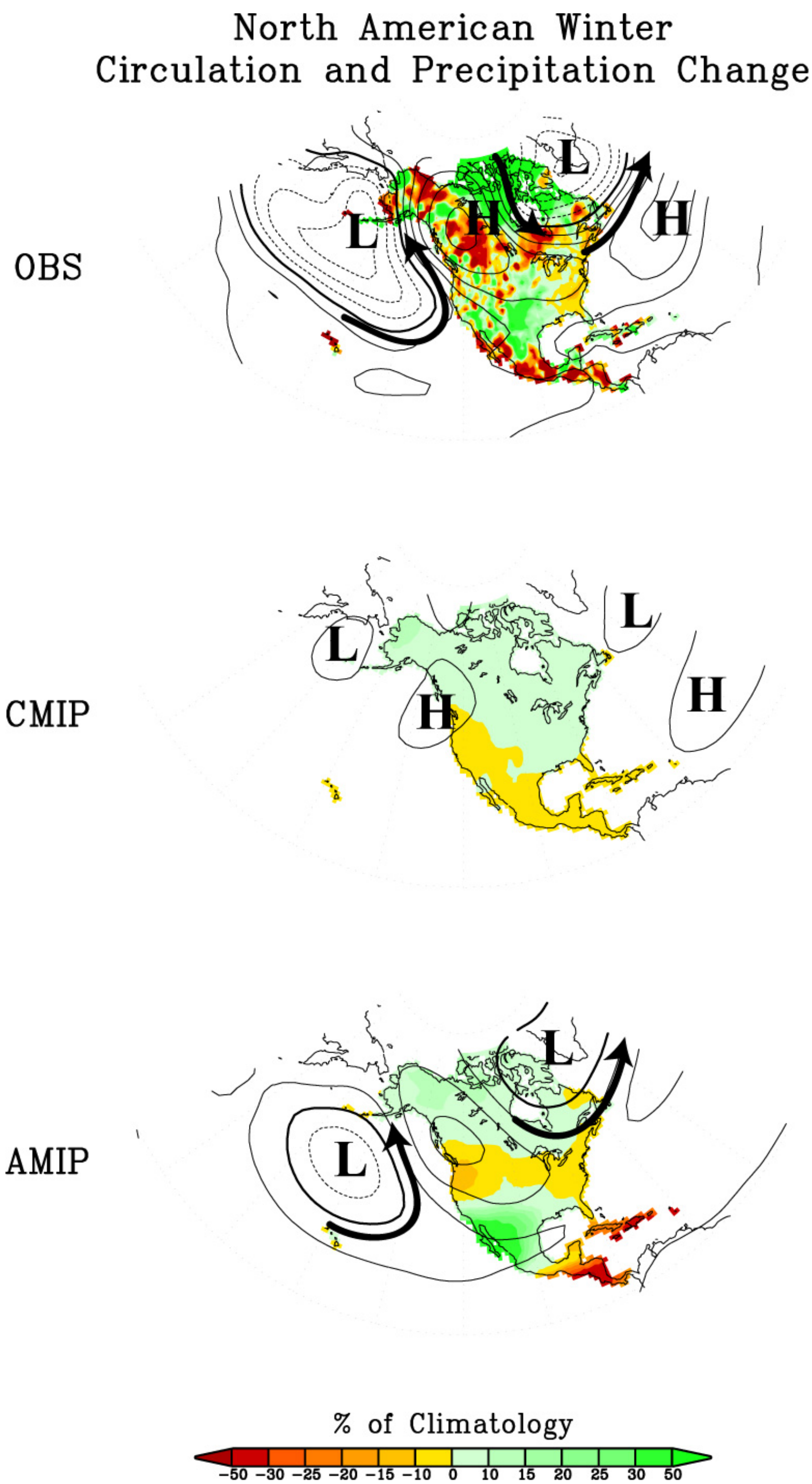

Figure 3.13 The 1951 to 2006 November to April trend of 500 mb heights (contours, units meters/56 years, contour interval 10 m) and North American precipitation (color shading, units 56-year change as % of climatology) for observations (top), CMIP ensemble mean (middle), AMIP ensemble mean (bottom). Anomalous High and Low Pressure regions are highlighted. Arrows indicate the anomalous wind direction, which circulates around the High and Low Pressure centers in a clockwise (counterclockwise) direction.

and northern Mexico in winter is consistent with the deeper southeastward shifted Aleutian low that is conducive for increased winter storminess across the southern region of the United States. Further south, drying again appears across southern Mexico and Central America. This regional pattern is unrelated to external forcing alone, as revealed by the lack of spatial agreement with the CMIP trend pattern (middle panel), and the lack a wavy tropospheric circulation response in the CMIP simulations. Many key features of the observed regional precipitation change are, however, consistent with the forced response to global SST variations during 1951 to 2006, as is evident from the AMIP trend pattern (bottom). In particular, the AMIP simulations generate the zonal band of enhanced high latitude precipitation, the band of reduce precipitation centered along 45°N, wetness in the southern United States and North Mexico, and dryness over Central America. These appear to be consistent with the SST forced change in tropospheric circulation. It is thus again important to determine, in future attribution research, the responsible regional SST variations, and to assess the origin of the SSTs anomalies themselves.

3.3.3.1 Conterminous United States

The observed seasonal-mean precipitation trends over the period 1951 to 2006 are compared with the ensemble mean responses of the CMIP and AMIP simulations for summer in Figure 3.14 and for winter in Figure 3.15. During all seasons in general, there are smaller scale spatial variations of the observed precipitation trends across the United States than for the temperature trends, and larger interannual and decadal variability. These factors undermine the detectability of any physical change in precipitation since 1951.

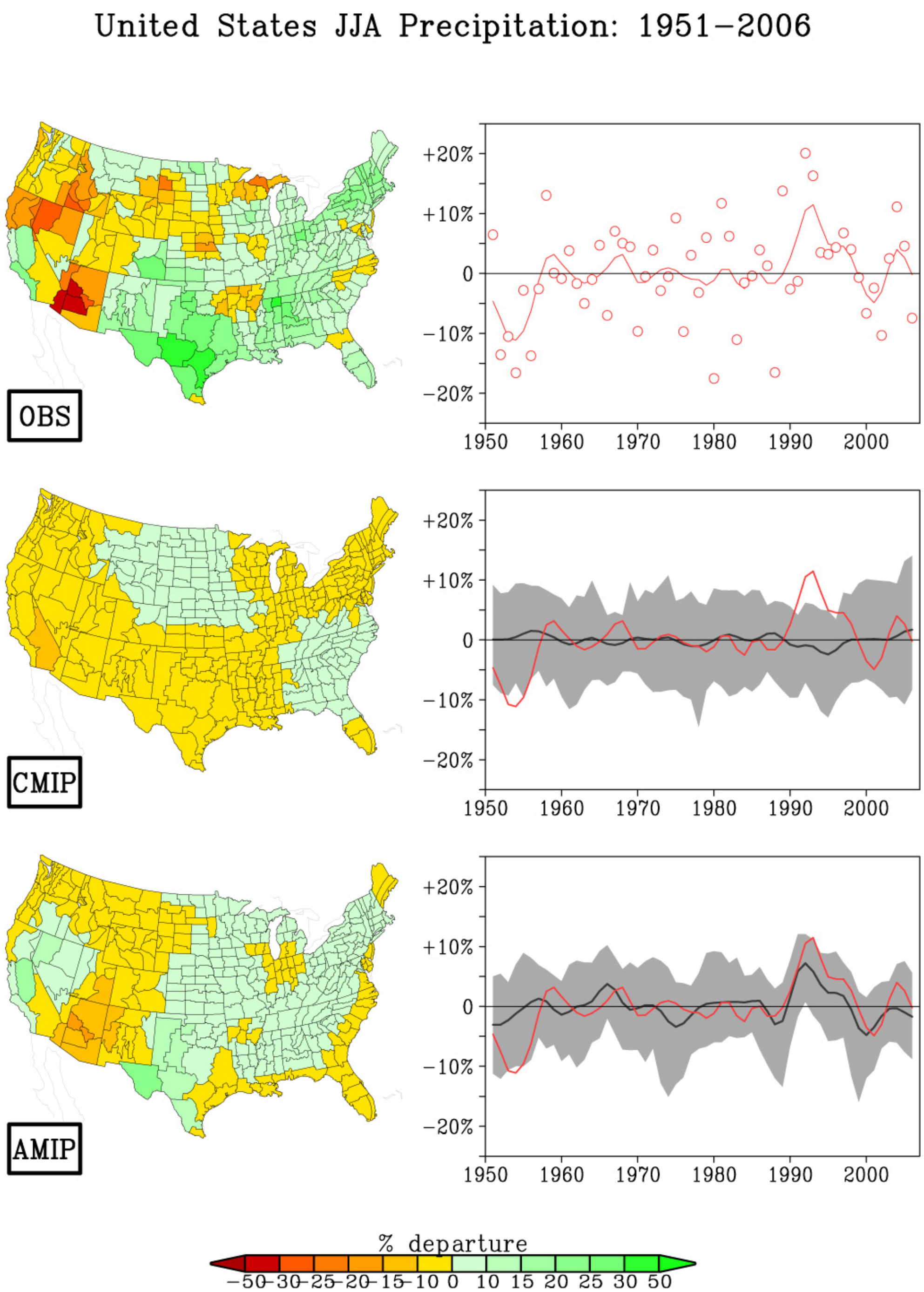

Figure 3.14 Spatial maps of the linear trend in precipitation (% change of seasonal climatology) in summer (June through August) (left side) and time series of the decadal variations of United States area-average precipitation in summer from observations, CMIP model simulations, and AMIP model simulations. Gray band in middle panel denotes the 5-95% range among 41 CMIP model simulations, and gray band in lower panel denotes the 5-95% range among 33 AMIP model simulations. Curves smoothed with 5-point Gaussian filter. Unsmoothed observed annual precipitation anomalies shown in open red circles.

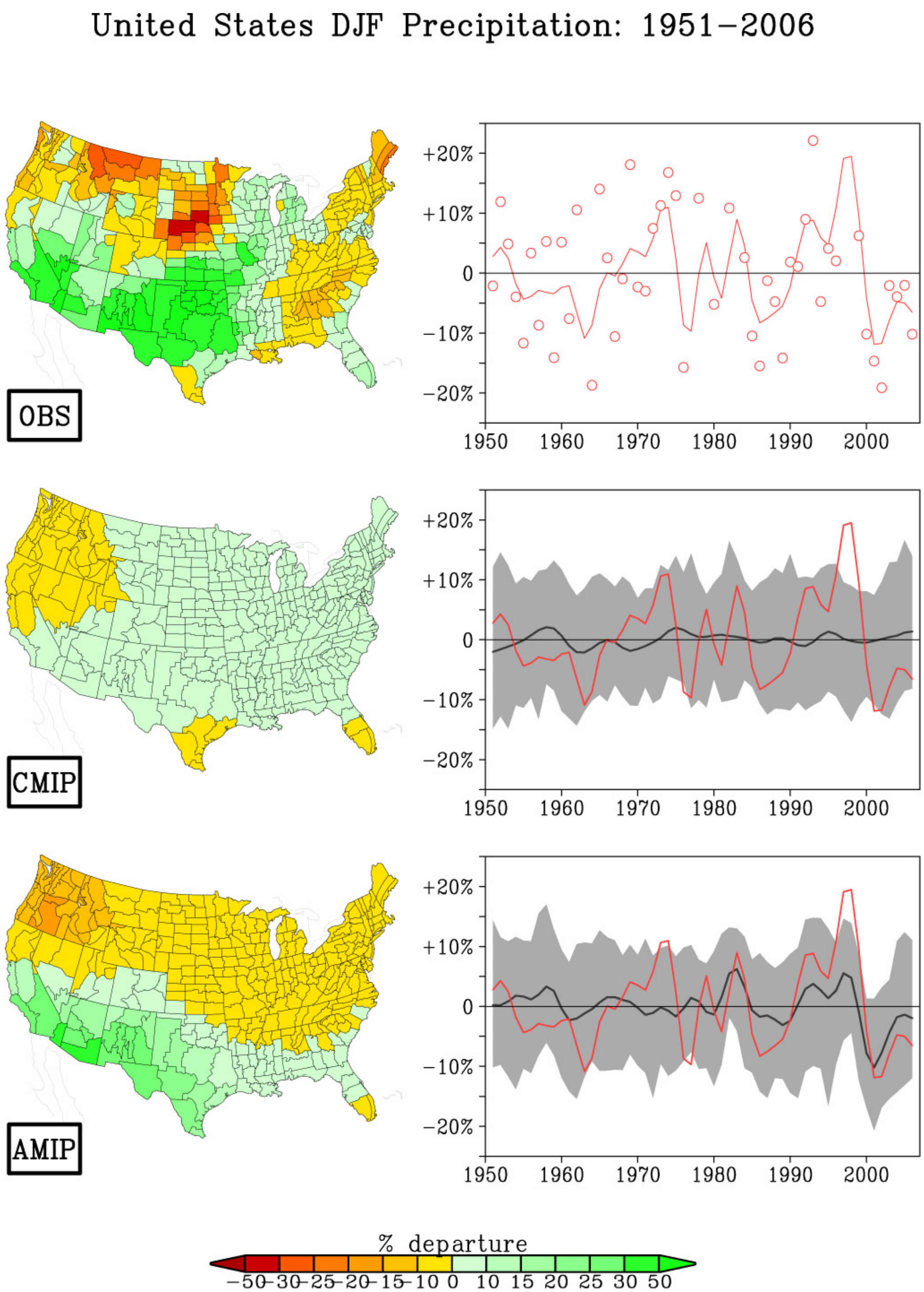

Figure 3.15 Spatial maps of the linear trend in precipitation (% change of seasonal climatology) in winter (December through February) (left side) and time series of the decadal variations of United States area-average precipitation in winter from observations, CMIP model simulations, and AMIP model simulations. Gray band in middle panel denotes the 5-95% range among 41 CMIP model simulations, and gray band in lower panel denotes the 5-95% range among 33 AMIP model simulations. Curves smoothed with 5-point Gaussian filter. Unsmoothed observed annual precipitation anomalies shown in open red circles.

During summer (Figure 3.14), there is a general pattern of observed rainfall reductions in the west and southwest United States and increases in the east. There is some indication of similar patterns in the CMIP and AMIP simulations, however, the amplitudes are so weak that the ensemble model anomalies are themselves unlikely to be significant. The time series of United States summer rainfall is most striking for a recent fluctuation between wet conditions in the 1990s, followed by dry conditions in the late 1990s and early 2000s. This prominent variation is well explained by the region's summertime response to SST variations, as seen by the remarkable correspondence of observations with the time evolving AMIP rainfall (lower panel). For the 56-year period as a whole, the temporal correlation of AMIP simulated and observed summer United States averaged rainfall is +0.64.

During winter (Figure 3.15), there is little agreement between the observed and CMIP modeled spatial patterns of trends, though considerably better agreement exists with the AMIP modeled spatial pattern. Again, the ensemble mean CMIP model simulations shows no significant long term trends during 1951 to 2006, and they also exhibit muted variability (middle), suggesting that changes in external forcing have had no appreciable influence on area-average precipitation in the United States. This is consistent with the published results of Zhang *et al.* (2007) who find disagreement between observed and CMIP simulated trends over the United States. In contrast, several key decadal variations are captured by the ensemble mean AMIP simulations including again the swing from wet 1990s to dry late 1990s early 2000 conditions. For the 56-year period as a whole, the temporal correlation of AMIP simulated and observed winter United States averaged rainfall is +0.59.

For the nine separate United States regions, Figures 3.16 and 3.17 illustrate the temporal variations of observed, ensemble CMIP, and ensemble AMIP precipitation for summer and winter seasons, respectively. These highlight the strong temporal swings in observed regional precipitation between wet and dry periods, such that no single region has a detectable change in precipitation during 1951 to 2006. These observed fluctuations are nonetheless of great societal relevance, being associated with floods and droughts having catastrophic local impacts. Yet, comparing to CMIP simulations indicates that it is *exceptionally unlikely* that these events are related to external forcing. There is some indication from the AMIP simulations that their occurrence is somewhat determined by SST events especially in the south and west during winter presumably related to the ENSO cycle.

It should be noted that other statistical properties of rainfall, including extremes in daily amounts and the fraction of annual rainfall due to individual wet days have exhibited a detectable change over the United States in recent decades, and such changes have been attributed to anthropogenic forcing in the companion CCSP SAP 3.3 report (CCSP, in press).

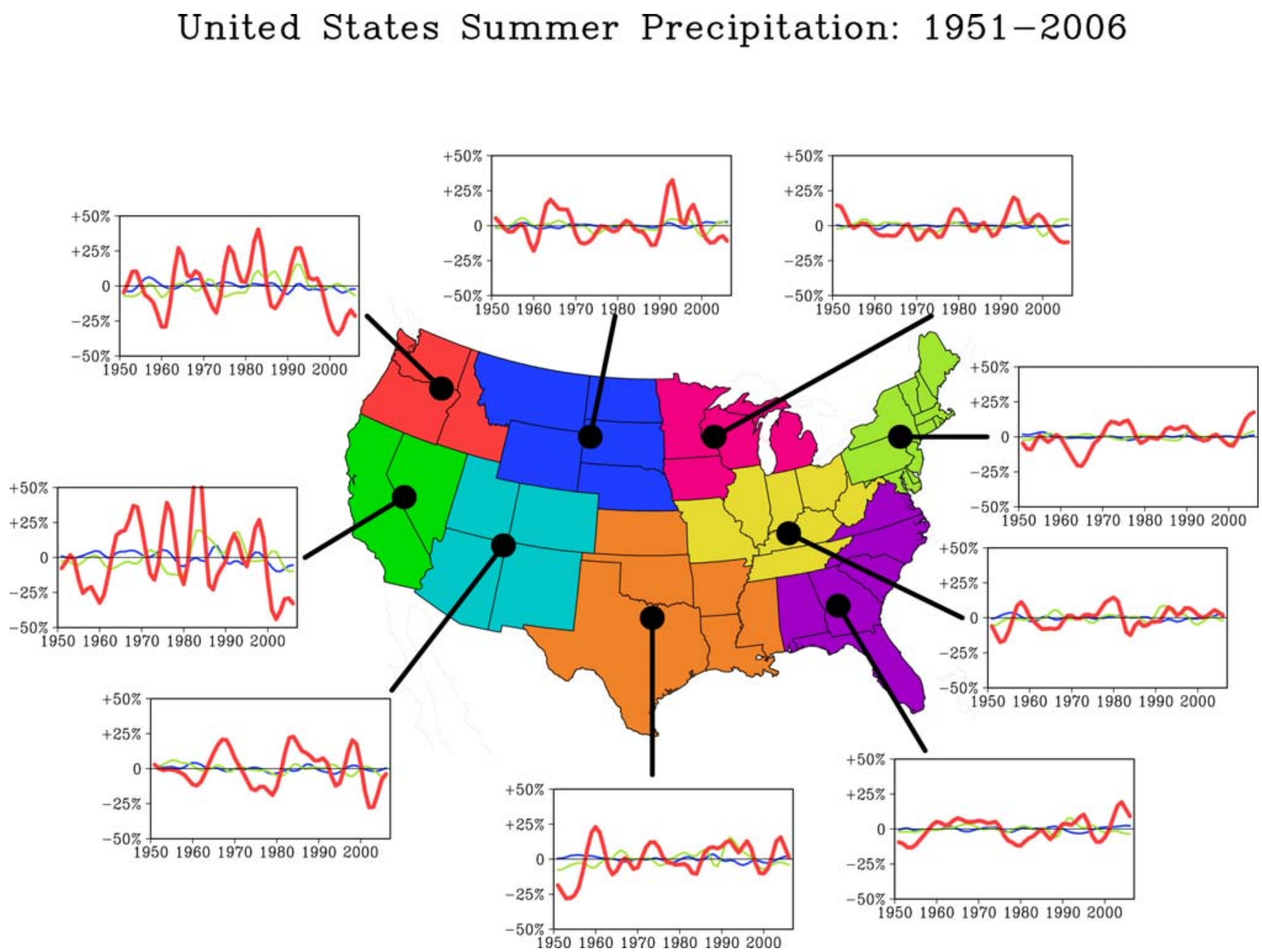

Figure 3.16 The 1951 to 2006 time series of regional United States precipitation in summer (June through August). The observations are shown in bold red, ensemble mean CMIP in blue, and ensemble mean AMIP in green. A 5-point Gaussian filter has been applied to the time series to emphasize multi-annual scale time variations.

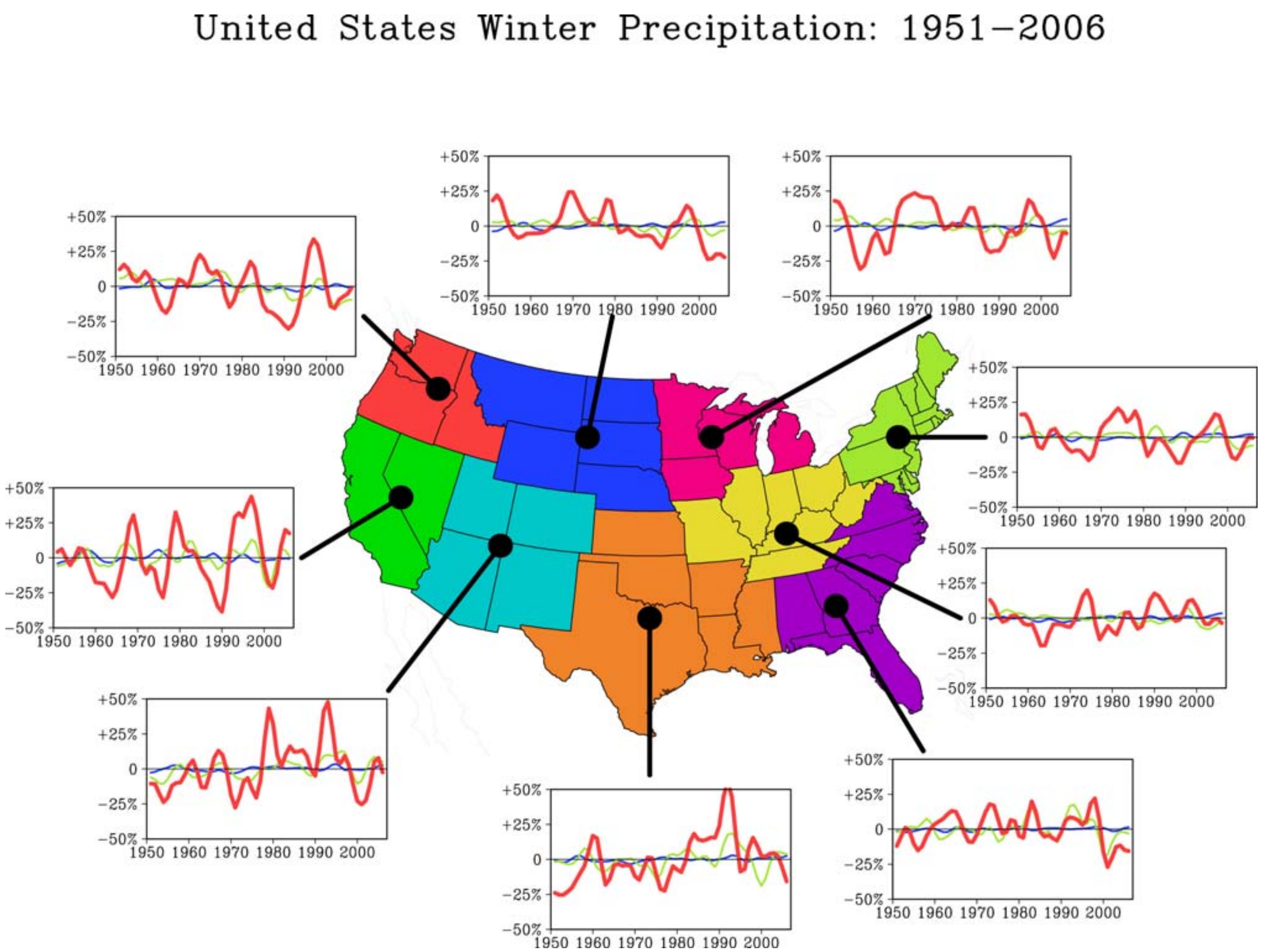

Figure 3.17 The 1951 to 2006 time series of regional United States precipitation in winter (December to February). The observations are shown in bold red, ensemble mean CMIP in blue, and ensemble mean AMIP in green. A 5-point Gaussian filter has been applied to the time series to emphasize multi-annual scale time variations.

3.4 WHAT IS THE NATURE AND CAUSE OF APPARENT RAPID CLIMATE SHIFTS, HAVING MATERIAL RELEVANCE TO NORTH AMERICA, OVER THE REANALYSIS PERIOD?

3.4.1 Introduction

Rapid climate shifts are of scientific interest and of public concern because of the expectation that such occurrences may be particularly effective in exposing the vulnerabilities of societies and ecosystems (Smith *et al.*, 2001). Such abrupt shifts are typically distinguished from the gradual pace of climate change associated, for instance, with anthropogenic forcing. However, through non-linear feedbacks the latter could also trigger rapid shifts in some parts of the climate system, a frequently cited example being a possible collapse of the global ocean's principal conveyor of heat between the tropics and high latitudes known as the thermohaline circulation (Clarke *et al.*, 2002).

By their very nature, abrupt shifts are unexpected events - climate surprises - and thus offer particular challenges to policy makers in planning for their impacts. A retrospective assessment of such "rare" events may offer insights on mitigation strategies that are consistent with the severity of impacts related to rapid climate shifts. Such an assessment would also consider impacts of abrupt climate shifts on societies and ecosystems and would also prepare us to anticipate consequences of gradual changes in climate, in so far as they may be no less severe than those related to rapid climate shifts.

3.4.2 Defining Rapid Climate Shifts

A precise definition for a climate shift that is either "rapid" or "abrupt" does not exist owing to limited knowledge about the full sensitivity of the climate system. For instance, due to nonlinearity, changes in external forcing need not lead to a proportionate climate response. It is conceivable that a *gradual* change in external forcing could yield an abrupt response when applied near a tipping point of sensitivity in the climate system, whereas an *abrupt* change in forcing may not lead to any abrupt response when it is applied far from the system's tipping point between various equilibrium climate states. To date, little is known about the threshold tipping points of the climate system (Alley *et al.*, 2003).

In its broadest sense, a "rapid" shift is a transition between two climatic states that individually have much longer duration than the transition period itself. From an impacts viewpoint, a rapid climate shift is one occurring so fast that societies and ecosystems have difficulty adapting to it.

3.4.3 Mechanisms for Rapid Climate Shifts

The National Research Council (NRC, 2002) has undertaken a comprehensive assessment of rapid climate change, summarizing evidence of such changes occurring before the instrumental and reanalysis records, and understanding abrupt changes in the modern era. The NRC (2002) report on abrupt climate change draws attention to evidence for severe swings in climate proxies of temperature (so-called paleo-reconstructions) during both the last ice age and the subsequent interglacial period known as the Holocene. Ice core data indicate that abrupt shifts in climate have often occurred during Earth's climate history, indicating that gradual and smooth movements do not always characterize climate variations. Identification of such shifts is usually empirical, based upon expert assessment of long time series of the relevant climate records, and in this regard their recognition is usually retrospective. Against this background of abundant evidence for the magnitude of rapid climate shifts, there is a dearth of information about the mechanisms that can lead to climate shifts and of the processes by which climate states are maintained in their altered states (Broecker, 2003). Understanding the causes of such shifts is a prerequisite to any early warning system that is, among other purposes, needed for planning the scope and pace of mitigation.

The National Academy report also highlights three candidate mechanisms for abrupt change: (1) an abrupt forcing, such as may occur through meteorite impacts or volcanic eruptions, (2) a threshold-like sensitivity of the climate system in which sudden changes can occur even when subjected to gradual changes in forcing, (3) an unforced behavior of the climate system resulting purely from chaotic internal variations.

3.4.4 Rapid Climate Shifts since 1950

Although changes in external forcing, whether natural or anthropogenic, are not yet directly assimilated in the current generation of reanalysis products, abrupt changes in external forcings can still influence the reanalyses indirectly thru their effect on other assimilated variables. Observational analyses of the recent instrumental record gives some clues of sudden climate shifts, ones having known societal consequences. These are summarized below according to the current understanding of the potential mechanism involved. For several reasons, the sustainability of these apparent shifts is not entirely known. First, multi-decadal fluctuations are readily seen in post-1950 North American time series of temperature (Figure 3.3) and precipitation (Figure 3.6). Although the post-1950 period is the most accurately observed period of Earth's climate history, the semi-permanency of any change cannot be readily judged from merely 50 years of data. This limited perspective of our brief modern climate record stands in contrast to proxy climate records within which stable climate was punctuated by abrupt change leading to new climate states lasting centuries to millennia. Second, it is not known whether any recent rapid transitions have involved threshold accidences in a manner that would forewarn of their permanence.

3.4.4.1 Abrupt natural external forcings since 1950

The period of the reanalysis record was a volcanically active one, particularly when compared to the first half of the 20th century. Three major eruptions included the Agung, El Chichon, and Pinatubo volcanoes of 1963, 1982, and 1991, respectively. Each of these injected aerosols into the stratosphere acting to significantly increase the stratospheric aerosol optical depth that led to an increase in the reflectance of incoming solar radiation (Santer *et al.*, 2006).

Each of these abrupt volcanic forcings has been found to exert a discernable impact on climate conditions. Observed sea surface temperatures cooled in the wake of the eruptions, the detectability of which was largest in oceans having small unforced, internal variability (Santer *et al.*, 2006). Surface based observational analyses of these and other historical volcanoes indicates North American surface temperatures tend to experience warming in the winters following strong eruptions, but cooling in the subsequent summer (Kirchner *et al.*, 1999). These abrupt forcings have not, however, led to sustained changes in climate conditions, in so far as the residence time for the stratospheric aerosol increases due to volcanism is less than a few years (depending on the particle distributions and the geographical location of the volcanic eruption), and the fact that major volcanic events since 1950 have been well separated in time.

The impact of the volcanic events is readily seen in Figure 3.18 (green curve) which plots time series of annual SSTs in various ocean basins derived from the ensemble mean CMIP simulations forced externally by estimates of the time evolving volcanic and solar forcings - so-called "natural forcing" runs. The SST cooling in the wake of each event is evident. Furthermore, in the comparison with SST evolutions in the fully forced natural and anthropogenic CMIP runs (Figure 3.18, bars), the lull in ocean warming in the early 1980s and early 1990s was likely the result of the volcanic aerosol effects. Similar lulls in warming rates are evident in the observed SSTs at these times (Figure 3.5). They are also evident in the observed and CMIP simulated North American surface temperature time series (Figure 3.3). Yet, while having detected the climate system's response to abrupt forcing, and while some model simulations detect decadal-long reductions in oceanic heat content following volcanic eruptions (Church *et al.*, 2005), their impacts on surface temperature have been relatively brief and transitory.

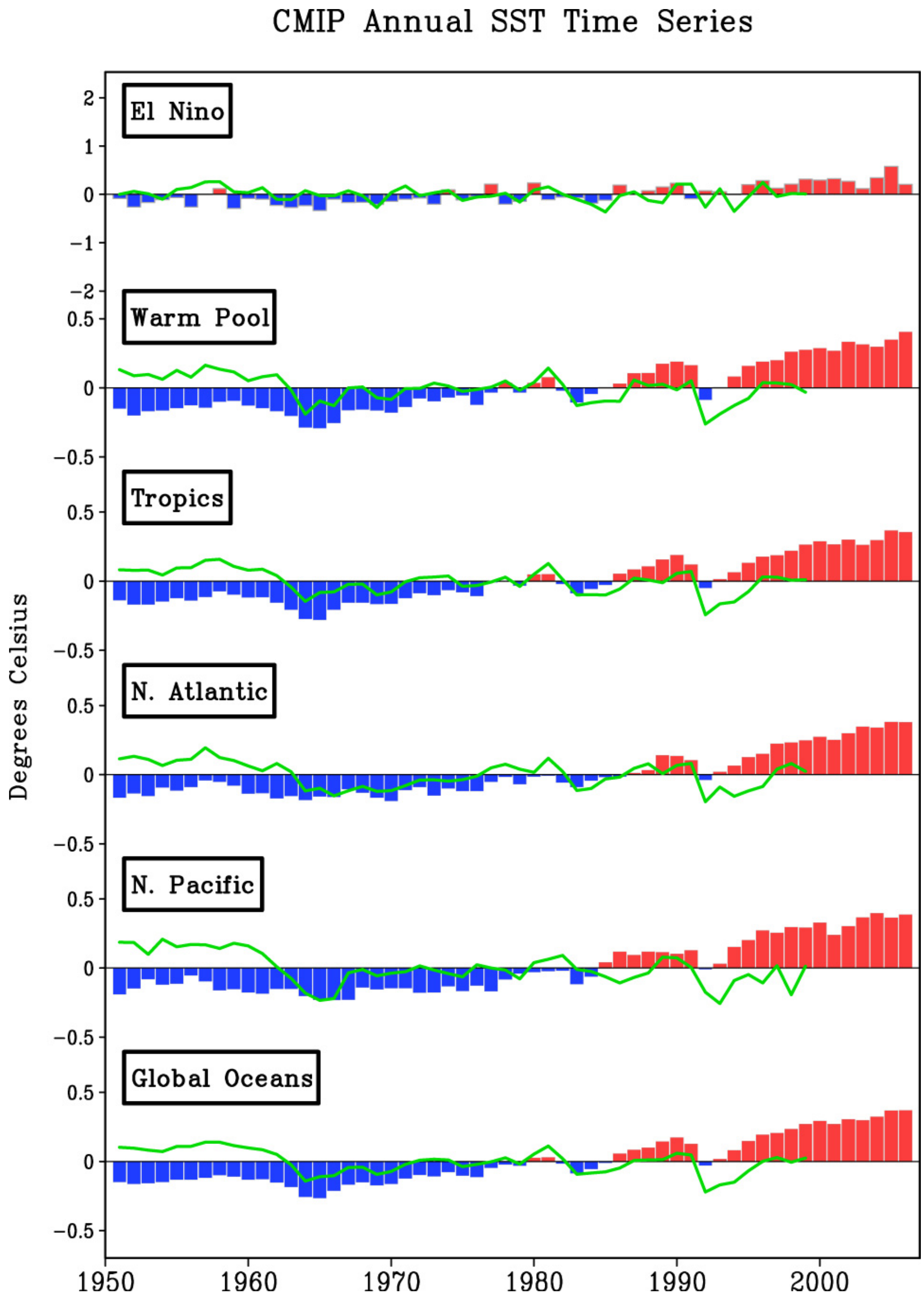

Figure 3.18 CMIP simulated annual mean SST time series for 1951 to 2006. The oceanic regions used to compute the indices are 5°N-5°S, 90°W-150°W for El Niño, 10°S-10°N, 60°E-150°E for the warm pool, 30°S-30°N for the tropics, 30°N-60°N for the North Atlantic, 30°N-60°N for the North Pacific, and 40°S-60°N for the global oceans. Data set is the ensemble mean of 19 CMIP models subjected to the combination of external anthropogenic and natural forcing , and anomalies are calculated relative to each model's 1951 to 2006 reference. Green curve is the surface temperature time series based on the ensemble mean of four CMIP models forced only by time evolving natural forcing (volcanic and solar).

3.4.4.2 Abruptness related to gradual increase of greenhouse gases since 1950

Has the gradual increase in greenhouse gas external forcing triggered threshold-like behavior in climate, and what has been the relevance for North America? There is evidence of abrupt changes of ecosystems in response to anthropogenic forcing that is consistent with tipping point behavior over North America (Adger *et al.*, 2007), and some elements of the physical climate system including sea ice, snow cover, mountainous snow pack, and streamflow have also exhibited rapid change in recent decades (IPCC, 2007a).

There is also some suggestion of abrupt change in ocean surface temperatures. Whereas the net global radiative forcing due to greenhouse gas increases has increased steadily since 1950 (IPCC, 2007a), observed sea surface temperature over the warmest regions of the world ocean - the so-called warm pool - have experienced a rapid shift to warm conditions in the late 1970s (Figure 3.5). In this region covering the Indian Ocean and western tropical Pacific Ocean where surface temperatures can exceed 30°C, the noise of internal SST variability is weak, increasing the confidence in the detection of change. While there is some temporal correspondence between the rapid 1970s emergent warm pool warming in observations and CMIP simulations (Figure 3.18), further research is required to confirm that a threshold-like response of the ocean surface heat balance to steady anthropogenic forcing occurred.

The matter of the relevance of abrupt oceanic warming for North American climate is even less clear. On the one hand, North American surface temperatures also warmed primarily after the 1970s, though not in an abrupt manner. The fact that the AMIP simulations yield a similar behavior suggests some cause-effect link to the oceans. On the other hand, the CMIP simulations generate a steadier rate of North American warming during the reanalysis period, punctuated by brief pauses due to volcanic aerosol-induced cooling events.

3.4.4.3 Abruptness due to unforced chaotic behavior since 1950

Some rapid climate transitions in recent decades appear attributable to chaotic natural fluctuations. One focus of studies has been the consequence of an apparent shift in the character of ENSO events after the 1970s, with more frequent El Niño warming in recent decades (Trenberth and Hoar, 1996).

Abrupt decreases in rainfall occurred over the southwest United States and Mexico in the 1950s and 1960s (Narisma *et al.*, 2007), with a period of enhanced La Niña conditions during that decade being a likely cause (Schubert *et al.*, 2004; Seager *et al.*, 2005). Nonetheless, this dry period, and the decadal period of the Dust Bowl that preceded it over the Great Plains, did not constitute permanent declines in those region's rainfall, despite meeting some criteria for detecting abrupt rainfall changes (Narisma *et al.*, 2007). In part, the ocean conditions that contributed to these droughts did not persist in their cold La Niña state.

An apparent rapid transition of the atmosphere-ocean system over the North Pacific was observed to occur in 1976 to 77. From an oceanographic perspective, changes in ocean heat content and SSTs that happened suddenly over the Pacific basin north of 30°N were caused by atmospheric circulation anomalies (Miller *et al.*, 1994). These consisted of an unusually strong Aleutian Low that developed in the fall season of 1976, a feature that recurred during many successive winters for the next decade (Trenberth, 1990). These surface features were linked with a persistent positive phase of the PNA teleconnection pattern in the free atmosphere as revealed by reanalysis data. The time series of wintertime Alaskan surface temperatures (Figure 3.19) reveals the mild conditions that suddenly emerged after 1976, and this transition in climate was accompanied by significant shifts in marine ecosystems throughout the Pacific basin (Mantua *et al.*, 1997). It is now evident that this Pacific basin-North American event, while perhaps meeting some criteria for a rapid transition, was mostly due to a large scale coupled-ocean atmosphere variation having multidecadal time scale (Latif and Barnett, 1996). It is thus best viewed as a climate "variation" rather than as an abrupt change in the coupled ocean-atmosphere system (Miller *et al.*, 1994). Such multidecadal variations are readily seen in the observed index of the North Pacific SSTs and also the North Atlantic SSTs. Nonetheless, the Alaskan temperature time series also indicates that there has been no return to cooler surface conditions in recent years. While the pace of anthropogenic warming alone during the last half-century has been more gradual that the rapid warming observed over Alaska, the superposition of an internal decadal fluctuation can lend the appearance of an abrupt warming, as Figure 3.19 indicates occurred over western North America in the mid-1970s. It is plausible that the permanency of the shifted surface warmth is rendered by the progressive increase in the strength of the external anthropogenic signal relative to the amplitude of internal decadal variability.

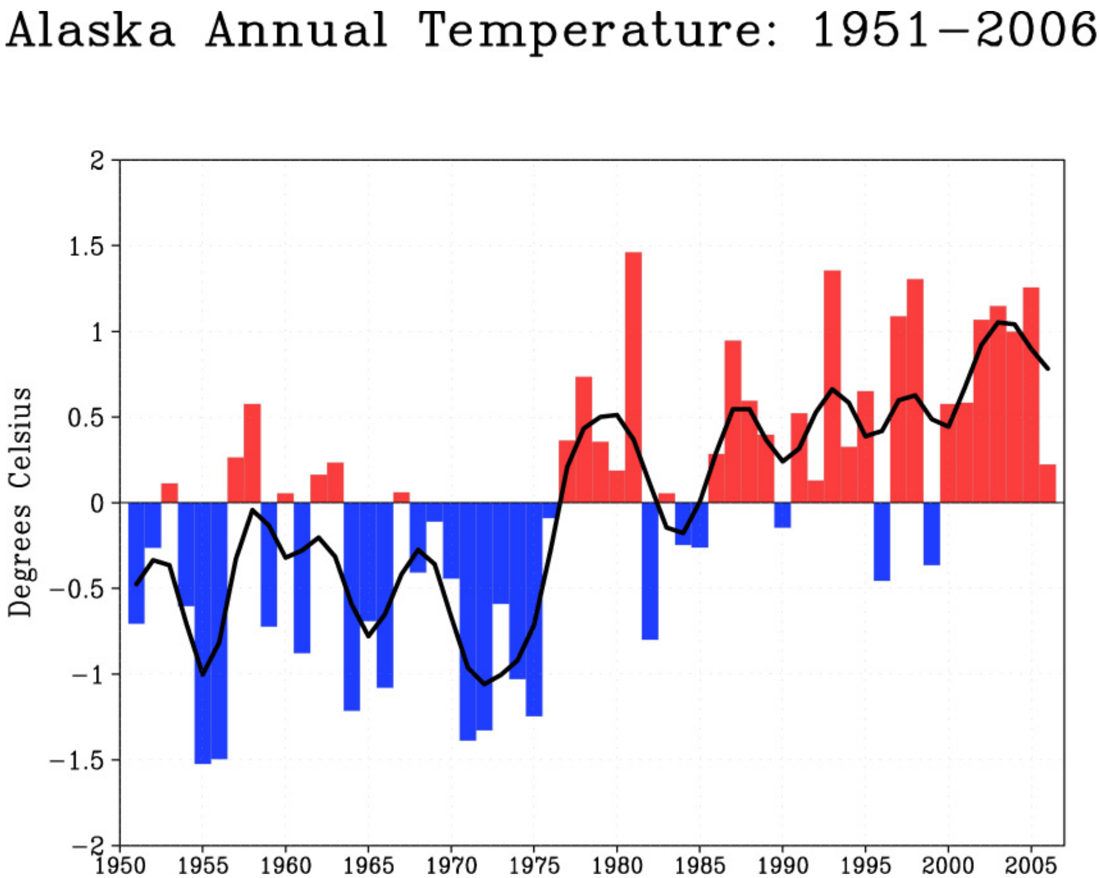

Figure 3.19 Observed Alaska annual surface temperature departures for 1951 to 2006. Anomalies are calculated relative to a 1951 to 2006 reference. Smoothed curve is a 5-point Gaussian filter of the annual departures to emphasize multi-annual variations.

3.5 WHAT IS OUR PRESENT UNDERSTANDING OF THE CAUSES FOR HIGH-IMPACT DROUGHT EVENTS OVER NORTH AMERICA OVER THE REANALYSIS RECORD?

3.5.1. Introduction

Climate science has made considerable progress in understanding the processes leading to drought, in large part owing to the emergence of global observing systems. The analysis of the observational data reveal relationships with atmospheric circulation patterns having large scale, and they illustrate linkages with sea surface temperature patterns as remote from North America as the equatorial Pacific and Indian Ocean. Computing infrastructure - only recently available - is permitting first ever quantifications of the sensitivity of North American climate to various forcings, including ocean temperatures and atmospheric chemical composition.

Such progress, together with the recognition that our Nation's economy suffers dearly during severe droughts, has led to the launch of a National Integrated Drought Information System (NIDIS, 2004) whose ultimate purpose is to develop a timely and useful early warning system for drought.

Credible prediction systems are always enhanced when supported by knowledge of the underlying mechanisms and causes for the phenomenon's variability. In this Chapter, we assess current understanding of the origins of North American drought, focusing on events during the period of abundant global observations since about 1950. Assessments of earlier known droughts (such as the Dust Bowl) serve to identify potential cause-effect relationships that may apply to more recent and future North American regional droughts, and this perspective is provided here as well (see Box 3.3 for discussion of the Dust Bowl).

3.5.2 Definition of Drought

Many definitions for drought appear in the literature, each reflecting its own unique social and economic context in which drought information is desired. Here the focus is on meteorological drought, as opposed to the numerous impacts (and measures) that could be used to characterize drought (*e.g.*, the hydrologic drought indicated by low river flow and reservoir storage, or the agricultural drought indicated by low soil moisture and deficient plant yield).

Meteorological drought has been defined as "a period of abnormally dry weather sufficiently prolonged for the lack of water to cause serious hydrologic imbalance in the affected area." (Huschke, ed.,1959). The American Meteorological Society’s policy statement defines meteorological drought as a departure from a region's normal balance between precipitation and evapotranspiration (AMS, 1997).

The Palmer Drought Severity Index (PDSI) (Palmer, 1965) measures the deficit in moisture supply relative to its demand at the Earth’s surface, and is employed in this Chapter to illustrate some of the major temporal variations of drought witnessed over North America. The Palmer Drought Index is also useful when intercomparing historical droughts over different geographical regions (*e.g.*, Karl, 1983; Diaz, 1983), and it has been found to be a useful proxy of soil moisture and streamflow deficits that relate to the drought impacts having decision-making relevance (*e.g.*, Dai *et al.*, 2004).

3.5.3 Drought Causes

3.5.3.1 Drought statistics, mechanisms and processes

The North American continent has experienced numerous periods of drought during the reanalysis period. Figure 3.20 illustrates the time variability of areal coverage of severe drought since 1951, and on average 10% (14%) of the area of the conterminous (western) United States experiences severe drought each year. The average PDSI for the western states during this time period is shown in the bottom panel; while it is very likely dominated by internal variability, the severity of the recent drought compared with others since 1950 is also apparent.

BOX 3.5 Drought Attribution and Use of Reanalysis Data

The indications for drought itself, such as the Palmer Drought severity Index (PDSI) or precipitation, are not derived from reanalysis data, but from the network of surface observations. The strength of reanalysis data lies in its depiction of the primary variables of the free atmospheric circulation and linking them with the variability in the PDSI. As discussed in Chapter 3, the development and maintenance of atmospheric ridges is the prime ingredient for drought conditions, and reanalysis data is useful for understanding the etymology of such events: their relationship to initial atmospheric conditions, potential downstream and upstream linkages, and the circulation response to soil moisture deficits and SST anomalies. Many drought studies compare model simulations of hypothetical causes to observed atmospheric circulation parameters; reanalysis data can help differentiate among the different possible causes by depicting key physical processes by which drought events evolved.

For final attribution, the drought mechanism must be related to either a specific forcing or internal variability. Reanalysis data, available only since about 1950, is of too short a length to provide a firm indication of internal variability. It also does not indicate (or utilize) direct impact of changing climate forcings, such as increased greenhouse gases or varying solar irradiance. The relationship of atmospheric circulation changes to these forcings must be provided by empirical correlation or, better yet, General Circulation Model (GCM) studies where cause and effect can be directly related.

************ END BOX 3.5 *************

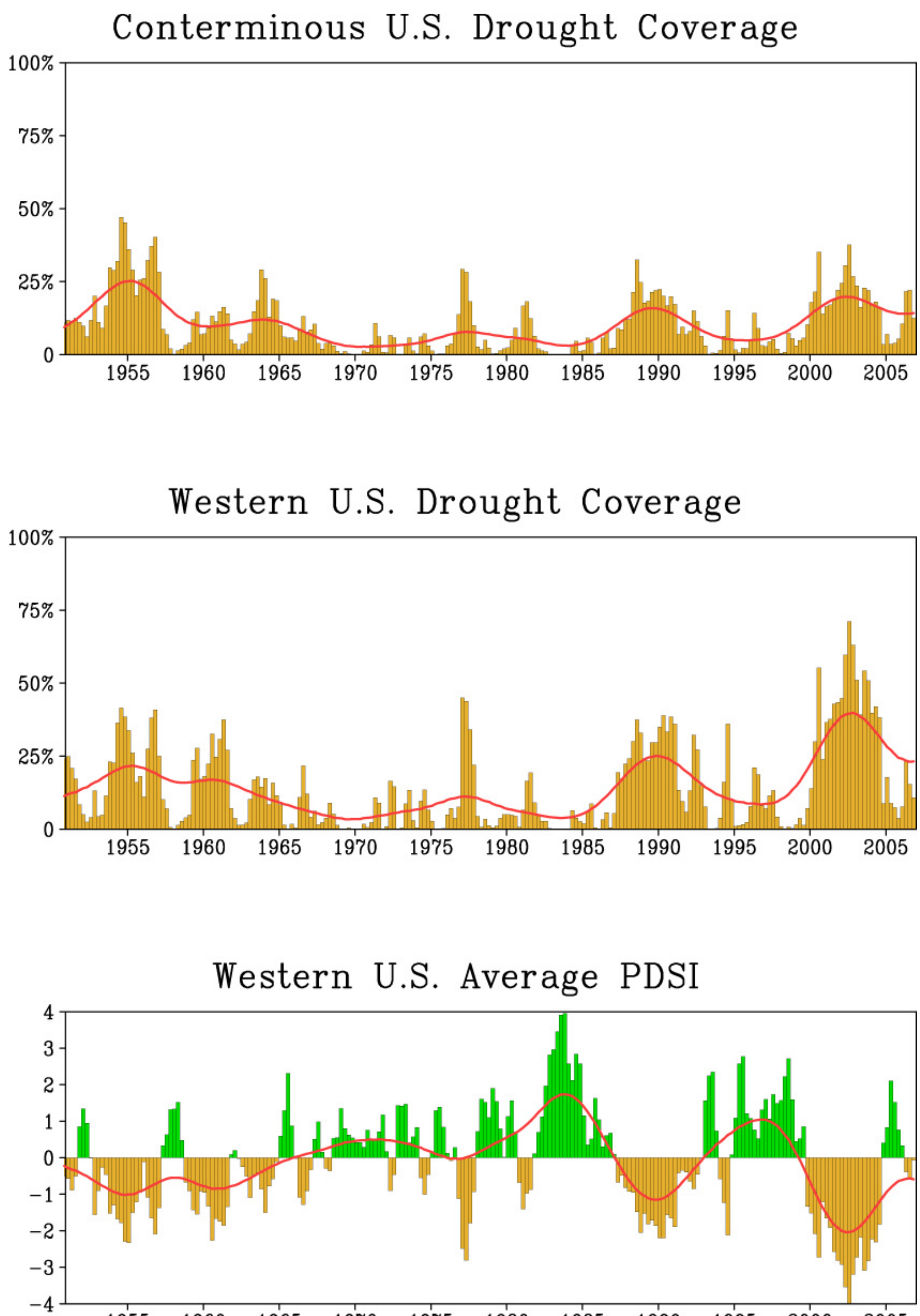

Figure 3.20 Percentage of conterminous United States (top) and western United States (middle) covered by severe or extreme drought, as defined by Palmer Drought Severity Index < -3. Time series of the western United States area averaged PDSI. Positive (Negative) PDSI indicative of above (below) average surface moisture conditions. The Western United States consists of the 11 western-most conterminous U.S. states. Red lines depict time series smoothed with a 9-point Gaussian filter in order to emphasize lower frequency variations.

The middle of the twentieth century began with severe drought that covered much of the United States. Figure 3.21 illustrates the observed surface temperature (top) and precipitation anomalies (bottom) during the early 1950s drought. The superimposed contours are of the 500 mb height from reanalysis data that indicates one of the primary causal mechanisms for drought: high pressure over and upstream that steers moisture-bearing storms away from the drought-affected region.

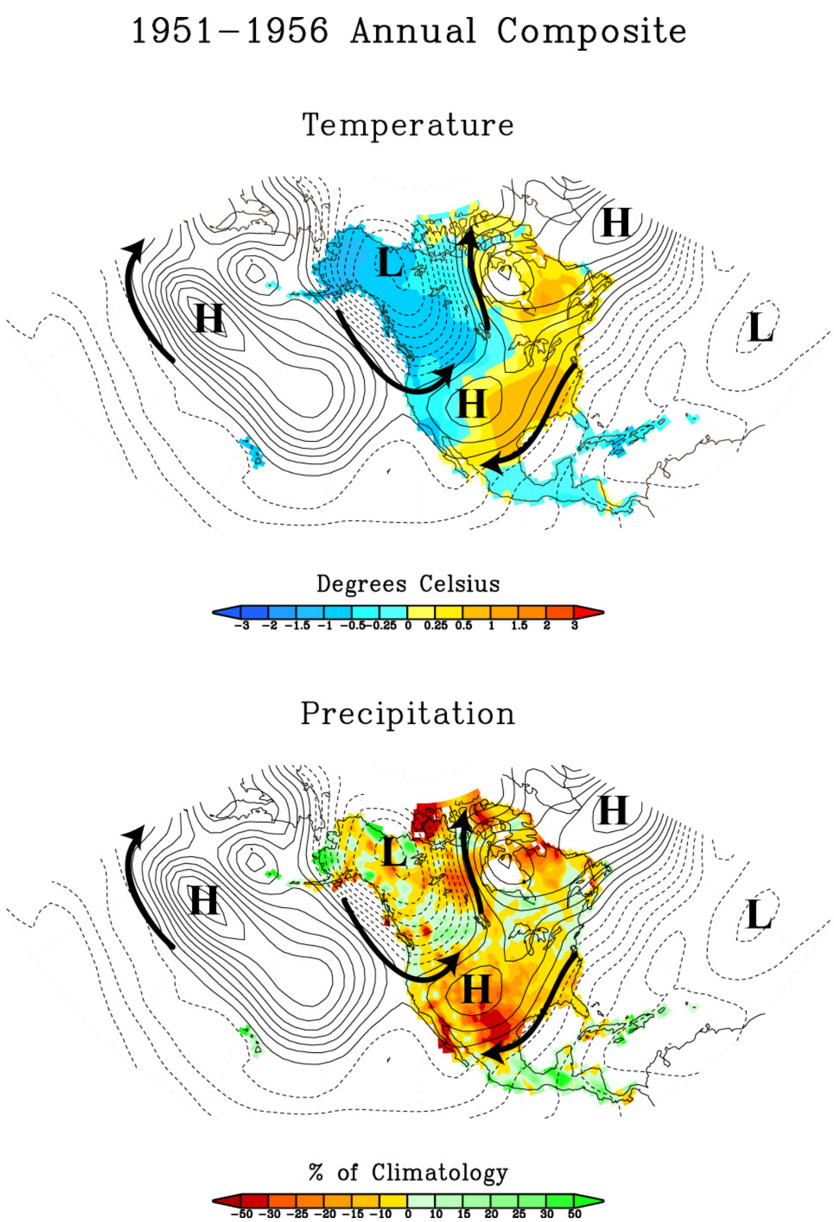

Figure 3.21 Observed climate conditions averaged for 1951 to 1956 during a period of severe Southwest United States drought. The 500mb height field (contours, units 2m) is from the NCEP/NCAR R1 reanalysis. The shading indicates the five-year averaged anomaly of the surface temperature (top) and precipitation (bottom). The surface temperature and precipitation are from independent observational data sets. Anomalous High and Low Pressure regions are highlighted. Arrows indicate the anomalous wind direction, which circulates around the High and Low Pressure centers in a clockwise (counterclockwise) direction.

The northeast United States had severe drought from about 1962 to 1966, with dry conditions extending southwestward into Texas. While the 1970s were relatively free from severe drought, since 1980 there has been an increased frequency of what the National Climatic Data Center (NCDC) refers to as “billion dollar U.S. weather disasters,” many of which are drought events: (1) Summer 1980, central/eastern U.S.;(2) Summer 1986, southeastern U.S.; (3) Summer 1988, central/eastern U.S.; (4) Fall 1995 to Summer 1996, U.S. southern plains; (5) Summer 1998, U.S. southern plains; (6) Summer 1999, eastern U.S.; (7) 2000 to 2002 western U.S./U.S. Great Plains; (8) Spring/summer 2006, centered in Great Plains but widespread.

The droughts discussed above cover various parts of the United States, but in fact droughts are much more common in the central and southern Great Plains. Shown in Figure 3.22 is the mean summer precipitation over the United States (top) and the seasonal standard deviation for the period 1951 to 2006 (bottom). The largest variability occurs along the 95W meridian, while the lowest variability relative to the average precipitation is in the northeast, a distribution that parallels the occurrence of summertime droughts. This picture is somewhat less representative of droughts in the western United States, a region which receives most of its rainfall during winter.

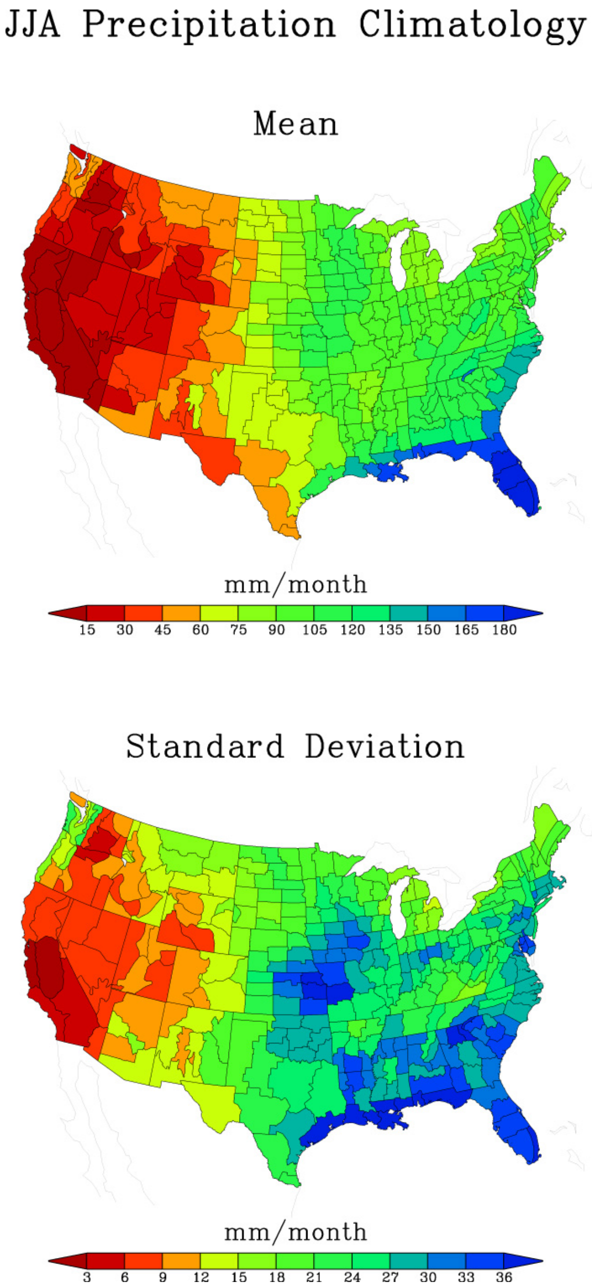

Figure 3.22 Climatological mean (top) and standard deviation (bottom) of summer seasonal mean precipitation over the continental United States for the period 1951 to 2006. Contour intervals are (a) 15 mm month $^{-1}$ and (b) 3 mm day $^{-1}$ (adopted from Ting and Wang, 1997). Data is the NOAA Climate Division data set.

It is natural to ask whether the plethora of recent severe drought conditions identified by NCDC is associated with anthropogenic effects, particularly greenhouse gas emissions. Figure 3.20 shows that the United States area covered by recent droughts (lower panel) is similar to that which prevailed in the 1950s, and is furthermore similar to conditions before the reanalysis period such as the "Dust Bowl" era of the 1930s (Box 3.3). For the western United States (upper panel), paleo-reconstructions of drought conditions indicate that recent droughts are considerably less severe and protracted than those that have been estimated for time periods in the 12th and 13th century from tree ring data (Cook *et al.*, 2004). Hence from a frequency/area standpoint, droughts in the recent decades are not particularly special. To better assess anthropogenic influences on drought, we need to understand the potential causes for these droughts.

While drought can have many definitions, all of the above episodes relate to a specific weather pattern that resulted in reduced rainfall, generally to amounts less than 50% of normal climatological totals. The specific weather pattern in question features an amplified broad-scale high pressure area (ridge) in the troposphere over the affected region (Figure 3.21). Sinking air motion associated with a ridge reduces summertime convective rainfall, results in clear skies with abundant sunshine reaching the surface, and provides for a low level wind flow that generally prevents substantial moisture advection into the region.

The establishment of a stationary wave pattern in the atmosphere is thus essential for generating severe drought. Such stationary, or blocked atmospheric flow patterns can arise due to mechanisms internal to the atmosphere, and the ensuing droughts can be thought of as due to internal atmospheric processes - so-called unforced variability.

However, the longer the anomalous weather conditions persists, the more likely it is to have some stationary forcing acting as a flywheel to maintain the anomalies.

The droughts discussed above can be distinguished by their duration, with longer lasting events more likely involving forcing of the atmosphere. The atmosphere does not have much heat capacity, and its "memory" of past conditions is relatively short (on the order of a few weeks). Hence the forcing required to sustain a situation over seasons or years would be expected to lie outside of the atmospheric domain, and an obvious candidate with greater heat capacity (and hence a longer "memory") is the ocean. Therefore, most studies have assessed the ability of particular ocean sea surface temperature patterns to generate the atmospheric wave pattern that would result in tropospheric ridges in the observed locations during drought episodes.

Namias (1983) pointed out that the flow pattern responsible for Great Plains droughts, with a ridge over the central United States, also includes other region of ridging, one in the East Central Pacific and the other in the East Central Atlantic. As described in Chapter 2 and Section 3.1, these teleconnections represent a standing Rossby wave pattern. Using 30 years of data, Namias showed that if the "tropospheric high pressure center in the Central Pacific is strong, there is a good probability of low heights along the West Coast and high heights over the Plains" (Namias, 1983). This further suggests that the cause for the stationary ridge is not (completely) local, and may have its origins in the Pacific.

Droughts in the western United States are also associated with an amplified tropospheric ridge, further west than for Great Plains droughts that in winter displaces storm tracks north of the United States/Canadian border. In winter, the ridge is also associated with an amplified Aleutian Low in the North Pacific, and this has been associated with forcing from the tropical eastern Pacific in conjunction with El Niño events (*e.g.*, Namias, 1978), whose teleconnection and resulting United States climate pattern has been discussed in Section 3.1

Could ENSO also be responsible for warm-season droughts? Trenberth *et al.* (1988) and Trenberth and Branstator (1992) suggested on the basis of observations and a simplified linear model of atmospheric wave propagation that colder sea surface temperatures in the tropical eastern Pacific (equatorward of 10°N), the La Niña phase of ENSO, in conjunction with the displacement of warmer water and the Intertropical Convergence Zone (ITCZ) northward in that same region (15-20°N), led to the amplified ridging over the United States in the spring of 1988. While this was the leading theory at the time, the general opinion now is that most of the short-term summer droughts are more a product of initial atmospheric conditions (Namias, 1991; Lyon and Dole, 1995; Liu *et al.*, 1998; Bates *et al.*, 2001; Hong and Kalnay, 2002) amplified by the soil moisture deficits that arise in response to lack of precipitation (Wolfson *et al.*, 1987; Atlas *et al.*, 1993; Hong and Kalnay, 2002).

For droughts that occur on the longer time-scale, various possibilities have been empirically related to dry conditions over specific regions of the United States and

Canada. Broadly speaking, they are associated with the eastern tropical Pacific (La Niñas in particular); the western Pacific/Indian Ocean; the north Pacific; and (for the eastern United States) the western Atlantic Ocean. Cool conditions in the eastern tropical Pacific have been related to annual United States droughts in various studies (Barlow *et al.*, 2001; Schubert *et al.*, 2004, Seager *et al.*, 2005), although they are more capable of influencing the United States climate in late winter when the atmospheric mean state is more conducive to allowing an extratropical influence (Newman and Sardeshmukh, 1998; Lau *et al.*, 2006). Warm conditions in the western Pacific/Indian Ocean region are capable of instigating drought in the United States year-round (Lau *et al.*, 2006) but especially in spring (Chen and Newman, 1998). Warmer conditions in the north Pacific have been correlated with drought in the Great Plains (Ting and Wang, 1997) and the northeast United States (Barlow *et al.*, 2001) although modeling studies often fail to show a causal influence (Wolfson *et al.*, 1987; Trenberth and Branstator, 1992; Atlas *et al.*, 1993). The North Pacific SST changes appear to be the result of atmospheric forcing, rather than the reverse – so even if they are contributing to drought conditions, they may not be the cause of the initial circulation anomalies. Alexander *et al.* (2002) concluded from GCM experiments that roughly one quarter to one half of the variance of the dominant pattern of low frequency (greater than ten year) variability in the North Pacific sea surface temperatures during winter was itself the result of ENSO, which helped intensify the Aleutian Low and increased surface heat fluxes (promoting cooling).

Sea surface temperature perturbations downstream of North America, in the North Atlantic have occasionally been suggested as influencing some aspects of United States drought. For example, Namias (1983) noted that the wintertime drought in the western United States in 1977, one of the most extensive Far Western droughts in recent history, appeared to be responsive to a downstream deep trough over the eastern United States. Warmer sea surface temperatures in the western North Atlantic have the potential to intensify storms in that region. Conversely, colder sea surface temperatures in summer can help intensify the ridge (*i.e.*, the "Bermuda High") that exists in that region. Namias (1966) suggested that just such a cold water regime played an integral part in the Northeast United States spring and summer drought of 1962 to 1965, and Schubert *et al.* (2004) also argue for an Atlantic SST effect on the Dust Bowl, while multi-decadal swings between wet and dry periods over the United States as a whole has been statistically linked with Atlantic SST variations of similar time-scale (McCabe *et al.*, 2004; Figure 3.5).

In Mexico, severe droughts during the reanalysis period were noted primarily in the 1950s, and again in the 1990s. This latter time period featured seven consecutive years of drought (1994 to 2000). As in the United States, droughts in Mexico have been linked to tropospheric ridges that can affect northern Mexico, and also to ENSO. However, there exist additional factors tied to Mexico's complex terrain and its strong seasonal monsoon rains. Mexican rainfall in the warm season is associated with the North American Monsoon System (NAMS) driven by solar heating, from mid-May into July. Deficient warm season rainfall over much of the country is typically associated with El Niño events. La Niña conditions often produce increased rainfall in southern and northeastern Mexico, but have been associated with drought in northwestern Mexico (Higgins *et al.*, 1999). During winter and early spring, there is a clear association with the ENSO cycle (*e.g.*, Stahle *et al.*, 1998), with enhanced precipitation during El Niño events, associated with a strengthened subtropical jet that steers storms to lower latitudes, and reduced rainfall with La Niñas when the jet moves poleward.

Therefore the occurrence of drought in Mexico is heavily dependent on the state of the ENSO cycle, or its teleconnection to the extratropics, and on solar heating variations. In the warm season there is often an out-of-phase relationship between southern and northern Mexico, and between spring and summer, dependent on the phasing of the NAMS (Therrell *et al.*, 2002). These aspects make attribution of recent droughts difficult. For example, the consecutive drought years from 1994 to 2000 occurred over several different phases of ENSO, suggesting multiple causes including El Niño conditions for warm season drought through 1998, the possible influence of Western Pacific/Indian Ocean warming during the subsequent La Niña phase, and internal atmospheric variability.

Because a large proportion of the variance of drought conditions over North America is unrelated to sea surface temepratature perturbations, it is conceivable that when a severe drought occurs, it is because numerous mechanisms are acting in tandem. This was the conclusion reached in association with the recent United States drought (1999 to 2005) that affected large areas of the southern, western and central United States. During this time, warm conditions prevailed over the Indian Ocean/Western Pacific region along with La Nina conditions in the eastern tropical Pacific – influences from both regions working together may have helped intensify/prolong the annual droughts (Hoerling and Kumar, 2003; Lau *et al.*, 2006).

3.5.3.2 Anthropogenic influences on North American drought since 1951

To the extent that ENSO cycle variations, in particular La Niñas, are the cause of drought in the United States it would be hard to make the case that they are related to greenhouse gas forcing. While it is true that some studies (Clement *et al.*, 1996) have suggested that La Niña conditions will be favored as climate warms, in fact more intense El Niño events have occurred since the late 1970s, perhaps due at least in part to anthropogenic warming of the eastern equatorial Pacific (Mendelssohn *et al.*, 2005). There is a tendency in model projections for the future greenhouse-gas warmed climate to indicate a mean shift towards more El Niño-like conditions in the tropical east Pacific Ocean including the overlying atmospheric circulation; this latter aspect may already be occurring (Vecchi and Soden, 2007). With respect to anthropogenic influence on ENSO variability, Merryfield (2006) surveyed 15 coupled atmosphere-ocean models and found that for future projections, almost half exhibited no change, five showed reduced variability, and three increased variability. Hence to the extent that La Niña conditions are associated with United States drought there is no indication that they have been or will obviously be influenced by anthropogenic forcing.

However, given that SST changes in the Western Pacific/Indian Ocean are a factor for long-term United States drought, a somewhat different story emerges. Shown in Figure 3.23 are the SST anomalies in this region, as well as the tropical central-eastern Pacific

(Lau *et al.*, 2006). As noted with respect to the recent droughts, the Western Pacific/Indian Ocean region has been consistently warm when compared with the 1971 to 2000 sea surface temperature climatology. What has caused this recent warming?

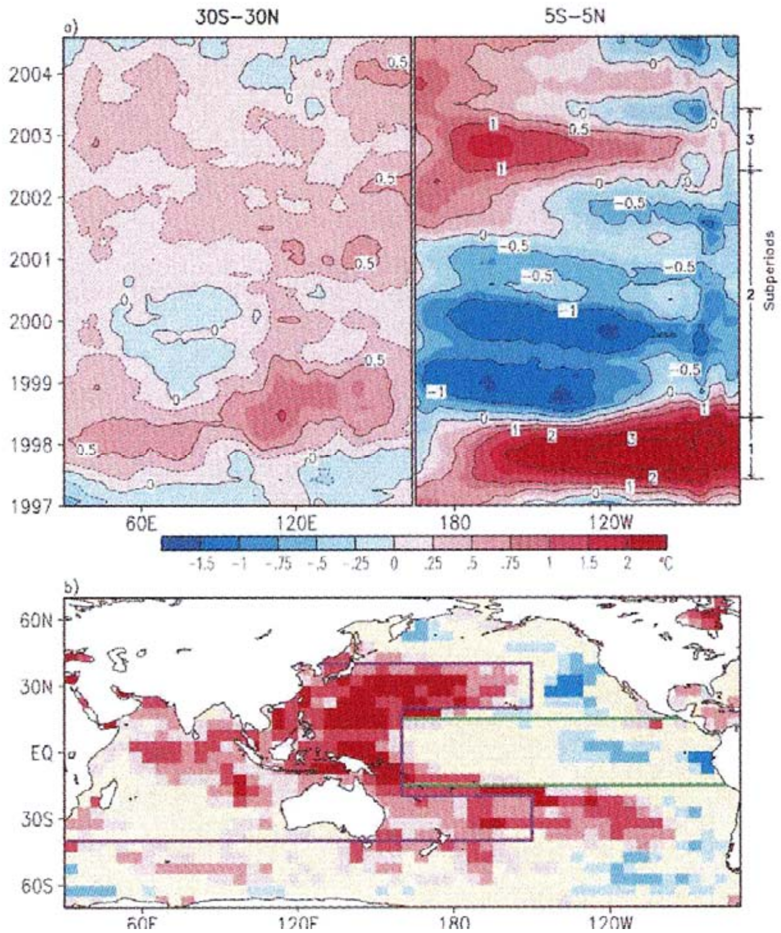

Figure 3.23 Top panel: Sea surface temperature anomalies relative to the period 1970 through 2000 as a function of year in the Indian Ocean/West Pacific (left) and Central-Eastern Pacific (right) (from Lau *et al.*, 2006). Bottom panel: Number of 12-month periods in June 1997-May 2003 with SST anomalies at individual 5° (lat) / 5° (lon) rectangles being above normal (red shading) or below normal (blue shading) by more than one-half of a standard deviation (0.5).

To be sure, more frequent El Niños would by themselves result in increased temperatures in the Indian Ocean, acting through an atmospheric bridge that alters the wind and perhaps cloud field in the Indian Ocean (Klein *et al.*, 1999; Yu and Rienecker, 1999; Alexander *et al.*, 2002; Lau and Nath, 2003); an oceanic bridge between the Pacific and

Indian Ocean has also been modeled ((Bracco *et al.*, 2007). (This effect could then influence droughts over the United States in the summer after an El Nino, as opposed to the direct influence of La Nina [Lau *et al.*, 2005]).

Nevertheless, as shown in Figure 3.23, the warming in the West Pacific/Indian Ocean region has occurred over different phases of the ENSO cycle, making it less likely that the overall effect is associated with it. Hoerling and Kumar (2003) note that "the warmth of the tropical Indian Ocean and the west Pacific Ocean was unsurpassed during the 20th century"; the region has warmed about 1°C since 1950. That is within the range of warming projected by models due to anthropogenic forcing for this region and is outside the range expected from natural variability, at least as judged by coupled atmosphere-ocean model output of the CMIP simulations. (Hegerl *et al.*, 2007, Chapter 9; see in particular Figure 9.12). The comparison of the observed warm pool SST time series with those of the CMIP simulations in previous sections of Chapter 3 indicates that it is very likely that the recent warming of SSTs over the Western Pacific/Indian Ocean region is of anthropogenic origins.

The possible poleward expansion of the subtropical region of descent of the Hadley Circulation is an outcome that is favored by models in response to a warming climate (IPCC, 2007a). It would in effect transfer the dry conditions of northern Mexico to the United States Southwest and southern Great Plains; Seager *et al.* (2007) suggest that may already be happening associated with drought in the southwestern United States.

Additional observations and modeling improvements will be required to assess with greater confidence the likelihood of its occurrence.

An additional impact of greenhouse warming is a likely increase in evapotranspiration during drought episodes because of warmer land surface temperatures. It was noted in the discussion of potential causes that reduced soil moisture from precipitation deficits helped sustain and amplify drought conditions, as the surface radiation imbalance increased with less cloud cover, and sensible heat fluxes increased in lieu of latent heat fluxes. This effect would not have *initiated* drought conditions but would be an additional factor, and one that is likely to grow as climate warms. For example, drier conditions have been noted in the northeast United States despite increased annual precipitation, due to a century-long warming (Groisman *et al.*, 2004), and this appears to be true for Alaska and southern and western Canada as well (Dai *et al.*, 2004). Droughts in the western United States also appear to have been influenced by increasing temperature (Andreadis and Lettenmaier, 2006; Easterling *et al.*, 2007). The area of forest fires in Canada has been high since 1980 compared with the previous 30 years and Alaska experienced record high years in 2004 and 2005 (Soja *et al.*, 2007). Hence global warming by adding additional water stress can exacerbate naturally occurring droughts, in addition to influencing the meteorological conditions responsible for drought.

A further suggestion of the increasing role played by warm surface temperatures on drought is given in Figure 3.24. Shown is a diagnosis of conditions during the recent Southwest United States drought, with contours depicting the atmospheric circulation pattern based on reanalysis data, and shading illustrating the surface temperature anomaly (top) and precipitation anomaly (bottom). High pressure conditions prevailed across the entire continent during the period, acting to redirect storms far away from the region. Continental-scale warmth during 1999 to 2004 was also consistent with the anthropogenic signal. It is plausible that the regional maximum in warmth seen over the Southwest during this period was in part a feedback from the persistently below normal precipitation, together with the anthropogenic signal. Overall, the warmth associated with this recent drought has been greater than that observed during the 1950s drought in the Southwest (Figure 3.21), likely augmenting its negative impacts on water resource and ecologic systems compared to its predecessor

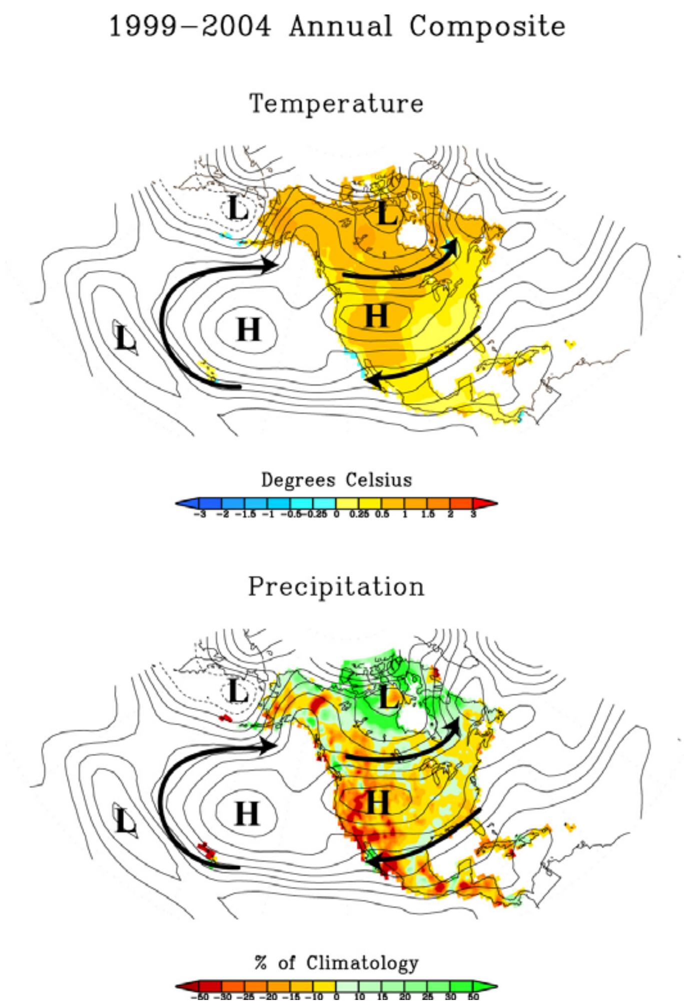

Figure 3.24 Observed climate conditions averaged for 1999 to 2004 during a period of severe southwest United States drought. The 500mb height field (contours, units 2m) is from the NCEP/NCAR R1 reanalysis. The shading indicates the 5-year averaged anomaly of the surface temperature (top) and precipitation (bottom). The surface temperature and precipitation are from independent observational data sets. Anomalous High and Low Pressure regions are highlighted. Arrows indicate the anomalous wind direction, which circulates around the High and Low Pressure centers in a clockwise (counterclockwise) direction.

Breshears *et al.* (2005) estimated the vegetation die-off extent across southwestern North America during the recent drought. The combination of drought with pine bark beetle infestation resulted in >90% loss in Piñon pine trees in some areas. They noted that such a response was much more severe than during the 1950s drought, arguing that the recent drought's greater warmth was the material factor explaining this difference.

Our current understanding is far from complete concerning the origin of individual droughts, both on the short- and long-time scale. While the assessment as discussed here has emphasized the apparently random nature of short-term droughts, a product of initial conditions which then sometimes develop rapidly into strong tropospheric ridges, the exact relationship of such phenomena to sea surface temperature patterns, including the ENSO cycle, is still being debated. The ability of North Atlantic sea surface temperature anomalies to influence the upstream circulation still needs further examination in certain circumstances, especially with respect to droughts in the eastern United States The exact mechanisms for influencing Rossby wave development downstream, including the role of transients relative to stationary wave patterns, will undoubtedly be the subject of continued research. The Hadley Cell response to climate change, as noted above, is still uncertain. And while some modeling studies have emphasized the role played by surface soil moisture deficits in exacerbating these droughts, the magnitude of the effect is somewhat model-dependent, and future generations of land-vegetation models may act somewhat differently.

Given these uncertainties, we conclude from the above analysis that of the severe droughts that have impacted North America over the past five decades, the short term (monthly-seasonal) events are most likely to be primarily the result of initial atmospheric conditions, subsequently amplified by local soil moisture conditions, and in some cases initiated by teleconnection patterns driven in part by SST anomalies. For the longer-term events, the effect of steady forcing through sea surface temperature anomalies becomes more important. Also, the accumulating greenhouse gases and global warming have increasingly been felt as a causative factor, primarily through their influence on Indian Ocean/West Pacific temperatures, conditions to which North American climate is sensitive. The severity of both short- and long-term droughts has *likely* been amplified by local greenhouse gas warming in recent decades.

CHAPTER 3 REFERENCES

Adger, W.N., S. Agrawala, M.M.Q. Mirza, C. Conde, K. O'Brien, J. Pulhin, R. Pulwarty, B. Smit and K. Takahashi, 2007: Assessment of adaptation practices, options, constraints and capacity. In: *Climate Change 2007: Impacts, Adaptation and Vulnerability.* Contribution of Working Group II to the Fourth Assessment Report (AR4) of the Intergovernmental Panel on Climate Change [M.L. Parry, O.F. Canziani, J.P. Palutikof, P.J. van der Linden and C.E. Hanson, (eds.)]. Cambridge University Press, Cambridge, UK, and New York, pp. 717-743.

Alexander, M.A., I. Bladé, M. Newman, J.R. Lanzante, N.-C. Lau, and J.D. Scott, 2002: The atmospheric bridge: the influence of ENSO teleconnections on air-sea interaction over the global oceans. *Journal of Climate*, **15(16)**, 2205-2231.

Allen, M.R. and S.F.B. Tett, 1999: Checking for model inconsistency in optimal fingerprinting. *Climate Dynamics*, **15(6)**, 419-434.

Alley, R.B., J. Marotzke, W.D. Nordhaus, J.T. Overpeck, D.M. Peteet, R.A. Pielke, Jr., R.T. Pierrehumbert, P.B. Rhines, T.F. Stocker, L.D. Talley, and J.M. Wallace, 2003: Abrupt climate change. *Science*, **299(5615)**, 2005-2010.

AMS (American Meteorological Society, 1997: Policy Statement on Meteorological Drought, at <http://www.ametsoc.org/policy/drought2.html>.

Andreadis, K.M. and D.P. Lettenmaier, 2006: Trends in 20th century drought over the continental United States. *Geophysical Research Letters*, **33**, L10403, doi:10.1029/2006GL025711.

Atlas, R., N. Wolfson and J. Terry, 1993: The effect of SST and soil moisture anomalies on GLA model simulations of the 1988 U. S. summer drought. *Journal of Climate*, **6(11)**, 2034-2048.

Barlow, M., S. Nigam and E.H. Berbery, 2001: ENSO, Pacific decadal variability, and U. S. summertime precipitation, drought and stream flow. *Journal of Climate*, **14(9)**, 2105-2128.

Barnston, A.G., A. Kumar, L. Goddard, and M.P. Hoerling. 2005. Improving seasonal prediction practices through attribution of climate variability. *Bulletin of the American Meteorological Society*, **86(1)**, 59-72.

Barsugli, J.J. and P.D. Sardeshmukh, 2002: Global atmospheric sensitivity to tropical SST anomalies throughout the Indo-Pacific basin. *Journal of Climate*, **15(23)**, 3427-3442.

Bates, G.T., M.P. Hoerling, and A. Kumar, 2001: Central U. S. springtime precipitation extremes: teleconnections and relationships with sea surface temperature. *Journal of Climate*, **14(17)**, 3751-3766.

Bengtsson, L., M. Kanamitsu, P. Kallberg, and S. Uppala, 1982: FGGE 4-dimensional data assimilation at ECMWF. *Bulletin of the American Meteorological Society*, **63(1)**, 29-43.

Bjerknes, J., 1966: A possible response of the atmospheric Hadley circulation to equatorial anomalies of ocean temperature. *Tellus*, **18(4)**, 820-828.

Bjerknes, J., 1969: Atmospheric teleconnections from the equatorial Pacific. *Monthly Weather Review*, **97(3)**, 163-172.

Bracco, A., F. Kucharski, F. Molteni, W. Hazeleger and C. Severjins, 2007: A recipe for simulating the interannual variability of the Asian summer monsoon and its relation with ENSO. *Climate Dynamics***, 28(5)**, 441-460.

Breshears, D.D., N.S. Cobb, P.M. Rich, K.P. Price, C.D. Allen, R.G. Balice, W.H. Romme, J.H. Kastens, M.L. Floyd, J. Belnap, J.J. Anderson, O.B. Myers, and C.W. Meyer, 2005: Regional vegetation die-off in response to global-change type drought. *Proceedings of the National Academy of Sciences*, **102(42)**, 15144-15148.

Broecker, W.S., 1975: Climatic change: Are we on the brink of a pronounced global warming? *Science*, **189(4201)**, 460-463.

Broecker, W.S., 2003: Does the trigger for abrupt climate change reside in the ocean or in the atmosphere? *Science*, **300(5625)**, 1519-1522.

Brohan, P., J.J. Kennedy, I. Harris, S.F.B. Tett and P.D. Jones, 2006: Uncertainty estimates in regional and global observed temperature changes: a new dataset from 1850. *Journal of Geophysical Research,* **111**, D12106, doi:10.1029/2005JD006548.

Cai, M. and. E. Kalnay, 2005: Can reanalysis have anthropogenic climate trends without model forcing? *Journal of Climate*, **18(11)**, 1844-1849.

Chen, P. and M. Newman, 1998: Rossby wave propagation and the rapid development of upper-level anomalous anticyclones during the 1988 U. S. drought. *Journal of Climate,* **11(10)**, 2491-2504.

Chen, M., P. Xie, J. E. Janowiak and P.A. Arkin, 2002: Global land precipitation: a 50-year monthly analysis based on gauge observations. *Journal of Hydrometeorology*, **3(3)**, 249-266.

Christy, J.R., W.B. Norris, K. Redmond, and K.P. Gallo, 2006: Methodology and results of calculating central California surface temperature trends: evidence of human-induced climate change? *Journal of Climate,* **19(4)**, 548-563.

Church, J.A., N.J. White, and J.M. Arblaster, 2005: Significant decadal-scale impact of volcanic eruptions on sea level and ocean heat content. *Nature*, **438(7064)**, 74-77.

Clarke, P., N. Pisias, T. Stocker, and A. Weaver, 2002: The role of the thermohaline circulation in abrupt climate change. *Nature*, **415**(6874), 863-869.

Clement, A.C., R. Seager, M.A. Cane, and S.E. Zebiak, 1996: An ocean dynamical thermostat. *Journal of Climate*, **9(9)**, 2190-2196.

CCSP (Climate Change Science Program), *In press*: Weather and Climate Extremes in a Changing Climate. Regions of Focus: North America, Hawaii, Caribbean, and U.S. Pacific Islands. A Report by the U.S. Climate Change Science Program and the Subcommittee on Global Change Research. T. R. Karl, G. A. Meehl, C. D. Miller, S. J. Hassol, A. M. Waple, W. L. Murray, editors. Department of Commerce, NOAA's National Climatic Data Center, Washington, D.C., USA, 166 pp.

Cole, J.E., J.T. Overpeck, and E.R. Cook, 2002: Multiyear La Niña events and persistent drought in the contiguous United States. *Geophysical Research Letters,* **29(13)**, 1647, doi:10.1029/2001GL013561.

Cook, E.R., C.A. Woodhouse, C.M. Eakin, D.M. Meko, and D.W. Stahle, 2004: Long-term aridity changes in the western United States. *Science*, **306(5698)**, 1015-1018.

Dai, A. and K.E. Trenberth, 2004: The diurnal cycle and its depiction in the Community Climate System Model. *Journal of Climate*, **17(5)**, 930-951.

Dai, A., K.E. Trenberth, and T.T. Qian, 2004: A global dataset of Palmer Drought Severity Index for 1870-2002: relationship with soil moisture and effects of surface warming. *Journal of Hydrometeorology,* **5(6)**, 1117-1130.

Daly, C., W.P. Gibson, G.H. Taylor, G.L. Johnson, P. Pasteris, 2002: A knowledge-based approach to the statistical mapping of climate. *Climate Research*, **22(2)**, 99-113.

Delworth, T.L. and T.R. Knutson, 2000: Simulation of early 20th century global warming. *Science*, **287(5461)**, 2246-2250.

Diaz, H.F., 1983: Some aspects of major dry and wet periods in the contiguous United States 1895-1981. *Journal of Climate and Applied Meteorology*, **22(1)**, 3-6.

Feldstein, S.B., 2000: The timescale, power spectra, and climate noise properties of teleconnection patterns. *Journal of Climate*, **13(24)**, 4430-4440.

Feldstein, S., 2002: Fundamental mechanisms of the growth and decay of the PNA teleconnection pattern. *Quarterly Journal of the Royal Meteorological Society*, **128(581)**, 775-796.

Gates, W.L., 1992: AMIP: The Atmospheric Model Intercomparison Project. *Bulletin of the American Meteorological Society*, **73(12)**, 1962-1970.

Gillett, N.P., G.C. Hegrel, M.R. Allen, and P.A. Stott, 2000: Implications of changes in the Northern Hemisphere circulation for the detection of anthropogenic climate change. *Geophysical Research Letters*, **27(7)**, 993-996.

Gillett, N.P., F.W. Zwiers, A.J. Weaver, and P. A. Stott, 2003: Detection of human influence on sea-level pressure. *Nature*, **422(6929)**, 292-294.

Gillett, N.P., A.J. Weaver, F.W. Zwiers, and M.F. Wehner, 2004: Detection of volcanic influence on global precipitation. *Geophysical Research Letters*, **31**(12), L12217, doi:10.1029/2004GL020044.

Glantz, M.H., R.W. Katz, and N. Nicholls, (eds.), 1991: *Teleconnections Linking Worldwide Climate Anomalies: Scientific Basis and Societal Impact.* Cambridge University Press, Cambridge, UK, and New York, 535 pp.

Groisman, P.Ya., R.W. Knight, T.R. Karl, D.R. Easterling, B. Sun, and J.H. Lawrimore, 2004: Contemporary changes of the hydrological cycle over the contiguous United States: Trends derived from *in situ* observations. *Journal of Hydrometeorology*, **5(1)**, 64-85.

Gwynne, P., 1975: Cooling world. *Newsweek*, **85(April 28)**, 64.

Hale, R.C., K.P. Gallo, T.W. Owen, and T.R. Loveland, 2006: Land use/land cover change effects on temperature trends at U.S. climate normals stations, *Geophysical Research Letters*, **33**, L11703, doi:10.1029/2006GL026358.

Halpert, M.S. and C.F. Roplewski, 1992: Surface temperature patterns associated with the Southern Oscillation. *Journal of Climate*, **5(6)**, 577-593.

Hansen, J., R. Ruedy, M. Sato, M. Imhoff, W. Lawrence, D. Easterling, T. Peterson, and T. Karl, 2001: A closer look at United States and global surface temperature change. *Journal of Geophysical Research,* **106(D20)**, 23947-23963.

Hasselmann, K., 1979: On the signal-to-noise problem in atmospheric response studies. In: *Meteorology Over the Tropical Oceans* [Shaw, D.B. (ed.)]. Royal Meteorological Society, Bracknell (UK), pp. 251-259.

Hasselmann, K., 1997: Multi-pattern fingerprint method for detection and attribution of climate change. *Climate Dynamics*, **13(9)**, 601-612.

Hegerl, G.C., F.W. Zwiers, P. Braconnot, N.P. Gillett, Y. Luo, J. Marengo, N. Nicholls, J.E. Penner, and P.A. Stott, 2007: Understanding and attributing climate change. In: *Climate Change 2007: The Physical Science Basis.* Contribution of Working Group I to the Fourth Assessment Report (AR4) of the Intergovernmental Panel on Climate Change [Solomon, S., D. Qin, M. Manning, Z. Chen, M. Marquis, K.B. Averyt, M.Tignor, and H.L. Miller (eds.)]. Cambridge University Press, Cambridge, UK, and New York, pp. 663-745.

Held, I.M. and M. Ting, 1990: Orographic versus thermal forcing of stationary waves: the importance of the mean low-level wind. *Journal of the Atmospheric Sciences*, **47(4)**, 495-500.

Herweijer, C., R. Seager and E.R. Cook, 2006: North American droughts of the mid to late nineteenth century: a history, simulation and implication for Mediaeval drought. *Holocene*, **16(2)**, 159-171.

Higgins, R.W., Y. Chen and A.V. Douglas, 1999: Interannual variability of the North American warm season precipitation regime. *Journal of Climate*, **12(3)**, 653-680.

Hoerling, M.P. and A. Kumar, 2000: Understanding and predicting extratropical teleconnections related to ENSO. In: "*El Niño and the Southern Oscillation: Multi-scale Variability, and Global and Regional Impacts* [Diaz, H.F. and V. Markgraf, (eds.)], Cambridge University Press, Cambridge, UK, and New York, pp. 57-88.

Hoerling, M.P. and A. Kumar, 2002: Atmospheric response patterns associated with tropical forcing. *Journal of Climate*, **15(16)**, 2184-2203.

Hoerling, M. and A. Kumar, 2003: The perfect ocean for drought. *Science*, **299(5607)**, 691-694.

Hoerling, M.P., J.W. Hurrell, T.Y. Xu, 2001: Tropical origins for recent North Atlantic climate change. *Science*, **292(5514)**, 90-92.

Hoerling, M.P., J. W. Hurrell , T. Xu , G. T. Bates, and A. Phillips, 2004: Twentieth century North Atlantic climate change. Part II: understanding the effect of Indian Ocean warming. *Climate Dynamics* **23(3-4)**, 391-405.

Hoerling, M., J. Eischeid, X. Quan, and T. Xu, 2007: Explaining the record US warmth of 2006. *Geophysical Research Letters*, **34**, L17704, doi:10.1029/2007GL030643.

Hong, S-Y. and E. Kalnay, 2002: The 1998 Oklahoma-Texas drought: mechanistic experiments with NCEP global and regional models. *Journal of Climate*, **15(9)**, 945-963.

Horel, J.D. and J.M. Wallace, 1981: Planetary-scale atmospheric phenomena associated with the Southern Oscillation. *Monthly Weather Review*, **109(4)**, 813-829.

Hoskins, B.J. and D.J. Karoly, 1981: The steady linear response of a spherical atmosphere to thermal and orographic forcing. *Journal of the Atmospheric Sciences,* **38(6)**, 1179-1196.

Houghton, J.T. , L.G. Meira Filho, B.A. Callander, N. Harris, A. Kattenberg, and K. Maksell (eds.), 1996: *Climate Change 1995: The Science of Climate Change*. Cambridge University Press, Cambridge, UK, and New York, 572 pp.

Houghton, J.T., Y. Ding, D.J. Griggs, M. Noguer, P.J. van der Linden, X. Dai, K. Maskell, and C.A. Johnson (eds.), 2001: *Climate Change 2001: The Scientific Basis*. Cambridge University Press, Cambridge, UK, and New York, 881 pp.

Hulme, M., 2003: Abrupt climate change: Can society cope? *Philosophical Transactions of the Royal Society of London. Series. A*, **361(1810)**, 2001-2021.

Hurrell, J.W., 1995: Decadal trends in the North-Atlantic Oscillation: regional temperatures and precipitation. *Science*, **269(5224)**, 676-679.

Hurrell, J.W., 1996: Influence of variations in extratropical wintertime teleconnections on Northern Hemisphere temperatures. *Geophysical Research Letters,* **23(6)**, 665-668.

Huschke, R.E. (ed.), 1959: *Glossary of Meteorology*: Boston, American Meteorological Society, 638 pp.

IDAG (International Ad Hoc Detection and Attribution Group), 2005: Detecting and attributing external influences on the climate system: A review of recent advances. *Journal of Climate*, **18(9)**, 1291-1314.

IPCC (Intergovernmental Panel on Climate Change) 2007a: *Climate Change 2007: The Physical Science Basis.* Contribution of Working Group I to the Fourth Assessment Report (AR4) of the Intergovernmental Panel on Climate Change [Solomon, S., D. Qin, M. Manning, Z. Chen, M. Marquis, K.B. Averyt, M.Tignor, and H.L. Miller (eds.)]. Cambridge University Press, Cambridge, UK, and New York, 987 pp. Available at http://www.ipcc.ch

IPCC (Intergovernmental Panel on Climate Change) 2007b: Summary for Policy Makers. In: *Climate Change 2007: Impacts, Adaptation and Vulnerability.* Contribution of Working Group II to the Fourth Assessment Report (AR4) of the

Intergovernmental Panel on Climate Change [Parry, M.L., O.F. Canziani, J.P. Palutikof, P.J. van der Linden and C.E. Hanson, (eds.)]. Cambridge University Press, Cambridge, UK, and New York, pp. 7-22. Available at http://www.ipcc.ch

Kalnay, E. and M. Cai, 2003: Impact of urbanization and land-use on climate change. *Nature*, **423(6939)**, 528-531.

Kalnay, E., M. Kanamitsu, R. Kistler, W. Collins, D. Deaven, L. Gandin, M. Iredell, S. Saha, G. White, J. Woollen, Y. Zhu, M. Chelliah, W. Ebisuzaki, W.Higgins, J. Janowiak, K. C. Mo, C. Ropelewski, J. Wang, A. Leetmaa, R. Reynolds, R. Jenne, and D. Joseph, 1996: The NCEP/NCAR 40-Year Reanalysis Project. *Bulletin of the American Meteorological Society*, **77(3),** 437–471.

Kalnay, E., M. Cai, H. Li, and J. Tobin, 2006: Estimation of the impact of land-surface forcings on temperature trends in eastern Unites States. *Journal of Geophysical Research*, **111**, D06106, doi:10.1029/2005JD006555.

Karl, T.R., 1983: Some spatial characteristics of drought duration in the United States. *Journal of Climate and Applied Meteorology*, **22(8)**, 1356-1366.

Karoly, D.J., and Q. Wu, 2005: Detection of regional surface temperature trends. *Journal of Climate*, **18(21)**, 4337–4343.

Karoly, D.J., K. Braganza, P.A. Stott, J. Arblaster, G. Meehl, A. Broccoli, K.W. Dixon, 2003: Detection of a human influence on North American climate. *Science* **302(5648)**, 1200-1203.

Kirchner, I, G. Stenchikov, H.-F. Graf, A. Robock, and J. Antuña, 1999: Climate model simulation of winter warming and summer cooling following the 1991 Mount Pinatubo volcanic eruption. *Journal of Geophysical Research*, **104(D16)**, 19039-19055.

Klein, S.A., B.J. Sodden, and N.-C. Lau, 1999: Remote sea surface variations during ENSO: Evidence for a tropical atmospheric bridge. *Journal of Climate*, **12(4)**, 917-932.

Knutson, T.R., T.L. Delworth, K.W. Dixon, I.M. Held, J. Lu, V. Ramaswamy, M.D. Schwarzkopf, G. Stenchikov, and R.J. Stouffer, 2006: Assessment of twentieth-century regional surface temperature trends using the GFDL CM2 coupled models. *Journal of Climate*, **19(9)**, 1624–1651.

Kueppers, L.M., M.A. Snyder, L.C. Sloan, D. Cayan, J. Jin, H. Kanamaru, M. Kanamitsu, N.L. Miller, M. Tyree, H. Du, B. Weare, 2007: Seasonal temperature responses to landuse change in the western United States. *Global and Planetary Change*, **60(3-4)**, 250-264.

Kukla, G.J. and R.K. Matthews, 1972: When will the present interglacial end? *Science*, **178(4057)**, 190-191.

Kumar, A., W. Wang, M.P. Hoerling, A. Leetmaa, and M. Ji, 2001: The sustained North American warming of 1997 and 1998. *Journal of Climate*, **14(3)**, 345-353.

Kumar, A., F. Yang, L. Goddard, and S. Schubert, 2004: Differing trends in the tropical surface temperatures and precipitation over land and oceans. *Journal of Climate*, **17(3)**, 653-664.

Kunkel, K.E., X.-Z. Liang, J. Zhu, and Y. Lin, 2006: Can CGCMS simulate the twentieth century "warming hole" in the central United States? *Journal of Climate*, **19(17)**, 4137–4153.

Kushnir, Y., W.A., Robinson, I. Bladé, N.M.J. Hall, S. Peng, and R. Sutton, 2002: Atmospheric GCM response to extratropical SST anomalies: synthesis and evaluation. *Journal of Climate*, **15(16)**, 2233-2256.

Lambert, F.H., P.A. Stott, M.R. Allen, and M.A. Palmer, 2004: Detection and attribution of changes in 20th century land precipitation. *Geophysical Research Letters*, **31(10)**, L10203, doi:10.1029/2004GL019545.

Latif, M. and T.P. Barnett, 1996: Decadal climate variability over the North Pacific and North America: dynamics and predictability. *Journal of Climate*, **9(10)**, 2407-2423.

Lau, N.-C and M.J. Nath, 2003: Atmosphere-ocean variations in the Indo-Pacific sector during ENSO episodes. *Journal of Climate*, **16(1)**, 3-20.

Lau, N.-C., A. Leetmaa, M. J. Nath, and H.-L. Wang, 2005: Influences of ENSO-induced Indo-Western Pacific SST anomalies on extratropical atmospheric variability during the boreal summer. *Journal of Climate*, **18(15)**, 2922-2942.

Lau, N.-C., A. Leetmaa and M.J. Nath, 2006: Attribution of atmospheric variations in the 1997-2003 period to SST anomalies in the Pacific and Indian Ocean basins. *Journal of Climate*, **19(15)**, 3607-3628.

L'Heureux, M.L. and D.W.J. Thompson, 2006: Observed relationships between the El Niño-Southern Oscillation and the extratropical zonal-mean circulation. *Journal of Climate*, **19(2)**, 276-287.

Lim, Y.-K., M. Cai, E. Kalnay, and L. Zhou, 2005: Observational evidence of sensitivity of surface climate changes to land types and urbanization. *Geophysical Research Letters*, **32**, L22712, doi:10.1029/2005GL024267.

Liu, A.Z., M. Ting and H. Wang, 1998: Maintenance of circulation anomalies during the 1988 drought and 1993 floods over the United States. *Journal of the Atmospheric Sciences*, **55(17)**, 2810-2832.

Livezey, R.D. and T.M. Smith, 1999: Covariability of aspects of North American climate with global sea surface temperatures on interannual to interdecadal timescales. *Journal of Climate*, **12(1)**, 289-302.

Livezey, R.E., M. Masutani, A. Leetmaa, H.L. Rui, M. Ji, and A. Kumar, 1997: Teleconnective response of the Pacific-North American region atmosphere to large central equatorial Pacific SST anomalies. *Journal of Climate*, **10(8)**, 1787-1820.

Lyon, B. and R.M. Dole, 1995: A diagnostic comparison of the 1980 and 1988 U. S. summer heat wave-droughts. *Journal of Climate*, **8(6)**, 1658-1675.

Mahmood, R., S.A. Foster, T. Keeling, K.G. Hubbard, C. Carlson, and R. Leeper, 2006: Impacts of irrigation on 20th century temperature in the northern Great Plains. *Global and Planetary Change,* **54(1-2)***,* 1-18.

Mantua, N.J., S.R. Hare, Y. Zhang, J.M. Wallace, and R.C. Francis, 1997: A Pacific inter-decadal climate oscillation with impacts on salmon production. *Bulletin of the American Meteorological Society*, **78(6)**, 1069-1079.

McCabe, G.J., M.A. Palecki, and J.L. Betencourt, 2004: Pacific and Atlantic Ocean influences on multidecadal drought frequency in the United States. *Proceedings of the National Academy of Sciences*, **101(12)**, 4136-4141.

McPherson, R.A., 2007: A review of vegetation–atmosphere interactions and their influences on mesoscale phenomena. *Progress in Physical Geography*, **31(3)**, 261-285.

Mendelssohn, R., S.J. Bograd, F.B. Schwing, and D.M. Palacios, 2005: Teaching old indices new tricks: A state-space analysis of El Nino related climate indices. *Geophysical Research Letters*, **32**, L07709, doi:10.1029/2005GL022350.

Merryfield, W.J., 2006: Changes to ENSO under CO_2 doubling in a multimodal ensemble. *Journal of Climate*, **19(16)**, 4009-4027.

Miller, A.J., D.R. Cayan, T.P. Barnett, N.E. Graham, and J.M. Oberhuber, 1994: The 1976-77 climate shift of the Pacific Ocean. *Oceanography*, **7(1)**, 21-26.

Mitchell, J.F.B., D.J. Karoly, G.C. Hegerl, F.W. Zwiers, M.R. Allen, and J. Marengo, 2001: Detection of climate change and attribution of causes. In: *Climate Change 2001: The Scientific Basis.* Contribution of Working Group I to the Third Assessment Report of the Intergovernmental Panel on Climate Change [Houghton, J. T., Y. Ding, D.J. Griggs, M. Noguer, P.J. van der Linden, X. Dai, K. Maskell, and C.A. Johnson (eds.)]. Cambridge University Press, Cambridge, UK, and New York, pp. 695-738.

Namias, J., 1966: Nature and possible causes of the northeastern United States drought during 1962-1965. *Monthly Weather Review*, **94(9)**, 543-554.

Namias, J. 1978: Multiple causes of the North American abnormal winter 1976-77. *Monthly Weather Review*, **106(3)**, 279-295.

Namias, J., 1983: Some causes of United States drought. *Journal of Climate and Applied Meteorology*, **22(1)**, 30-39.

Namias, J., 1991: Spring and summer 1988 drought over the contiguous United States – causes and prediction. *Journal of Climate*, **4(1)**, 54-65.

Narisma, G., J. Foley, R. Licker, and N. Ramankutty, 2007: Abrupt changes in rainfall during the twentieth century. *Geophysical Research Letters*, **34**, L06710, doi:10.1029/2006GL028628.

NIDIS (National Integrated Drought Information System), 2004: Creating a Drought Early Warning System for the 21st Century: The National Integrated Drought Information System (NIDIS). A report of the National Oceanic and Atmospheric Administration and the Western Governor's Association. Available online at: http://www.westgov.org.

NCDC (National Climatic Data Center), 1994: *Time Bias Corrected Divisional Temperature-Precipitation-Drought Index*. Documentation for dataset TD-9640. National Climatic Data Center, Asheville, NC, 12pp. Available at http://www1.ncdc.noaa.gov/pub/data/documentlibrary/tddoc/td9640.pdf

Newman, M. and P.D. Sardeshmukh, 1998: The impact of the annual cycle on the North Pacific/North American response to remote low-frequency forcing. *Journal of the Atmospheric Sciences*, **55(8)**, 1336-1353.

NRC (National Research Council), 1975: *Understanding Climatic Change*. National Academy of Sciences, Washington DC, 239 pp.

NRC (National Research Council), 2002: *Abrupt Climate Change: Inevitable Surprises*. National Academy Press, Washington DC, 230 pp.

Palmer, W.C. 1965. Meteorological drought. Research Paper No. 45, U.S. Department of Commerce Weather Bureau, Washington, D.C.

Peterson, T.C., T.R. Karl, P.F. Jamason, R. Knight, and D.R. Easterling, 1998: First difference method: Maximizing station density for the calculation of long-term global temperature change, *Journal of Geophysical Research,* **103(D20)**, 25967-25974.

Pielke, R.A., Sr., G. Marland, R.A. Betts, T.N. Chase, J.L. Eastman, J.O. Niles, D.S. Niyogi, and S.W. Running, 2002: The influence of land-use change and landscape dynamics on the climate system: relevance to climate-change policy beyond the radiative effect of greenhouse gases. *Philosophical Transactions of the Royal Society of London Series* A, **360(1797)**, 1705-1719.

Rasmusson, E.M. and J.M. Wallace 1983: Meteorological aspects of the El Niño/Southern Oscillation. *Science*, **222(4629)**, 1195-1202.

Robertson, A.W., J.D., Farrara, and C.R. Mechoso, 2003: Simulations of the atmospheric response to South Atlantic sea surface temperature anomalies. *Journal of Climate*, **16(15)**, 2540-2551.

Robinson, W.A., R. Reudy, and J.E. Hansen, 2002: General circulation model simulations of recent cooling in the east-central United States. *Journal of Geophysical Research*, **107(D24)**, 4748, doi:10.1029/2001JD001577

Roeckner, E., K. Arpe, L. Bengtsson, M. Christoph, M. Claussen, L. Dümenil, M. Esch, M. Giorgetta, U. Schlese, U. Schulzweida, 1996: *The Atmospheric General Circulation Model ECHAM-4: Model Description and Simulation of Present-Day Climate*. MPIM Report 218, Max-Planck-Institute for Meteorology, Hamburg, Germany, 90 pp.

Ropelewski, C., 1999: The great El Niño of 1997 and 1998: impacts on precipitation and temperature. *Consequences*, **5(2)**, 17-25.

Ropelewski, C.F. and M.S. Halpert, 1986: North American precipitation and temperature patterns associated with the El Niño/Southern Oscillation (ENSO). *Monthly Weather*

Review, **114(12)**, 2352–2362.

Rossby, C.G., 1939: Relation between variations in the intensity of the zonal circulation of the atmosphere and the displacements of the semi-permanent centers of action. *Journal of Marine Research*, **2(1)**, 38-55.

Rudolf, B. and U. Schneider, 2005: Calculation of gridded precipitation data for the global land-surface using in-situ gauge observations. In: *Proceedings of the 2nd Workshop of the International Precipitation Working Group IPWG*, Monterey, October 2004, pp. 231-247.

Santer, B.D., W. Brüggemann, U. Cubasch, K. Hasselmann, E. Maier-Reimer, and U. Mikolajewicz, 1994: Signal-to-noise analysis of time-dependent greenhouse warming experiments. Part 1: Pattern analysis. *Climate Dynamics*, **9**, 267-285.

Santer, B.D., M.F. Wehner, T.M.L. Wigley, R. Sausen, G.A. Meehl, K.E. Taylor, C. Ammann, J. Arblaster, W.M. Washington, J.S. Boyle, and W. Brüggemann, 2003: Contributions of anthropogenic and natural forcing to recent tropopause height changes. *Science*, **301(5632)**, 479-483.

Santer, B.D., T.M.L. Wigley, P.J. Gleckler, C. Bonfils, M.F. Wehner, K. AchutaRao, T.P. Barnett, J.S. Boyle, W. Brüggemann, M. Fiorino, N. Gillett, J.E. Hansen, P.D. Jones, S.A. Klein, G.A. Meehl, S.C.B. Raper, R.W. Reynolds, K.E. Taylor, and W.M. Washington, 2006: Forced and unforced ocean temperature changes in the Atlantic and Pacific tropical cyclogenesis regions. *Proceedings of the National Academy of Sciences*, **103(38)**, 13905-13910.

Schubert, S.D., M.J. Suarez, P.J. Pegion, R.D. Koster and J.T. Bacmeister, 2004: Causes of long-term drought in the U.S. Great Plains. *Journal of Climate*, **17(3)**, 485-503.

Seager, R., N. Harnik, Y. Kushnir, W. Robinson and J. Miller, 2003: Mechanisms of hemispherically symmetric climate variability. *Journal of Climate*, **16(18)**, 2960-2978.

Seager, R., Y. Kushnir, C. Herweijer, N. Naik and J. Velez, 2005: Modeling of tropical forcing of persistent droughts and pluvials over western North America: 1856-2000. *Journal of Climate*, **18(19)**, 4065-4088.

Seager, R., M. Ting, I. Held, Y. Kushnir, J. Lu, G. Vecchi, H.-P. Huang, N. Harnik, A. Leetmaa, N.-C. Lau, C. Li, J. Velez and N. Naik, 2007: Model projections of an imminent transition to a more arid climate in southwestern North America. *Science*, **316(5828)**, 1181-1184.

Simmons, A.J., J.M. Wallace, and G. Branstator, 1983: Barotropic wave propagation and instability and atmospheric teleconnection patterns. *Journal of the Atmospheric Sciences*, **40(6)**, 1363-1392.

Smith, T.M. and R.W. Reynolds, 2005: A global merged land-air-sea surface temperature reconstruction based on historical observations (1880-1997). *Journal of Climate*, **18(12)**, 2021-2036.

Smith, J.B., H.-J. Schellnhuber, and M.M.Q. Mirza, 2001: Vulnerability to climate change and reasons for concern: a synthesis. In: *Climate Change 2001: Impacts, Adaptation, and Vulnerability*. Contribution of Working Group II to the Report of the Intergovernmental Panel on Climate Change [McCarthy, J.J., O.F. Canziani, M.A. Leary, D.J. Dokken, and K.S. White (eds)]. Cambridge University Press, Cambridge, UK, and New York, pp. 913-967.

Soja, A.J., N.M. Tchebakova, N.H.F. French, M.D. Flannigan, H.H. Shugart, B.J. Stocks, A.I. Sukhinin, E.I. Parfenova, F.S. Chapin III, and P.W. Stackhouse Jr., 2007: Climate-induced boreal forest change: predictions versus current observations. *Global and Planetary Change*, **56(3-4)**, 274-296.

Solomon, S, D. Qin, M. Manning, M. Marquis, K. Averyt, M. Tignor, H. Miller, Z. Chen, 2007: *Climate Change 2007: The Physical Science Basis*, Cambridge University Press, 996 pp.

Stahle, D.W., M.K. Cleaveland, M.D. Therrell, D.A. Gay, R.D. D'Arrigo, P.J. Krusic, E.R. Cook, R.J. Allan, J.E. Cole, R.B. Dunbar, M.D. Moore, M.A. Stokes, B.T. Burns, J. Villanueva-Diaz, and L.G. Thompson, 1998: Experimental dendroclimatic reconstruction of the Southern Oscillation. *Bulletin of the American Meteorological Society*, **79(10)**, 2137-2152.

Stott, P.A., 2003: Attribution of regional-scale temperature changes to anthropogenic and natural causes. *Geophysical Research Letters,* **30(14)**, 1724, doi:10.1029/2003GL017324.

Stott, P.A. and S.F.B. Tett, 1998: Scale-dependent detection of climate change. *Journal of Climate*, **11(12)**, 3282–3294.

Therrell, M.D., D.W. Stahle, M.K. Cleaveland and J. Villanueva-Diaz, 2002: Warm season tree growth and precipitation over Mexico. *Journal of Geophysical Research*, **107(D14)**, 4205, doi:10.1029/2001JD000851.

Thompson, D.W.J. and J.M. Wallace., 1998: The Arctic Oscillation signature in the wintertime geopotential height temperature fields. *Geophysical Research Letters,* **25(9),** 1297–1300.

Thompson, D.W.J. and J.M. Wallace 2000a: Annular modes in the extratropical circulation. Part I: month-to-month variability. *Journal of Climate,* **13(5),** 1000–1016.

Thompson, D.W.J. and J.M. Wallace, 2000b: Annular modes in the extratropical circulation. Part II: trends. *Journal of Climate,* **13(5),** 1018–1036.

Ting, M. and H. Wang, 1997: Summertime U. S. precipitation variability and its relation to Pacific sea surface temperature. *Journal of Climate*, **10(8)**, 1853-1873.

Tippett, M. K. and A. Giannini, 2006: Potentially predictable components of African summer rainfall in an SST-forced GCM simulation. *Journal of Climate*, **19(13)**, 3133-3144.

Trenberth, K.E., 1990: Recent observed interdecadal climate changes in the Northern Hemisphere. *Bulletin of the American Meteorological Society*, **71(7)**, 988-993.

Trenberth, K.E., 2004: Rural land-use change and climate. *Nature,* **427(6971)**, 213.

Trenberth, K.E. and G.W. Branstator, 1992: Issues in establishing causes of the 1988 drought over North America. *Journal of Climate*, **5(2)**, 159-172.

Trenberth, K. and T.J. Hoar, 1996: The 1990-1995 El Niño-Southern Oscillation event: longest on record. *Geophysical Research Letters*, **23**, 57-60.

Trenberth, K.E., G.W. Branstator and P.A. Arkin, 1988: Origins of the 1988 North American drought. *Science*, **242(4886)**, 1640-1645.

Trenberth, K.E., G.W. Branstrator, D. Karoly, A. Kumar, N.-C. Lau, and C. Ropelewski, 1998: Progress during TOGA in understanding and modeling global teleconnections associated with tropical sea surface temperatures. *Journal of Geophysical Research*, **103(C7)**, 14291-14324.

Vecchi, G.A. and B. Soden, 2007: Global warming and the weakening of the tropical circulation. *Journal of Climate*, **20(17)**, 4316-4340.

Von Storch, H., and F.W. Zwiers, 1999: *Statistical Analysis in Climate Research*. Cambridge University Press, Cambridge, UK, and New York, 484 pp.

Vose, R.S., T.R. Karl, D.R. Easterling, C.N. Williams, and M.J. Menne, 2004: Impact of land-use change on climate. *Nature,* **427(6971)**, 213–214.

Walker, G.T. and E.W. Bliss, 1932: World weather V. *Memoirs of the Royal Meteorological Society*, **4(36)**, 53-84.

Wallace, J.M. and D.S. Gutzler, 1981: Teleconnections in the geopotential height field during the Northern Hemisphere winter. *Monthly Weather Review*, **109(4)**, 784-812.

Wolfson, N., R. Atlas, and Y.C. Sud, 1987: Numerical experiments related to the summer 1980 U.S. heat wave. *Monthly Weather Review*, **115(7)**, 1345-1357.

Wu, Q. and D.J. Karoly, 2007: Implications of changes in the atmospheric circulation on the detection of regional surface air temperature trends. *Geophysical Research Letters*, **34**, L08703, doi:10.1029/2006GL028502.

Yu, L. and M.M. Rienecker, 1999: Mechanisms for the Indian Ocean warming during the 1997-1998 El Niño. *Geophysical Research Letters*, **26(6)**, 735-738.

Zhang, X., F.W. Zwiers, and P.A. Stott, 2006: Multimodel multisignal climate change detection at regional scale. *Journal of Climate*, **19(17)**, 4294–4307.

Zhang, X., F.W. Zwiers, G.C. Hegerl, F.H. Lambert, N. P. Gillett, S. Solomon, P.A. Stott, and T. Nozawa, 2007: Detection of human influence on twentieth-century precipitation trends. *Nature*, **448(7152)**, 461–465.

Zwiers, F.W. and X. Zhang, 2003: Towards regional scale climate change detection. *Journal of Climate,* **16(5),** 793–797.

Appendix 3.A

Data and Methods Used for Attribution

3.A.1 OBSERVATIONAL DATA

North American surface temperatures during the assessment period of 1951 to 2006 are derived from four data sources. These are the U.K. Hadley Centre's HadCRUT3v (Brohan *et al.*, 2006), NOAA's land/ocean merged data (Smith and Reynolds, 2005), NOAA's global land gridded data (Peterson *et al.*, 1998), and NASA's gridded data (Hansen *et al.*, 2001). For analysis of United States surface temperatures, two additional data sets used are NOAA's U.S. Climate Division data (NCDC, 1994) and the PRISM data (Daley *et al.*, 2002).

Spatial maps of the surface temperature trends shown in Chapter 3 are based on combining all the above data sets. For example, the North American and United States surface temperature trends during 1951 to 2006 were computed for each data set, and the trend map is based on equal-weighted averages of the individual trends. The uncertainity in observations is displayed by plotting the extreme range among the time series of the 1951 to 2006 trends from individual data sets.

North American precipitation data are derived from the Global Precipitation Climatology Project (GPCC) (Rudolf *et al.*, 2005); also consulted is the NOAA gridded precipitation data (Chen *et al.*, 2002), however the North American analysis shown in Chapter 3 is based on the GPCC data alone which is judged to be superior owing to its greater volume of input stations over Canada and Alaska in particular. For analysis of United States precipitaton, two additonal data sets used are NOAA's U.S. Climate Division data and PRISM data. Spatial maps of United States precipitation trends during 1951 to 2006 were computed for each of these three data sets, and the United States trend map is based on equal-weighted averages of the individual trends.

Free atmospheric conditions during 1951 to 2006, including 500 hPa geopotential heights, are derived from the NCEP/NCAR reanalysis (Kalnay *et al.*, 1996). A comparison of various reanalysis data is provided in Chapter 2, but only the NCEP/NCAR version is available for the entire 1951 to 2006 assessment period.

3.A.2 CLIMATE MODEL SIMULATION DATA

Two configurations of climate models are used in this SAP; atmospheric general circulation models (AMIP), and coupled ocean-atmosphere general circulation models (CMIP). For the former, the data from two different atmospheric models are studied; the European Center/Hamburg model (ECHAM4.5) (Roeckner *et al.*, 1996) whose simulations were performed by the International Research Institute for Climate and Society at LaMont Doherty (L. Goddard, personal communication), and the NASA Seasonal-to-Interannual Prediction Project (NSIPP) model (Schubert *et al.*, 2004) whose simulations were conducted at NASA/Goddard. The models were subjected to specified monthly varying observed global sea surface temperatures during 1951 to 2006. In a procedure that is commonly used in climate science, multiple realizations of the 1951 to

2006 period were conducted with each model in which the separate runs started from different atmospheric initial conditions but were subjected to identically evolving SST conditions. A total of 33 AMIP runs (24 ECHAM and 9 NASA) were available.

The coupled models are those used in the IPCC Fourth Assessment. These are forced with estimated greenhouse gases, aerosols, solar irradiance and the radiative effects of volcanic activity for 1951 to 1999, and with the IPCC Special Emissions Scenario (SRES) A1B (IPCC, 2007) for 2000 to 2006. The model data are available from the Program for Climate Model Diagnosis and Intercomparison (PCMDI) archive as part of the Coupled Model Intercomparison Project (CMIP3). Table 3.1 lists the 19 different models used and the number of realizations conducted with each model. A total of 41 runs were available.

The SST-forced (externally-forced) signal of North American and United States surface temperature and precipitation variability during 1951 to 2006 is estimated by averaging the total of 33 AMIP (41 CMIP) simulations. Trends during 1951 to 2006 were computed for each model run in a manner identical to the observational method; the trend map shown in Chapter 3 is based on an equal-weighted ensemble average of the individual trends. The uncertainty in these simulated trends is displayed graphically by plotting the 5%-95% range amongst the individual model runs.

All the observational and model data used in this SAP are available in the public domain. Further, these data have been widely used for a variety of climate analysis studies as reported in the refereed scientific literature. Table 3.2 provides URLs for each of these data sets.

3.A.3 DATA ANALYSIS AND ASSESSMENT

Analysis of observational and model data is based on standard statistical procedures used extensively in climate research and the physical sciences (von Storch and Zwiers, 1999). Trends for 1951 to 2006 are computed using a linear methodology based on least-squares. Statistical estimates of the significance of the observed trends are based on a non-parametric test in which the 56-year trends are ranked against those computed from CMIP simulations subjected to only natural forcing (solar irradiance and volcanic aerosol). The principal uncertainty in such an analysis is knowing the population of 56-year trends that are expected in the absence of anthropogenic forcing. This Section uses four different coupled models, and a total of sixteen 100-year simulations to estimate the statistical population of naturally occurring 56-year trends, though the existence of model biases is taken into account in making expert assessments.

Observed and model data are compared using routine linear statistical methods. Time series are intercompared using standard temporal correlations. Spatial maps of observed and simulated trends over North America are compared using standard spatial correlation and congruence calculations. Similar empirical methods have been applied for pattern analysis of climate change signals in the published literature (Santer *et al.*, 1994).

Chapter 3 employs expert judgment in arriving at probabilistic attribution statements. The analyses described above are only a small part of the information available to the authors, who also make extensive use of the scientific peer-reviewed literature. For more details on the use of expert assessment in this SAP, the reader is referred to Box 3.4 and the Preface.